KINETICS OF PRION ACCUMULATION IN SPLENIC CELL TYPES OF THE LYMPHORETICULAR SYSTEM

A thesis submitted in partial fulfillment for the degree of

Doctor of Philosophy to the University College London

by

Rocío Castro Seoane

BSc (Hons) University of London

Declaration

I, Rocío Castro Seoane confirm that the work presented in this thesis is my own. Where information has been derived from other sources, I confirm that this has been indicated in the thesis.

Acknowledgments

I would like to thank my supervisor and my 'compañero de batalla' Peter Klöhn for all his help and shared enthusiasm in the project. Thanks to Parmjit as my secondary supervisor, the MRC and John Collinge for supporting my work. Many thanks to our collaborator Prof. Trevor Sweeting for his contribution in the statistical modelling presented in this thesis and the invaluable help of Dr Holger Hummerich. Thanks to Dr Malin Sandberg for allowing us to use her bioassay data and to Dr Howard Tattum for his help with the EM analysis. Special thanks to Ray Young for the figures and to the various people in the department for helping me with my training on different experimental techniques. The Wakefield street staff has been incredible and I like to pass my gratitude to Chris, Gavin, Helen and many others. I would like to thank all my catIII bench mates, especially Nunu, my closest competitor in plate spliting, Nathalie Gross for being such a sweetheart and listen to my endless talk about the PhD, and Anna Harvey for being always happy to give me a hand on those long days in the lab. Thanks to the robot guys, Jeremie and Michael, for their inestimable help and efforts to fit my experiments in their busy schedule. Very special thanks to Joo-Hee for her help with my drafts but most of all for indulge me on my 'new life' dreams and for the fun moments.

A very special thanks goes out to Professor Graham Goldsworthy and Mary Lightfoot from Birkbeck College and Dr Abdul Matin without whose motivation and encouragement I would not have considered doing a PhD.

A big thank you to my 'adoptive family': Margui, Jose, Jaimito and my stress ball Carmen, whose support during the last year has been incredible. I have no words to describe how fortunately I feel for having such good friends. To all my friends who have put on with me all these years THANKS, specially Natalia for being one of my pillars in

London, Cristina and María for the unforgettable trips together, Juan for being a best friend, Sandra for sharing her PhD experiences with me and her words of advice and of course Musta my friend and favourite handy man.

Thanks to my parents and my brother for their love. Mum for her patience with the 'adulescente' that has for a daugther. And dad many thanks for worrying way too much.

A mis padres,

"There is a theory which states that if ever anyone discovers exactly what the Universe is for and why it is here, it will instantly disappear and be replaced by something even more bizarre and inexplicable. There is another theory which states that this has already happened."

- DOUGLAS ADAMS

ABSTRACT

Prions accumulate in the lymphoreticular system (LRS) at early stages of prion disease, long before they are detected in the brain. A considerable body of evidence showed that both haematopoietic and stromal cells play a role in prion pathogenesis. However, the contribution of different cell types to the accumulation and the spread of prions in the LRS are not well understood. Taking advantage of a quantitative *in-vitro* infectivity assay, the Scrapie Cell Assay (SCA) and high density magnetic-activated cell sorting (MACS), we studied the kinetics of prion accumulation in various splenic cell types at early stages of prion disease. The determination of statistically robust infectious titres was achieved by statistical modelling using generalised linear model (GLM) regression. With this novel procedure time-dependent changes of prion titres were monitored in seven distinct splenic cells and identified two cell types that have previously not been associated to prion pathogenesis, plasmacytoid dendritic (pDC) and natural killer (NK) cells. Notably, in *Prnp*$^{-/-}$ mice, e.g. in absence of prion replication, infectivity was detected in macrophages and dendritic cells (DC) after 3 dpi, but not in lymphocytes, underscoring the importance of prion sequestration by antigen-presenting cells which are among the first cells of the immune system to encounter pathogens. Reports of the secretion of endosome-derived membrane particles, so called exosomes by immune-competent cells and prion-infected cell lines raised the question whether prion secretion could be a potential route for the spread of prions. We here present the first evidence that MACS-isolated lymphocytes and DCs from scrapie-infected mice secrete prions which are associated to the release of exosome-like membrane particles into the cell culture supernatant *ex vivo*.

TABLE OF CONTENTS

Declaration 2

Acknowledgements 3

Abstract 6

Index of figures and tables 11

Abbreviation List 14

CHAPTER 1: Introduction 16

1.1 Transmissible spongiform encephalopathies 17

1.2 Nature of the infectious agent 18

1.2.1 The 'protein-only' hypothesis 18

1.2.2 PrP^{Sc} as a surrogate marker for infectivity 21

1.2.3 PrP^{C} trafficking and PrP^{Sc} formation 22

1.3 Pathogenesis of prion diseases 25

1.3.1 The immune system in prion diseases 25

1.3.2 Peripheral replication of prions 28

The role of follicular dendritic cells. 29

Other cell candidates for prion replication 31

Complement system 32

1.3.3 Transport of prions to the LRS and the CNS 33

Lymphocytes 34

Macrophages and dendritic cells 34

1.3.4 Neuroinvasion 36

1.4 Mechanisms for the lateral spread of prions 37

The role of exosomes in the spread of prions 38

1.5 Aims of the thesis 41

CHAPTER 2: Materials and Methods 43

2.1 Isolation of cell fractions from spleen tissue 44

2.1.1 Isolation of splenocytes 44

2.1.2 Isolation of splenic cell types by magnetic-activated cell sorting . . 45

Isolation of plasmacytoid dendritic cells and lymphocytes from blood 46

2.1.3 Isolation of follicular dendritic cell clusters 46

2.2 Cell culture 47

2.2.1 Short-term primary cultures of splenic cells 47

2.2.2 Long-term stroma cell cultures 48

2.2.3 Culture and maintenance of neuroblastoma N2a cells 49

2.3 Isolation of exosome-enriched membrane fractions and analysis by electron microscopy 49

2.4 Protein determination 51

2.5 *In vivo* depletion of plasmacytoid dendritic cells and RML inoculation 51

2.6 Infectivity measurements 52

2.6.1 Animals and scrapie inoculation 52

2.6.2 Preparation of samples for infectivity testing 52

Preparation of the RML standards 52

Preparation of tissue and cell homogenates 53

Infectivity of exosome pellets 53

2.6.3 Infectivity assays 54

Scrapie Cell Assay in End Point format 54

Bioassay with Tg20 indicator mice 55

Calculation of infectious titres 55

2.6.4 Detection of PrP^{Sc} 55

NaPTA precipitation and immuno-detection of PrP^{Sc} by WB 55
2.7 Fluorescence techniques 57
2.7.1 Flow cytometry 57
Immune complex labeling 58
2.7.2 Fluorescence microscopy 59
CHAPTER 3: Kinetics of prion accumulation in splenic cell types of mice . 60
3.1 Quantification of infectious titres using a generalized linear model 62
3.1.1 Validation of a GLM for the estimation of infectious titres by SCEPA 63
3.1.2 Determination of the sensitivity of SCEPA 66
3.2 Validation of a homogenization method for cell titre determination by SCEPA 71
3.3 Sequential isolation of splenic cell types by magnetic-activated cell sorting . 74
3.4 Prion accumulation in the lymphoreticular system at early stages of prion disease 78
3.5 Contribution of the stroma compartment 87
3.5.1 Isolation of follicular dendritic cells 88
Immune complex labelling 92
3.5.2 Infectious titres of follicular dendritic cell clusters 93
3.5.3 Stroma cultures isolated from spleens of scrapie-infected mice do not propagate prions *ex vivo* 95
3.6 *Ex-vivo* release of prions from scrapie-infected splenic cells 98
CHAPTER 4: Discussion 103
4.1 Establishment of a method to determine infectious titres of splenic cell types involved in prion pathogenesis 104
4.2 Role of antigen presenting cells in prion sequestration 107

4.3 Contribution of the stroma compartment to prion pathogenesis 116
4.4 *Ex-vivo* release of prions from scrapie-infected splenic cells 118
4.5 Concluding remarks 120
References 121
Appendices 142

INDEX OF FIGURES AND TABLES

CHAPTER 1

Figure 1.1 Model for prion propagation. Molecular strain typing of human prions 20

Figure 1.2 Endocytosis and subcellular localisation of PrP^C 24

Figure 1.3 Peripheral prion pathogenesis 27

Figure 1.4 Mechanisms for the lateral spread of prions 40

CHAPTER 2

Figure 2.1 Standard isolation procedures of splenic cells by MACS 46

Figure 2.2 Purification of follicular dendritic cell clusters by a four step 1 x *g* sedimentation procedure 47

Figure 2.3 Separation of low density cells using a Percoll gradient 49

Figure 2.4 Isolation of exosomes from primary cultures of splenic cells 50

Table 2.1 List of primary antibodies and isotype controls used for cell characterization 58

CHAPTER 3

Figure 3.1 Initial validation of Poisson distribution 64

Figure 3.2 Regression analysis of SCEPA end point titration assay by GLM 66

Figure 3.3 Regression analysis of mouse bioassay data by GLM 68

Figure 3.4 Flow cytometry analysis of isolated splenic cell types 77

Figure 3.5 Purification of macrophages by fluorescent activated cell sorting . . 78

Figure 3.6 Kinetics of prion accumulation in spleen and mesenteric lymph nodes 80

Figure 3.7 Distribution of infectivity in splenic cell types at 30 dpi 83
Figure 3.8 PrP^C expression of splenic pDCs 85
Figure 3.9 No abnormalities of splenic B cells subsets at preclinical disease . . . 87
Figure 3.10 Summary of FDC isolation from spleen tissue 91
Figure 3.11 Internalization of OVA immune complexes 93
Figure 3.12 Characterization of follicular dendritic cell clusters 94
Figure 3.13 Characterisation of stroma cultures 96
Figure 3.14 Infectivity of stroma cell cultures after splitting 97
Figure 3.15 Effects of different culture conditions on the viability of primary cultures of B lymphocytes 100
Figure 3.16 Exosomes are released from scrapie-infected B cells *ex vivo* 102

Table 3.1 Sensitivity for prion detection of SCEPA and mouse bioassay 70
Table 3.2 Infectious titres of MACS-isolated cells after homogenisation by ribolysation and sonication 73
Table 3.3 Summary of yields and purities of isolated splenic cell types 76
Table 3.4 Infectious titres of different splenic cell types in the absence of prion replication at 3dpi 81
Table 3.5 Time dependent accumulation of prion infectivity in isolated splenic cell types 82
Table 3.6 Effects of *in vivo* depletion of pDCs on prion titres of spleen and mesenteric lymph nodes 84
Table 3.7 Infectivity associated to FDC clusters in *wild-type* and *Prnp*$^{-/-}$ mice . . 95
Table 3.8 Prions are released from scrapie-infected splenic cell cultures *ex vivo* 101

CHAPTER 4

Figure 4.1 Areas of antigen encounter in lymphoid organs 109

APPENDICES

Table A1 *In-vitro* endpoint titration of RML I6200 146

Table A2 Serial mouse bioassays to determine endpoint titres of RML I6200 . . 147

ABBREVIATION LIST

2-ME	2-Mercaptoethanol
7-AAD	7-Aminoactinomycin D
AP	alkaline phosphatase
APC	antigen presenting cell
BSA	bovine serum albumin
BSE	bovine spongiform encephalopathy
CJD	Creutzfeld-Jakob disease
CNS	central nervous system
CWD	chronic wasting disease
DC	dendritic cells
dpi	days post inoculation
ECM	extracellular matrix
EDTA	ethylene diamine tetra-acetic acid
ELISPOT	enzyme-linked immunospot
ER	endoplasmic reticulum
FACS	fluorescent activated cell sorting
FCS	foetal calf serum
FcR	Fc Receptor
FDC	follicular dendritic cells
FITC	fluorescein isothiocyanate
FLC	foetal liver cells
FRC	fibroblastic reticular cells
g	gravity (acceleration due to)
G	gauge
GLM	generalized linear model
GM-CSF	Granulocyte-macrophage colony stimulating factor
GPI	glycosyl-phosphatidylinositol
GSCN	guanidinium thiocyanate
GSS	Gerstmann-Straussler-Scheinker syndrome
i.c.	intracerebrally
IC	immune complex
IL4	interleukine 4
IMDM	Iscove's modified Dulbecco's medium
i.p.	intraperitoneally
lDC	lymphoid DCs
LPS	lipopolysaccharide
LRS	lymphoreticular system
LT	lymphotoxin
MACS	magnetic activated cell sorting
mDC	myeloid DCs
MLN	mesenteric lymph nodes
MVB	multivesicular bodies
N2a	murine neuroblastoma cells
NaPTA	sodium phosphotungstic acid
NK	natural killer cells
OFCS	OptiMEM + 10 % FBS + 1 % pen-strep
OVA	ovalbumine

PBS	phopho-buffered saline
pDC	plasmacytoid dendritic cells
PE	phycoerythrin
PerCP	Peridinin chlorophyll protein
PFA	paraformaldehyde
pH	hydrogen ion concentration
PK	proteinase K
PMCA	protein misfolding cyclic amplification
PMSF	phenylmethylsuphonyl fluoride
Prnp	prion protein gene (mouse)
PrP	prion protein
$PrP^{0/0}$	PrP null
PrP^{C}	normal isoform of the prion protein
PrP^{res}	protease resistant prion protein
PrP^{Sc}	disease-associated prion protein
RBC	red blood cells
RML	Rocky Mountain Laboratory
RT	room temperature
SCA	scrapie cell assay
SCID	Severe combined immunodeficiency
SCEPA	scrapie cell end-point assay
SD	standard deviation
SDS	sodium dodecyl sulphate
SE	standard error
S-K	Spearman-Karber
TBM	tingible body macrophages
TCIU	tissue culture infectious units
TNF	tumour necrosis factor
TNT	tunnelling nanotubes
TSE	transmissible spongiform encephalopathies
WB	western blot
wt	*wild-type*
w/v	weight in volume

CHAPTER 1

INTRODUCTION

INTRODUCTION

1.1 Transmissible spongiform encephalopathies

Transmissible spongiform encephalopathies (TSE) or prion diseases are a group of lethal neurodegenerative diseases that affect humans and other animal species. Examples are Creutzfeldt-Jakob disease (CJD), Gerstmann-Sträussler-Scheinker (GSS), and kuru in humans, bovine spongiform encephalopathy (BSE) in cattle, scrapie in sheep and chronic wasting disease (CWD) in cervids. TSEs are characterized by long disease incubation times followed by a rapidly progressing and severe degeneration. Spongiform degeneration, astrocyte and microglia proliferation, and deposition of misfolded proteins are the main characteristic histopathological features of prion diseases (Kretzschmar, 1993).

Although prion diseases are rare transmissible diseases with a prevalence of one case per million people each year[1], they made international headlines during the European BSE crisis in the 1990s. With hundreds of thousands of infected cattle and the risk of a foodborne transmission to humans, prion diseases have caused massive economic losses and form a public health concern. Although the BSE crisis has been largely resolved, a recent increase in the number of cases of CWD and first cases of BSE in the United States (Belay *et al.*, 2004; Richt *et al.*, 2007; Aguzzi *et al.*, 2008), renders these diseases a current topic, but also a fascinating one, given the uniqueness of the biology of prions.

The nature of the infectious agent distinguishes TSEs from all known infectious diseases and renders them to date a unique biological phenomenon. According to the broadly accepted 'protein-only' hypothesis the infectious agent is devoid of nucleic acids and consists mainly, if not entirely of protein (Griffith, 1967). An abnormal conformer of a

[1] World Health Organization (WHO). http://www.who.int/zoonoses/diseases/prion_diseases/en/

host membrane glycoprotein known as the prion protein was identified as a major component of the infectious agent (Prusiner, 1982). How a protein can be transmissible and encode for different conformational variants is still unresolved and remains a matter of debate.

Another remarkable feature of prions is that they fail to induce an immune response in the host. But surprisingly, the immune system plays an important role in prion pathogenesis and is possibly involved in the accumulation, replication of prions and their transport to the brain (Aucouturier and Carnaud, 2002; Aguzzi *et al.*, 2008).

1.2 Nature of the infectious agent

1.2.1 The 'protein-only' hypothesis

Early observations led to the conclusion that TSEs are unconventional infectious diseases, since their disease-causing agents are resistant to procedures that inactivate nucleic acids, but are sensitive to procedures that inactivate proteins (Alper *et al.*, 1967; Alper *et al.*, 1978; Prusiner, 1982). In 1967, Griffith suggested that the transmissible agent is an infectious protein that is propagated by autocatalytic misfolding. The nature of the TSE agent was defined in more detail by Prusiner in 1982, who coined the term 'prion' for proteinaceous infectious particle (Griffith, 1967; Prusiner, 1982). Purification protocols for the infectious agent in hamster brain homogenates led to the detection of a 27-30 kDa protease resistant protein, the PrP^{27-30} (Bolton *et al.*, 1982; Prusiner *et al.*, 1982). This protein, the protease-resistant core of a 33-35 kDa protein designated PrP^{Sc}, was suggested to be a major constituent of the infectious fraction. Further research conducted in the laboratories of S. Prusiner and C. Weissmann led to the discovery that PrP^{Sc} is encoded by a host gene (Basler *et al.*, 1986). Both PrP^{Sc} and the normal cellular prion protein, PrP^{C} are encoded by a single gene and share the same amino acid sequence (Oesch *et al.*, 1985; Basler *et al.*,

1986; Stahl and Prusiner, 1991). PrP^{Sc} and PrP^{C} are conformational variants of the same protein that differ in their biochemical properties. While PrP^{C} is predominately α-helical, soluble and protease sensitive, PrP^{Sc} has a higher β-sheet content, forms insoluble aggregates and is partially resistant to proteinase K (PK) (Stahl and Prusiner, 1991; Caughey *et al.*, 1991; Riek *et al.*, 1997).

According to the 'protein-only' hypothesis, the replication of misfolded protein results from the recruitment by PrP^{Sc} of endogenous PrP^{C} monomers and their conversion into PrP^{Sc} by a conformational change (Griffith, 1967; Prusiner, 1982). The most widely accepted model of prion propagation, the seeded polymerization model, postulates that PrP^{Sc} conformers are stabilized by recruitment into a stable PrP^{Sc} seed which accelerates the addition of monomers. Prion propagation is driven by the fragmentation of large PrP^{Sc} aggregates resulting in more infectious PrP^{Sc} seeds (**figure 1.1 A**) (Come *et al.*, 1993). Oligomers of 14 to 28 PrP molecules were reported as the most infectious entities (Silveira *et al.*, 2005). The aetiology of sporadic and inherited prion diseases can also be explained with this model, since PrP mutations could alter the $PrP^{C} \leftrightarrow PrP^{Sc}$ equilibrium and favour nucleation (Jarrett and Lansbury, 1993).

A wealth of evidence supports the 'protein-only' hypothesis as exemplified by the following: Abrogation of PrP^{C} prevents prion disease (Bueler *et al.*, 1993; Brandner *et al.*, 1996a; Blattler *et al.*, 1997), certain PrP gene mutations have been linked to inherited prion diseases (Hsiao *et al.*, 1992) and conversion of PrP^{C} into PK resistant PrP (PrP^{res}) can be recapitulated in cell-free systems using PrP^{Sc} seeds in large excess, a process that is species-specific (Kocisko *et al.*, 1994; Kocisko *et al.*, 1995). A number of recent reports demonstrate the *de-novo* generation of prions from recombinant prion protein, albeit at extremely low titres (Wang *et al.*, 2010; Colby *et al.*, 2010). Historically, the presence of distinct prion strains constituted the main argument against the 'protein-only' hypothesis (Weissmann, 1991), but the coexistence of

distinct conformational variants whose clonal selection is favoured by unknown host factors could resolve this paradox (Collinge and Clarke, 2007). Prion strains are defined by their characteristic incubation periods, biochemical properties and neuropathological features. According to our current understanding prion-strain features are encoded as PrP^{Sc} oligomers with different conformations and glycosylation patterns (**figure 1.1 B**). Structural information is propagated by recruitment of PrP monomers (in a strain-specific manner) into pre-existing PrP^{Sc} conformers which serve as templates (Bessen *et al.*, 1995; Khalili-Shirazi *et al.*, 2005). Differences in the aminoacid sequence of PrP^{C} between animal species may define what conformations can be acquired; the overlap of permitted PrP^{Sc} conformers between species could explain the efficiency of transmission and the species barrier effect (Collinge and Clarke, 2007).

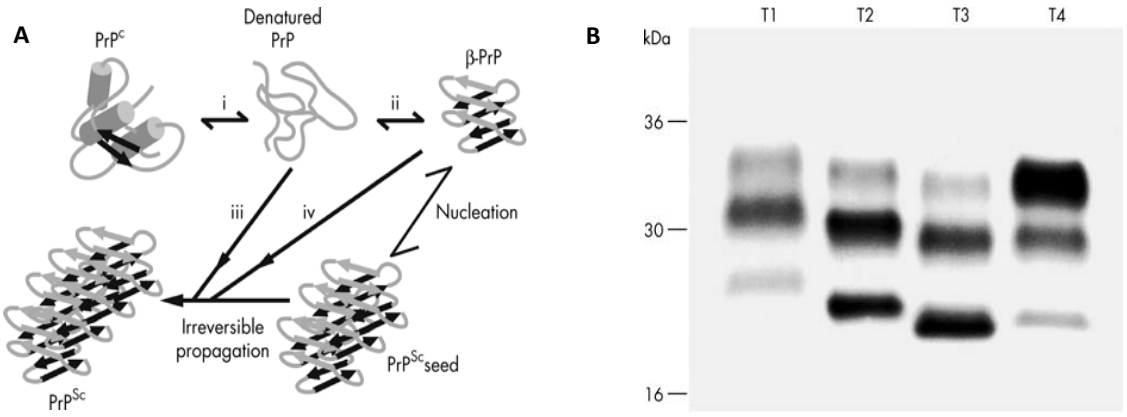

Figure 1.1 (**A**) **Model for prion propagation.** PrP fluctuates between the native state and a minor misfolded conformation, which self-aggregates into a stable PrP^{Sc} seed (nucleation). Once the seed is formed, addition of new monomers occurs rapidly. (**B**) **Molecular strain typing of human prions.** Different prion strains can be distinguished by their biochemical properties such as the size of protease-resistant core, revealed by distinct mobilities and ratios of di-, mono- and un-glycosylated forms. Variant CJD (T4) is characterised by a diglycosylated-dominant PrP^{Sc} pattern and is readily distinguishable from strains associated with sporadic and iatrogenic CJD (T1-3). Reproduced from the J. Neurol. Neurosurg. Psychiatry, Collinge, J., 2005, Vol 76, pp 906-919 (Collinge, 2005).

1.2.2 PrP^{Sc} as a surrogate marker for infectivity

Studies by Bolton *et al.* with 263K hamster scrapie led to the identification of PrP^{Sc} as a major component of the infectious isolates (Bolton *et al.*, 1982). A strong correlation between PrP^{Sc} and infectivity was inferred from experiments that showed a proportional relationship between infectious titres and the concentration of $PrP^{27\text{-}30}$, the protease resistant core of PrP^{Sc} (Bolton *et al.*, 1982; Gabizon *et al.*, 1988). However, formation of PrP^{Sc} does not always correlate with infectivity and several results have challenge the hypothesis that PrP^{Sc} is the TSE agent. Prion diseases are transmitted in the absence of detectable levels of PrP^{Sc} (Sakaguchi *et al.*, 1993; Lasmezas *et al.*, 1997; Barron *et al.*, 2007). Likewise, abnormal deposits of PrP were detected in the absence of infectivity (Piccardo *et al.*, 2007). Relatively protease-sensitive forms of PrP were identified in atypical cases of scrapie in sheep (Nor98) and cattle (BASE) (Everest *et al.*, 2006; Benestad *et al.*, 2008) indicating that both protease-sensitive ($sPrP^{Sc}$) and protease-resistant ($rPrP^{Sc}$) conformers may co-exist (Taraboulos *et al.*, 1992; Safar *et al.*, 1998; Tzaban *et al.*, 2002). PrP^{Sc}, defined by its partial resistance to proteases should therefore be considered a surrogate marker for prions. Although in most cases $rPrP^{Sc}$ correlates with infectivity, the determination of PrP^{Sc} levels cannot be used in quantitative terms to determine infectious titres and infectivity assays remain the gold standard. Until recently, infectivity assays were based on the transmission of prions to laboratory animals, which are time consuming and inaccurate. An important improvement in titre determination is the establishment of cell-based infectivity assay, e.g. the scrapie cell assay (SCA), developed for measuring *de novo* infectivity (Klohn *et al.*, 2003). Unfortunately, most known prion-replicating cell lines are only susceptible to murine prions, which limit their application for diagnostic purposes. An interesting application of *in vitro* infectivity assays has recently been published by Mahal *et al.* where different strains could be distinguished in cell culture using a panel of

susceptible cell lines with different responses to various mouse prions (Mahal *et al.*, 2007).

Limitations of infectivity assays in regards to assay duration and prion susceptibility to multiple prion strains render PrP^{Sc} detection on Western Blot the method of choice for the diagnosis of prion diseases in humans and ruminants. To improve detection of PrP^{Sc} in tissues and clinical diagnosis, procedures like the selective precipitation of PrP^{Sc} by sodium phosphotungstic acid (NaPTA) or the amplification of PrP^{Sc} by protein misfolding cyclic amplification (PMCA) have been used (Safar *et al.*, 1998; Wadsworth *et al.*, 2001; Castilla *et al.*, 2005b).

1.2.3 PrP^{C} trafficking and PrP^{Sc} formation

Clear experimental evidence confirms that PrP^{C} expression is a prerequisite for prion propagation (Bueler *et al.*, 1993; Brandner *et al.*, 1996a) and subsequent neurodegeneration (Brandner *et al.*, 1996b). A better understanding of the function and cell biology of PrP are essential to characterise molecular events that trigger prion formation.

The prion protein is a highly conserved cell surface glycoprotein abundant in neurons and glia, but also expressed in other cells types including immune cells (Aguzzi and Polymenidou, 2004). Although numerous studies have identified a role of PrP^{C} in cell signalling, copper metabolism, resistance to oxidative stress, immuno-regulation and synaptic transmission, the functional role of PrP^{C} remains largely unknown (reviewed in Martins *et al.*, 2002). Interestingly, despite its highly conserved aminoacid sequence, PrP^{C} seems to be dispensable, since no obvious phenotypic changes were observed in PrP-knockout mice (Bueler *et al.*, 1992) and in mice after the postnatal ablation of the PrP gene in neurons (Mallucci *et al.*, 2002).

PrP^{C} is a glycosyl-phosphatidylinositol (GPI)-anchored glycoprotein (Stahl *et al.*, 1987), attached to the outer leaflet of the lipid membrane and is associated with lipid rafts,

i.e. membrane domains rich in cholesterol and sphingolipids. Synthesised in the rough endoplasmic reticulum (ER), PrP^{C} is transported via the Golgi to the plasma membrane. PrP^{C} is post-translationally modified by addition of N-linked oligosaccharide chains, the formation of a disulphide bond and the attachment to the GPI anchor (Taylor and Hooper, 2006). Following its transport to the membrane, newly synthesised PrP^{C} is rapidly internalised and recycled constitutively between the plasma membrane and the endocytic compartment (Shyng *et al.*, 1993). The conversion of PrP^{C} into PrP^{Sc} seems to occur after newly formed PrP^{C} reaches the membrane, either at the surface or after internalisation, as supported by the observation that blocking the transport to the plasma membrane or inhibition of endocytosis prevents PrP^{Sc} formation (Borchelt *et al.*, 1992; Taraboulos *et al.*, 1992; Marijanovic *et al.*, 2009). Different internalisation pathways have been suggested including caveolae- and clathrin-mediated processes (reviewed in Prado *et al.*, 2004; Campana *et al.*, 2005) (**figure 1.2**). Internalisation of PrP through caveolae was shown for Chinese hamster ovary cells (Vey *et al.*, 1996; Peters *et al.*, 2003), whereas in neuronal cells PrP^{C} clustered in clathrin-coated vesicles as shown by immunogold detection *in vitro* and *in vivo* (Shyng *et al.*, 1994; Shyng *et al.*, 1995; Sunyach *et al.*, 2003). The mechanism by which PrP^{C} is internalized remains unclear and may be cell- or tissue-specific. Irrespective of the internalisation pathway, proteins like PrP^{C} are directed to early endosomes from where they enter the endosomal recycling compartment and are delivered back to the membrane. Alternatively, if targeted for degradation, proteins are sorted into multivesicular bodies (MVB) and lysosomes (Maxfield and Mcgraw, 2004).

Despite experimental evidence for PrP^{Sc} formation in recycling endosomes it remains controversial whether this compartment constitutes the principal site of prion conversion (Borchelt *et al.*, 1992; Campana *et al.*, 2005; Marijanovic *et al.*, 2009). A role of the ER in PrP conversion was proposed for familial prion diseases where mutant PrP misfolds as it is synthesized (Harris, 2003). Furthermore, it was suggested that

retrograde transport of surface PrP^{Sc} to the Golgi and the ER could interfere with newly synthesized PrP^{C} and prime its conversion (Beranger *et al.*, 2002). Plasma membrane, endosomal recycling compartment, Golgi, late endosomes, lysosomes and exosomes were all shown to accumulate PrP^{Sc} (McKinley *et al.*, 1991; Arnold *et al.*, 1995; Sunyach *et al.*, 2003; Fevrier *et al.*, 2004; Barmada and Harris, 2005; Marijanovic *et al.*, 2009).

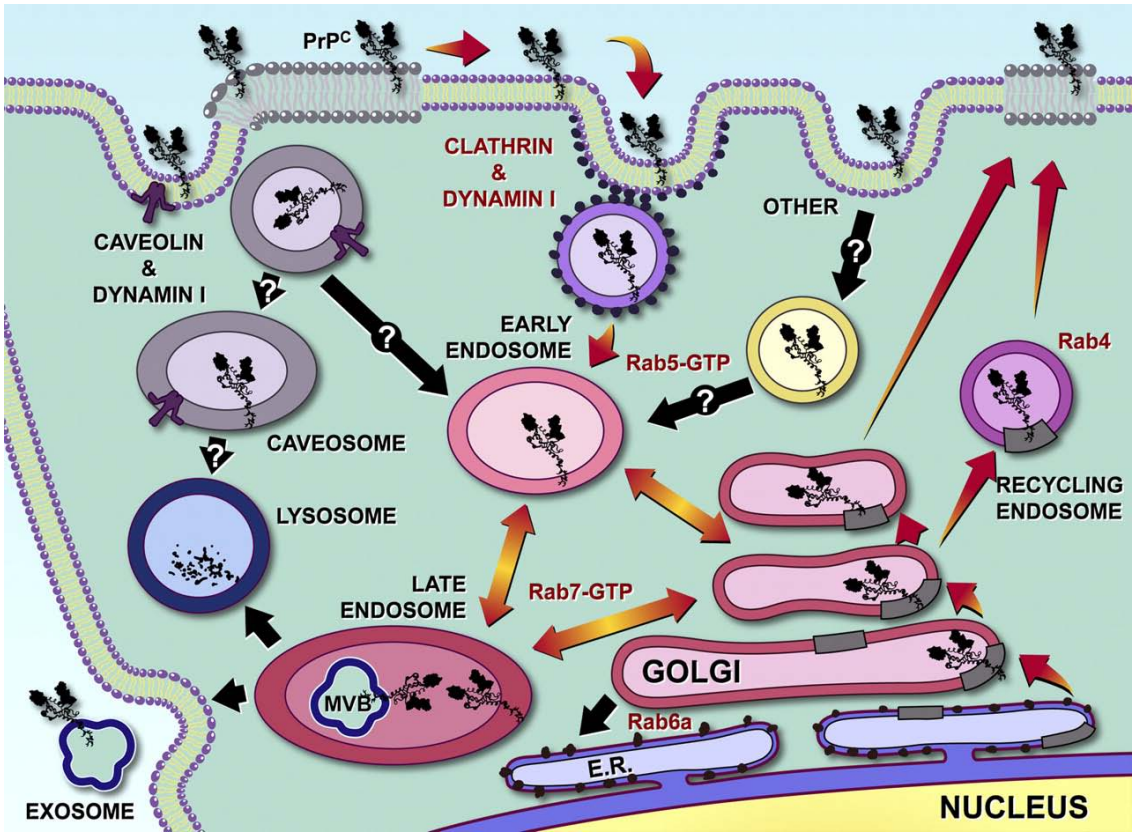

Figure 1.2 Endocytosis and subcellular localisation of PrP^{C}. After its synthesis in the ER and transport to the membrane through the Golgi, PrP^{C} is internalized. Several pathways may be involved in PrP^{C} endocytosis that may vary between cell types (Fivaz *et al.*, 2002). Clathrin-dependent endocytosis requires translocation of PrP^{C} to non-raft regions before internalisation. Caveolin dependent and non-clathrin non-caveolae endocytosis were also suggested. After internalisation PrP^{C} transits through endosomes and lysosomes. PrP^{C} in late endosomes or MVBs could be secreted as exosomes. Reproduced from the Physiol. Rev., Linden R. *et al.*, 2008, Vol 88, pp 673-728 (Linden *et al.*, 2008).

1.3 Pathogenesis of prion diseases

Acquired forms of TSE are characterized by long incubation times during which prions, invisible to the host immune defences (Kasper *et al.*, 1982), travel from the peripheral sites of infection to sites of replication in the lymphoreticular system (LRS) and ultimately to the central nervous system (CNS). A thorough understanding of early events in prion pathogenesis in the LRS is of great interest, since it opens the possibility for therapeutic intervention and early diagnosis before clinical symptoms are manifest.

1.3.1 The immune system in prion diseases

The involvement of lymphoid organs in prion pathogenesis has been known for a long time. In most prion diseases, including variant CJD (Hill *et al.*, 1999; Bruce *et al.*, 2001), natural scrapie (Hadlow *et al.*, 1982; van Keulen *et al.*, 1996) and CWD (Sigurdson *et al.*, 2002), prions are detected in the LRS where they accumulate and replicate before they reach the CNS (Eklund *et al.*, 1967; Fraser and Dickinson, 1970). Still, the importance of the lymphoid route in prion pathogenesis greatly varies among animal species and seems to be strain-specific (Aguzzi and Heikenwalder, 2005). For example, PrP^{Sc} was detected in the spleens of all vCJD cases, but only in 30 % of sporadic CJD cases (Glatzel *et al.*, 2003) and even less in BSE (Somerville *et al.*, 1997).

Even though rodents are broadly used to characterise the prion colonisation of different lymphoid organs and the CNS following different routes of inoculation, it should be noted that most natural prion diseases occur in ruminants. Differences between the distribution and dissemination of prions may be relevant. Experimental limitations when working with natural cases, however, renders mouse models a necessary option. The spleen and lymph nodes are the first sites of prion replication after peritoneal, cutaneous or intravenous inoculation, while after oral inoculation prions accumulate first in Peyer's patches of the gut-associated lymphoid tissue (Eklund *et al.*, 1967; Fraser and Dickinson, 1970; Kimberlin and Walker, 1979; Kimberlin and

Walker, 1989a; Kimberlin and Walker, 1989b; Bueler *et al.*, 1993). In particular, disease-specific deposits of PrP are detected in the germinal centres of lymphoid organs in vCJD and scrapie cases associated to follicular dendritic cells (van Keulen *et al.*, 1996; Hill *et al.*, 1999). Only after the establishment of infectivity in the LRS are prions detectable in the CNS. Sympathetic nerves which innervate lymphoid organs and parasympathetic nerves are thought to be main sites for the entrance of prions from the LRS to the brain (Kimberlin and Walker, 1980; McBride and Beekes, 1999; Glatzel *et al.*, 2001) (**Figure 1.3**). That this early accumulation in the LRS is essential and precedes neuroinvasion has been demonstrated by targeted interventions of the immune system where the susceptibility of the host to prions is greatly altered. Disease is significantly delayed in mice with impaired immune system, e.g. SCID, RAG, and μMT after peripheral prion inoculation (Klein *et al.*, 1997). Similar effects were observed after treatments aimed to stimulate or inhibit the immune system (Outram *et al.*, 1974; Dickinson *et al.*, 1978; Mabbott *et al.*, 2000). Susceptibility to oral infection was also shown to depend on the number of Peyer's patches present in the ileum (Outram *et al.*, 1974). Likewise, splenectomy resulted in prolonged incubation times and delayed the infection of the spinal cord (Kimberlin and Walker, 1989b).

Following oral inoculation, a natural route for prion transmission in acquired TSE forms, prions first replicate and colonise the LRS, a process that is critical for the manifestation of prion disease. The identification of the cell types and mechanisms involved in the uptake, dissemination, accumulation and replication of prions in the LRS is essential to identify potential targets for therapy. Early research to address the cellular distribution of prions in the LRS showed that both, haematopoietic and stromal compartments are involved in the spread and replication of prions. Using cell separation techniques, based on density gradient centrifugation, high prion titres were found to be associated to low density cells like macrophages, myeloblasts and lymphoblast (Lavelle *et al.*, 1972; Kuroda *et al.*, 1983). A critical role of the stromal compartment was inferred from

early experiments, where ten-fold higher infectious titres were detected in the stroma as compared to the pulp fraction of the spleen (Clarke and Kimberlin, 1984). In addition, sublethal whole body γ-irradiation of mice before or after inoculation with prions, which eliminates actively dividing haematopoietic cells, had no effect on the disease incubation time for the ME7 strain (Fraser and Farquhar, 1987). The contribution of macrophages, B cells, dendritic cells (DC) and follicular dendritic cells (FDC) in prion dissemination and replication are discussed in the next sections.

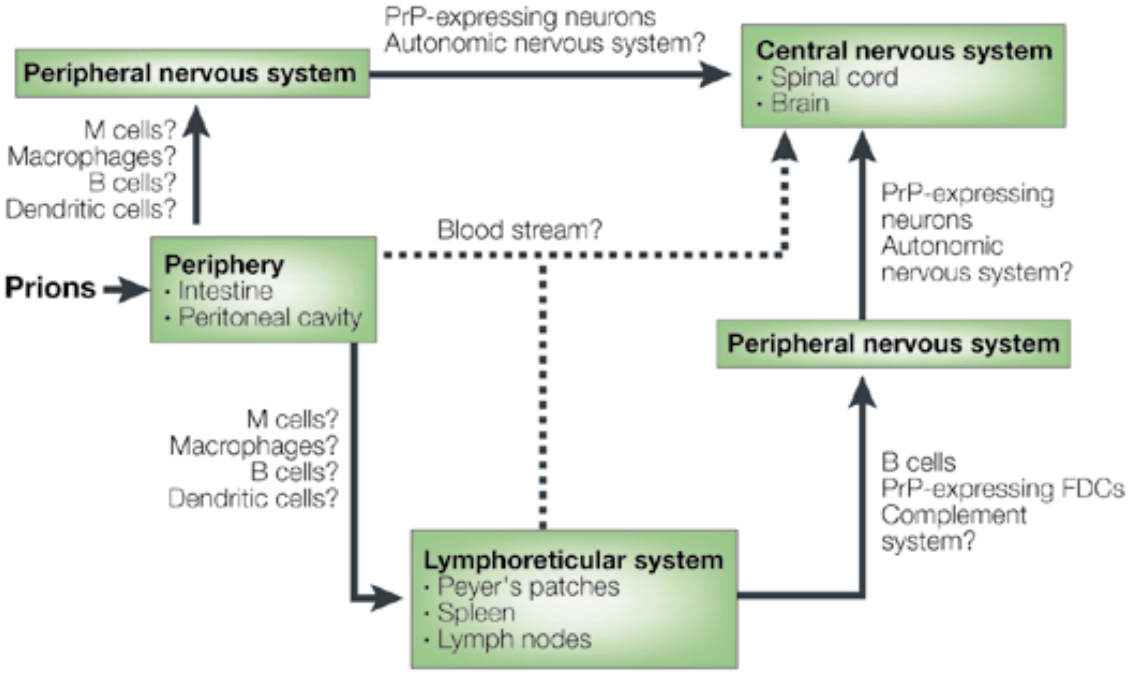

Figure 1.3 Peripheral prion pathogenesis. Following oral infection, prions accumulate in lymphoid organs, like the spleen, lymph nodes and Peyer's patches. Macrophages, lymphocytes and DCs are potential candidates for the transport of prions to the peripheral nervous system. From the sites of infection prions travel to the lymphoid organs and to the peripheral nervous system, alternatively, direct invasion of the CNS might occur after peripheral infection. Replication of prions in the lymphoid organs requires FDCs and B cells. Prions reach the brain via sympathetic and parasympathetic nerves where neuronal damage occurs. Reproduced from the Nat. Rev. Mol. Cell Biol., Aguzzi A. *et al.*, 2001, Vol 2, pp 118-126 (Aguzzi *et al.*, 2001).

1.3.2 Peripheral replication of prions

Although pathology of prion disease is confined in the central nervous system (CNS), lymphoid organs, particularly the spleen and lymph nodes, accumulate infectivity and PrP^{Sc} long before they are detectable in the CNS (Eklund *et al.*, 1967; Kimberlin and Walker, 1989b). The reduced susceptibility of immuno-deficient mice to scrapie after peripheral but not intracerebral inoculation, illustrates the importance of prion replication in the LRS for neuroinvasion. Mice with severe combined immunodeficiency (SCID) which lack lymphocytes and mature FDCs were in general resistant to peripheral, inoculation (O'Rourke *et al.*, 1994). Importantly, susceptibility and accumulation of infectivity in the spleen of SCID mice was restored by reconstitution with immuno-competent cells (Fraser *et al.*, 1996). Several mouse models helped to identify the cell types involved in prion replication and neuroinvasion, i.e. immuno-deficient mice, knockout mice lacking specific components of the immune system and chimeric mice where PrP expression was restricted to the stroma or haematopoietic compartment.

That T cells are dispensable for prion pathogenesis was first inferred from early studies where incubation times in nude or thymectomised mice were unchanged when compared to *wild-type* (*wt*) mice (Mohri *et al.*, 1987). Supporting this initial observation, T cell-deficient mice (e.g. $CD4^{-/-}$, $CD8^{-/-}$) were as susceptible to prion disease as *wt* mice (Klein *et al.*, 1997) and T cells over-expressing PrP failed to replicate prions in the spleen of $Prnp^{-/-}$ mice (Raeber *et al.*, 1999b), excluding them as sites for prion replication. Still, T cells were shown to accumulate infectivity (Raeber *et al.*, 1999a) and thus may contribute to the dissemination of the infectious agent in the LRS.

B cells, in contrast, play a dominant role in neuroinvasion. B cell-deficient mice (e.g. RAG, μMT) do not succumb to prion disease after intraperitoneal (i.p.) inoculation with high doses of RML (Klein *et al.*, 1997) and susceptibility to scrapie was restored by adoptive transfer with foetal liver cells (FLC) from $Prnp^{+/+}$ or $Prnp^{-/-}$ mice, implying that

B cells do not support prion replication, but may instead play an indirect role by supporting prion-replicating cells. Interestingly, PrP^{Sc} was detected in reconstituted mice associated with FDCs (Klein *et al.*, 1998). While prions are replicated in the spleen of transgenic mice where PrP expression was restricted to the LRS, no infectivity was detected in spleens of mice when PrP expression was targeted to B cells, suggesting that B cells alone do not suffice to support prion replication, or alternatively, that transport of prions to B cells may be PrP dependent (Raeber *et al.*, 2001; Montrasio *et al.*, 2001). Since B cells support the differentiation and maintenance of FDCs, the role of FDCs in disease pathogenesis came under scrutiny.

The role of follicular dendritic cells

Grafting of PrP-deficient B cells restored susceptibility to scrapie in SCID, RAG and μMT immunodeficient mice (Klein *et al.*, 1998), which excludes B cells as main replication sites. Early evidence for the role of radiation-resistant long-lived stroma cells in prion pathogenesis came from studies that demonstrated that sublethal γ-irradiation of mice before or after peripheral inoculation with ME7 prions failed to prolong incubation times (Fraser and Farquhar, 1987). Likely candidates for prion replication, known to express high levels of PrP^{C} are FDCs. Indeed, abnormal deposits of PrP were detected in association with FDCs membranes following experimental or natural TSE infection (Kitamoto *et al.*, 1991; Hill *et al.*, 1999; Jeffrey *et al.*, 2000).

FDCs are stroma cells in the germinal centres of lymphoid organs with long dendritic processes that form intricate membrane networks and are intimately associated with B cells. FDCs are specialized cells that capture and retain naïve antigens on their surfaces for long periods of time for B cell recognition (Kosco *et al.*, 1992). The differentiation and maturation of FDCs and the micro-architecture of lymphoid organs depend on cytokines such as tumour necrosis factor (TNF) α and lymphotoxins (LT) that are secreted by B cells. B cell-deficient mice like SCID, RAG and μMT mice, devoid of

functional FDCs, are resistant to prion infection, which suggests a critical role of B cells in FDC maintenance. Indeed, reconstitution of these mice with replication-deficient stem cells restored FDC maturation and susceptibility to scrapie (Mabbott and Bruce, 2002; Aguzzi and Heikenwalder, 2006).

To differentiate between the role of FDC and B cells in prion pathogenesis, a series of seminal studies aimed to disrupt the TNF and LT signalling pathways were performed. The temporary depletion of FDCs by treatment with lymphotoxin-β-receptor and immunoglobulin fusion protein (LTβR-Ig) abolished prion infectivity in the spleen of mice and extended incubation periods significantly as reported in two independent studies using ME7 and RML prion strains (Mabbott *et al.*, 2000; Montrasio *et al.*, 2000). Similarly, knockout mice with deficient LT pathways (e.g. $LT\alpha^{-/-}$, $LT\beta^{-/-}$ and $LT\beta R^{-/-}$ mice) which lack FDCs, but have functional lymphocytes, provided further evidence of a dominant role of FDCs in prion replication (Prinz *et al.*, 2002). However, mice with disruptions in TNF signalling (e.g. $TNFR1^{-/-}$) were devoid of FDCs, but almost fully susceptible to prions and accumulated high prion titres in lymph nodes (Prinz *et al.*, 2002). Furthermore, high prion titres were detected in lymph nodes of $Prnp^{-/-}$ mice reconstituted with $TNFR1^{-/-}$ FLCs, suggesting that other cell types of haematopoietic origin might also be involved in prion replication alongside stromal FDCs (Prinz *et al.*, 2002; Heikenwalder *et al.*, 2004b). Importantly, targeting of LT and TNF signalling pathways also severely affects the micro-architecture of the lymphoid organs with unknown consequences on prion propagation (Heikenwalder *et al.*, 2004b). Effects of FDC abrogation were more pronounced in LT deficient than in TNF deficient mice. Of note, the ablation of the LT pathways also affected other cell types like DCs in the spleen (Wu *et al.*, 1999) and marginal zone macrophages (Heikenwalder *et al.*, 2004b).

To avoid pleiotropic effects on cells other than the intended targets in knockout and immunodeficient mice alternative approaches using PrP-chimeric mice were pursued. Reconstitution of γ-irradiated *wt* or $Prnp^{-/-}$ mice with stem cells of $Prnp^{-/-}$ or *wt* mice

permitted to study chimeric mice where PrP expression was restricted to the stroma or the haematopoietic compartment, respectively (Mabbott and Bruce, 2001). Studies with the prion strain ME7 showed that splenic prion replication occurred only when PrP was expressed in the stromal compartment. No infectivity, however was detected when PrP expression was restricted to the haematopoietic compartment, providing further evidence for the involvement of FDCs in prion replication (Brown *et al.*, 1999; Mohan *et al.*, 2005). However, in similar studies using the RML strain, prions were replicated in both the haematopoietic and the stromal compartment provided PrP was expressed (Blattler *et al.*, 1997). Furthermore, at low doses of RML both PrP-expressing haematopoietic and stromal cells were required for efficient replication of prions (Kaeser *et al.*, 2001). Strain-dependent effects might explain the discrepancies between the ME7 and RML as different strains might favour different routes of neuroinvasion, e.g. LT-deficient mice were susceptible to Fukuoka-1 (mouse adapted CJD strain) challenge (Manuelidis *et al.*, 2000).

In summary, these studies clearly show the dominant role of FDCs in the replication and accumulation of prions (Brown *et al.*, 1999; Mabbott *et al.*, 2000; Montrasio *et al.*, 2000), but also present evidence of other undefined cell types that may maintain prion replication in the absence of FDCs (Blattler *et al.*, 1997; Kaeser *et al.*, 2001; Prinz *et al.*, 2002).

Other cell candidates for prion replication

Macrophages were suggested as alternative sites for prion replication and indeed abnormal PrP co-localised with macrophage markers in lymph nodes of TNFR1$^{-/-}$ and TNFα$^{-/-}$ mice (Prinz *et al.*, 2002). Interestingly, the localisation of macrophage subsets to the marginal zone in lymph nodes was severely disrupted in LTβ$^{-/-}$ mice (refractory to scrapie), but not in prion-susceptible TNFR1$^{-/-}$ mice (Heikenwalder *et al.*, 2004b). Disease-specific PrP was detected intracellularly in tingible body macrophages (TMB) of

germinal centres (Jeffrey *et al.*, 2000) and in CD68 macrophages in Peyer's patches on natural scrapie (Andreoletti *et al.*, 2000). However, a direct evidence for the involvement of macrophages in prion replication is lacking.

In a recent study with granulomas, a common form of chronic inflammation, Heikenwalder *et al.* showed that prions replicate in granulomas despite the lack FDCs. Replication was restricted to radiation-resistant stromal cells distinct from FDCs in a lymphotoxin-dependent manner. Fibroblastic reticular cells (FRC) and mesenchymal cells were identified as likely candidates of prion replication in granuloma-bearing mice (Heikenwalder *et al.*, 2008). Fibroblast cell lines have been shown to replicate prions *in vitro* (Vorberg *et al.*, 2004; Mahal *et al.*, 2007). High PrP^{C} expression was also detected in splenic capsule and trabeculae, probably from fibroblasts, the predominant cell type (Lotscher *et al.*, 2003).

Complement system

The accumulation of infectivity and PrP^{Sc} in lymphoid organs is a hallmark of most prion diseases. Deposits of disease-associated PrP are detected in germinal centres associated to FDCs, possibly in association with immune complexes (Jeffrey *et al.*, 2000). FDCs are specialized antigen presenting cells that capture and retain unprocessed antigens for their presentation to B cells (Kosco-Vilbois *et al.*, 1993). Antigens opsonised by antibody and/or complement molecules (e.g. C1q, C3) bind to FDC membranes via complement receptors (e.g. CD21/CD35) or Fc receptors (FcR) (Mabbott, 2004). The ability of FDCs to retain naïve antigens for long periods of time is exploited by many viruses like HIV-1 that accumulate on FDC for months to years, evading degradation (Smith *et al.*, 2001). The involvement of the complement system in prion accumulation was demonstrated in studies that targeted various components of the complement system. Depletion of C1q, C3 or the receptor CD21/CD35, but not FcR, prolonged incubation times and impaired prion accumulation in spleen (Klein *et*

al., 2001; Mabbott *et al.*, 2001; Zabel *et al.*, 2007). Binding of antibodies and/or complement factors target antigens not only to FDCs but also to other cell types expressing CD21/CD35 such as B cells, dendritic cells and macrophages. C1q was shown to participate in PrP^{Sc} endocytosis by DCs (Flores-Langarica *et al.*, 2009). Adoptive transfer experiments where CD21/CD35 expression was restricted to stromal or haematopoietic cells demonstrated that its expression in both compartments is required for efficient prion propagation although longer incubation times were observed when CD21/35 expression was restricted to the stromal compartment (Zabel *et al.*, 2007).

1.3.3 Transport of prions to the LRS and the CNS

Following peripheral inoculation, prions are transported to lymphoid organs where they replicate and accumulate long before they are detected in the brain (Eklund *et al.*, 1967). While most research focused on the identification of cell types that support prion replication in the LRS, the molecular mechanisms that lead to prion dissemination remain largely unknown. Circulating haematopoietic cells like lymphocytes, macrophages and DCs are plausible candidates for the transport of prions from initial sites of infection to their replication sites. The molecular link of prion dissemination from immobile FDCs, widely recognized as the major sites of prion replication (Mabbott and Bruce, 2002) to the brain via peripheral nerves remains unclear.

Upon oral challenge, prions are detected in the gut-associated lymphoid tissue, mainly in Peyer's patches, before they are found in lymph nodes and spleen (Kimberlin and Walker, 1989a). Transport of prions across the intestinal epithelium is thought to be mediated by microfold (M) cells, specialised epithelial cells that sample and deliver antigens from the gut lumen to immune cells in Peyer's patches (Heppner *et al.*, 2001). After crossing the epithelium, lymphocytes, macrophages and DCs could be involved in the transport of prions to their sites of replication in Peyer's patches and mediate the

transport to other organs via the lymphatics or the blood to the spleen (Huang and MacPherson, 2004; Defaweux *et al.*, 2005).

Lymphocytes

Targeted defects in T cell subsets did not affect incubation times indicating that T cells are dispensable for lymphoinvasion (Klein *et al.*, 1997; Raeber *et al.*, 1999b). The prevention of clinical disease in B cell-deficient mice after i.p. inoculation with prions highlights the critical role of B cells in prion propagation (Klein *et al.*, 1997; Klein *et al.*, 1998). It was suggested that B cells play an indirect role in the disease process by supporting the maturation of stromal cells by LT signalling. While B-cell deficient mice were entirely resistant to peripheral inoculation with prions, FDC-deficient mice were only partially resistant (Heikenwalder *et al.*, 2004b). However, since splenic B cells and T cells isolated from scrapie infected mice were infectious both could contribute to prion dissemination within the lymphoid organs (Raeber *et al.*, 1999a). Due to their close contact to FDCs circulating B cells were suggested to constitute the link between infected FDCs and nerve endings. However depletion of germinal centre B cells by interference of CD40 signalling did not affect pathogenesis (Heikenwalder *et al.*, 2007).

Macrophages and dendritic cells

Because of their migratory properties and their role as antigen presenting cells, macrophages and DCs were suggested as candidates for the dissemination of prions. Both, enriched fractions of macrophages (Kuroda *et al.*, 1983; Carp *et al.*, 1994) and highly purified DCs are infectious and retain more infectivity than lymphocytes (Aucouturier *et al.*, 2001). The rapid uptake and degradation of PrP^{Sc} was demonstrated *in vitro* for DCs and macrophages (Rybner-Barnier *et al.*, 2006). In Peyer's patches PrP^{Sc} is first found in $CD68^{+}$ cells, i.e. macrophages and some DCs, before it was detectable on FDCs (Andreoletti *et al.*, 2000; Huang and MacPherson, 2004). Abnormal PrP deposits were also detected in tingible body macrophages of germinal centres (Jeffrey

et al., 2000). Macrophages might contribute to prion propagation (Prinz *et al.*, 2002), but might also be involved in the clearance of prions as suggested by *in vitro* experiments that showed a reduction of infectivity in the presence of macrophages (Carp and Callahan, 1982; Rubenstein *et al.*, 1984; Beringue *et al.*, 2000). A series of *in-vivo* treatments known to interfere with the normal macrophage status failed to affect disease progression (reviewed in Beringue *et al.*, 2002). The activation of Toll-like receptors (innate immune receptors) has a protective effect to prion diseases (Sethi *et al.*, 2002). Treatment with clodronate, known to deplete macrophages *in vivo* resulted in a significant increase of PrP^{Sc} in the spleen (Beringue *et al.*, 2000) and Peyer's patches (Maignien *et al.*, 2005) at early stages, suggesting a protective role of macrophages. This treatment, however, also affects FDCs and B cells and could therefore have an impact on PrP^{Sc} levels (Beringue *et al.*, 2000).

DCs are migratory cells involved in antigen sampling and presentation to T cells in the lymphoid organs. Contrary to macrophages, some subsets of DCs have been shown to retain native antigen for long periods of time, making them ideal candidates for a role in prion dissemination (Banchereau *et al.*, 2000). Indeed, DCs, but not lymphocytes, isolated from lymph by thoracic duct cannulation acquired PrP^{Sc} following oral inoculation, yet no infectivity was detected in these cells (Huang *et al.*, 2002). The close contact between DCs and nerve endings in T cell areas of lymphoid organs suggests a role of DCs in neuroinvasion, although intervention studies to verify this hypothesis are pending. Intravenous inoculation of infectious and viable DCs restored prion susceptibility of Rag-$1^{-/-}$ mice, suggesting the DCs might suffice to propagate prions from the periphery to the CNS (Aucouturier *et al.*, 2001). These results however, were not confirmed by other experiments (Rybner-Barnier *et al.*, 2006; Raymond and Mabbott, 2007). Differences in the lymphoid microarchitecture between different mouse models that result in a higher innervation of Rag-$1^{-/-}$ mice as compared to TNFR$1^{-/-}$ may explain differences in the transfer rates of prions (Raymond and Mabbott,

2007). The role of DCs in prion dissemination was investigated in several depletion studies. However, the rapid replenishment of DCs from precursors was not well controlled in these studies, and therefore the conclusions are dubious. While disruption of lymphoid DCs ($DEC205^+$ $CD11c^+$) did not affect disease onset following intraperitoneal or oral inoculation (Oldstone *et al.*, 2002), longer incubation times were observed in mice defective for lymphoid DCs ($CD8^+$ $CD11c^+$) after i.p., but not oral inoculation (Sethi *et al.*, 2007). Temporal depletion of migratory DCs delayed disease onset and resulted in reduced infectious titres in Peyer's patches, mesenteric lymph nodes (MLN) and the spleen after oral inoculation (Raymond *et al.*, 2007). In a similar study reduced levels of PrP^{Sc} were found in the spleen and brain, and incubation times were prolonged as compared to controls following i.p., but not oral inoculation (Cordier-Dirikoc and Chabry, 2008). The disruption of DC migration by targeted disrupton of chemokine CCL19/CCL21 release, required for homing to T cell zones did not affect prion pathogenesis (Levavasseur *et al.*, 2007). In summary, to date no clear evidence for a role of DCs in prion dissemination has been provided.

1.3.4 Neuroinvasion

From their sites of replication in the LRS, prions are thought to be transported to the CNS via the autonomic nervous system. Abnormal PrP was detected along the spinal cord and peripheral nerves (Kimberlin and Walker, 1980; McBride and Beekes, 1999). In particular, prions seem to gain access to the nervous system via sympathetic nerves that innervate the lymphoid organs as demonstrated by the fact that incubation times were shortened by impairment of the sympathetic nervous system and prolonged by sympathetic hyperinnervation (Glatzel *et al.*, 2001). Alternative routes for neuroinvasion through parasympathetic nerves (e.g. vagus nerve) have been proposed (Baldauf *et al.*, 1997; McBride *et al.*, 2001). Neuroinvasion is accelerated in mouse models where the distance between FDCs and nerve endings is reduced (Prinz *et al.*,

2003), but the mechanisms by which prions gain access to peripheral nerves are not well understood. Nerve endings are rarely found in B cell follicles, where FDCs are located, but instead in T cell areas. Interactions between DCs and nerve fibres were observed by confocal microscopy in scrapie infected lymphoid organs (Dorban *et al.*, 2007).

Irrespective of the routes by which prions reach the CNS, the expression of PrP^C is required for neuroinvasion. The requisite of PrP^C expression for neuroinvasion and prion dissemination is evident from several experiment paradigms. Adoptive transfer of bone marrow from *wt* mice to *Prnp*$^{-/-}$ mice reconstituted the capability of the spleen to accumulate prions but not neuroinvasion (Blattler *et al.*, 1997; Kaeser *et al.*, 2001). Furthermore, no prion pathology was observed in *Prnp*$^{+/+}$ neurografts introduced into *Prnp*$^{-/-}$ mice after peripheral infection (Blattler *et al.*, 1997), but after intracerebral inoculation (Brandner *et al.*, 1996a). Taken together these data indicate that PrP^C expression is crucial for prion transport to the CNS and within the CNS.

1.4 Mechanisms for the lateral spread of prions

The cellular mechanisms underlying the transfer of prions between cells *in vivo* are unknown and may involve close contacts between membranes (Baron *et al.*, 2006). Several routes for transmission of prions have been proposed, including direct cell-to-cell contact (Kanu *et al.*, 2002), transmission of prions via membrane nanotubes (Gousset *et al.*, 2009) and the release of prions via exosomes (Fevrier *et al.*, 2004) (**figure 1.4**).

The detection of newly infected cells in co-cultures of infected and uninfected cells showed that prions are preferentially transferred to neighbouring cells, although long-range intercellular transfer cannot be excluded (Paquet *et al.*, 2007). The transfer of infectivity by direct cell-to-cell contact was shown *in vitro* by co-culture of fixed prion-infected cells with uninfected cells (Kanu *et al.*, 2002). The mechanisms involved in the

cell-to-cell transfer of prions are unknown, but may involve panning of PrP^{Sc} as documented for GPI-proteins (Medof *et al.*, 1996; Liu *et al.*, 2002), or *trans* conversion of PrP^{C} into PrP^{Sc} by PrP^{Sc} on the adjacent cell (Kanu *et al.*, 2002; Hooper, 2002). Although a transfer of prions between fixed prion-infected cells and uninfected cells was observed, the efficiency of this transfer was much higher in viable infected cells, implying that active biological processes may be involved in the transfer of infectivity (Kanu *et al.*, 2002). Although co-cultures of infected and uninfected cells that are separated by a porous membrane are frequently used to address prion release into the extracellular medium the possibility of a focal release of infectivity at sites of close juxtaposition between cells cannot be excluded (Ashok and Hegde, 2006). Several neuronal cell lines secrete infectivity into the culture medium and conditioned media from prion-infected cells can be used to initiate infection (Schatzl *et al.*, 1997; Baron *et al.*, 2006). Membranous channels, known as tunnelling nanotubes (TNT) that connect different cell types were recently suggested as a route for the intercellular transfer of prions where fluorescent-tagged PrP was shown to travel along nanotubes between cells (Gousset *et al.*, 2009).

The role of exosomes in the spread of prions

During endocytic trafficking proteins from the plasma membrane are internalized and recycled back to the membrane or sorted into late endosomes and lysosomes for degradation. Exosomes are small vesicles (30-100 nm) of endosomal origin that are formed by inward budding of the late endosome membrane into maturing multivesicular bodies (MVB). Mature MVBs either fuse with lysosomes to deliver their cargo for degradation, or fuse with the plasma membrane to release exosomes into the extracellular medium. Once released, exosomes could be endocytosed by neighbouring cells (Thery *et al.*, 2002). Endosomes, lysosomes and exosomes were shown to accumulate PrP^{Sc} (McKinley *et al.*, 1991; Arnold *et al.*, 1995; Fevrier *et al.*, 2004).

Secreted by a variety of cells including reticulocytes, mast cells, DCs, lymphocytes and macrophages, as well as a number of immortalized cell lines (Johnstone *et al.*, 1987; Stoorvogel *et al.*, 2002; Thery *et al.*, 2002; Couzin, 2005; van Niel *et al.*, 2006), exosomes could enable the transfer of prions between cells without the requirement of direct cell-to-cell contact (Vella *et al.*, 2008b). Exosomes are found in body fluids *in vivo* (Pisitkun *et al.*, 2004; Caby *et al.*, 2005; Knepper and Pisitkun, 2007; Vella *et al.*, 2008a) and in germinal centres, associated to FDCs (Denzer *et al.*, 2000). Similarly, extracellular deposits of disease-associated PrP were shown in proximity to FDC surfaces (Jeffrey *et al.*, 2000). Interestingly, exosomes on the surface of FDCs are not released by FDCs themselves but by other cell types, most likely B cells (Denzer *et al.*, 2000). However, no evidence for the presence of disease-specific PrP in exosomes attached to FDCs was found (McGovern and Jeffrey, 2007). *In vitro* studies showed that B cell-derived exosomes bind to extracellular matrix (ECM) proteins (collagen I and fibronectin) and activated fibroblasts (Clayton *et al.*, 2004).

Purified exosomes from infected cell lines are PrP^{Sc} positive and infectious (Fevrier *et al.*, 2004; Vella *et al.*, 2007; Alais *et al.*, 2008). Furthermore, transfer of infectivity was shown to occur between neuronal and non-neuronal cell lines (Vella *et al.*, 2007). Retroviruses including HIV-1 and murine leukaemia virus (MuLV) have been shown to use the endosomal route of cells to bud out of infected cells. Interestingly, retroviral infection strongly enhances the release of infectivity (Leblanc *et al.*, 2006). Despite several *in-vitro* studies that support the role of exosomes in the spread of infectivity, *in vivo* evidence is missing.

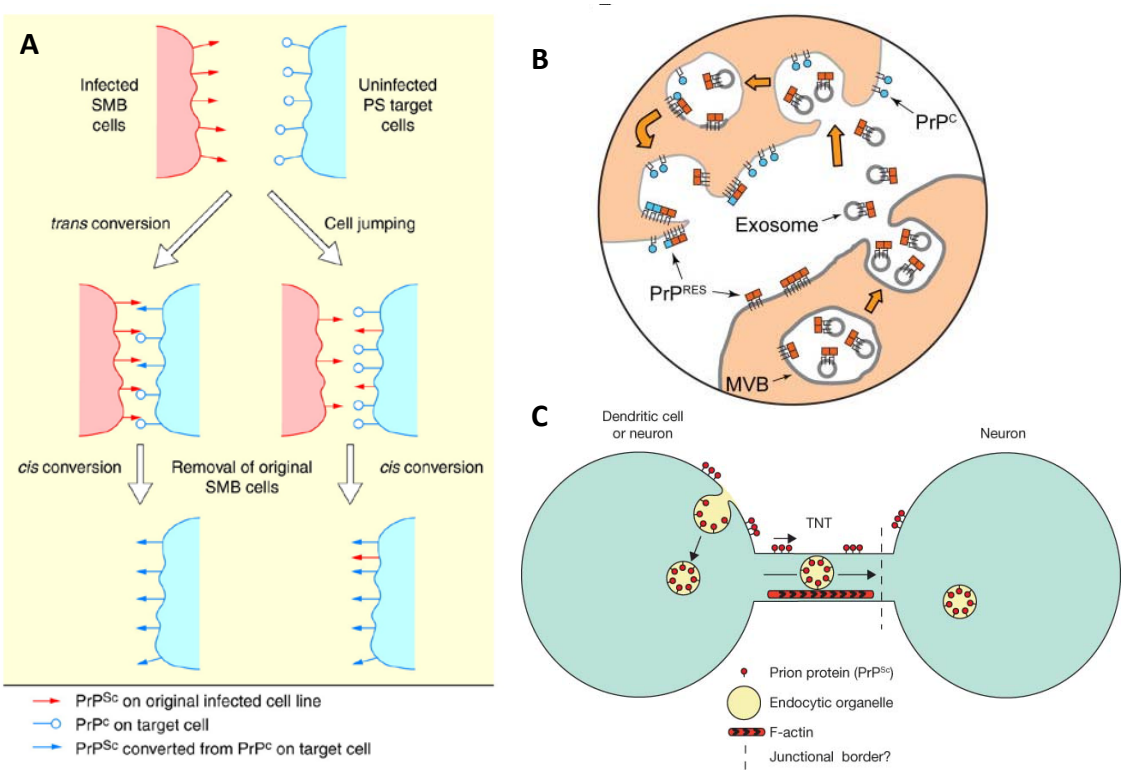

Figure 1.4 Mechanisms for the lateral spread of prions. (**A**) Two mechanisms for the transfer of infectivity by direct cell-to-cell contact were suggested. PrP^{Sc} on one membrane could promote the conversion of PrP^{C} on the adjacent membrane. Alternatively, as documented for GPI-anchored proteins, PrP^{Sc} could jump and be inserted into the contiguous membrane. (**B**) Exosomes, vesicles of endocytic origin, formed by invagination of the MVB membrane, are released into the extracellular medium by fusion of MVBs with the plasma membrane. Exosomes could be endocytosed by the neighbouring cell and deliver their cargo. (**C**) Nanotubes, membranous bridges between different cell types were suggested to mediate the transfer of PrP^{Sc} between cells by active vesicle transport. Reproduced from (**A**) Curr. Biol., Hooper N. M., 2002, Vol. 12, pp R248-R249 (Hooper, 2002) (**B**) Annu. Rev. Biochem., Caughey *et al.*, 2009, Vol. 78, pp 177-204 (Caughey *et al.*, 2009) (**C**) Nat. Cell. Biol., Gerdes H. H., 2009, Vol 11, pp 235-236 (Gerdes, 2009).

1.5 Aims of the thesis

To establish a standardised and statistically robust infectivity assay

A reliable determination of prion titres is fundamental to study prion diseases where differences in titres may be critical to assess the efficacy of therapeutic interventions. Where the size of experimental groups in bioassays is greatly restricted by ethical and economical factors, resulting in underpowered studies, *in-vitro* determination of prion titres may overcome these limitations by extending the experimental scope. We therefore aim to establish a standardised and statistically robust method for titre determination of tissue and cell homogenates.

To determine the kinetics of prion accumulation in splenic cell types

Studies with immuno-deficient and knockout mice showed that both haematopoietic and stromal cells play fundamental roles in prion pathogenesis (Blattler *et al.*, 1997; Kaeser *et al.*, 2001). Comprehensive studies to determine the infectious state of candidate cell types during early stages of pathogenesis have not been performed to date due to the prohibitively large number of animals required for *in-vivo* infectivity testing. By taking advantage of fast *in-vitro* titre determination (SCA) and high-capacity cell sorting we aim to establish a procedure to determine the infectious titres of various splenic cell types including B and T cells, DCs, the DC subset plasmacytoid DCs (pDC), macrophages and natural killer (NK) cells at early stages of prion pathogenesis.

To determine prion titres of stromal cell types

FDCs were shown to accumulate disease-specific PrP (Jeffrey *et al.*, 2000; Sigurdson *et al.*, 2002) and are considered prime candidates for prion replication in the LRS (Mabbott and Bruce, 2002). However, to date no study reported prion titres of FDCs. We therefore aim to establish a method to isolate FDCs by immuno-affinity separation

and to determine their infectious state. Evidence of prion replication in the absence of FDCs suggests that other stromal cells are replication-competent (Prinz *et al.*, 2002). For instance, mesenchymal or fibroblastic reticular cells were proposed to replicate prions in granulomas-bearing mice (Heikenwalder *et al.*, 2008) and several fibroblasts lines have been shown to replicate prions *in vitro* (Vorberg *et al.*, 2004). We therefore aim to establish splenic stromal cell culture models from scrapie-infected mice to confirm that stromal cell types are permissive to prions and to study prion propagation *ex vivo*.

To investigate the role of exosomes for the spread of prions

A potential role of exosomes for the intercellular transmission of prions was deducted from *in-vitro* studies with immortalised cell lines. In these studies secreted exosomes were purified from culture supernatants and were shown to be PrP^{Sc} positive and infectious (Fevrier *et al.*, 2004; Vella *et al.*, 2007; Alais *et al.*, 2008). Exosomes are found *in vivo* in body fluids (Pisitkun *et al.*, 2004; Caby *et al.*, 2005) and in germinal centres of lymphoid organs associated to FDCs (Denzer *et al.*, 2000), but their role in prion dissemination in the LRS remains unknown. Furthermore, all major immune cells including DCs, B cells, T cells and macrophages secrete exosomes (Thery *et al.*, 2002). We will therefore investigate whether infectious exosomes are secreted from splenic cells of scrapie infected mice *ex vivo.*

CHAPTER 2

MATERIALS AND METHODS

MATERIALS AND METHODS

2.1 Isolation of cell fractions from spleen tissue

2.1.1 Isolation of splenocytes

Splenocytes were isolated by enzymatic digestion from freshly dissected spleens. To maximise the release of non-haematopoietic stromal cells and other resident cells that are strongly attached to connective tissue, spleens were digested in successive cycles as described previously by Kosko *et al.* with minor modifications (Kosco *et al.*, 1992). Briefly, spleens were cut into small pieces and incubated at 37 °C with an enzyme cocktail, containing 2.5 mg/ml collagenase IV (Worthington Biochemical Corp., Lakewook, NJ), 0.05 % dispase 2 (Sigma-Aldrich, Dorset, UK) and 1 mg/ml DNase I (Roche Diagnostics Ltd, West Sussex, UK) in Iscove's Modified Dulbecco's Media (IMDM) (Invitrogen, Paisley, UK). After 15-20 min, partially digested tissue was gently dispersed with a serological pipette and released cells were transferred into a tube on ice. Fresh enzyme cocktail was added to the remaining tissue fragments and digested for another three cycles. Pooled cells were then passed through a 70 µm nylon mesh and pelleted at 300 x *g* for 10 min. To remove erythrocytes, splenocytes were resuspended in 10 ml erythrocyte lysis buffer [155 mM NH_4Cl, 10 mM $KHCO_3$, 0.1 mM Ethylene-diamine-tetra-acetic acid (EDTA), pH 7.0] and incubated at room temperature for no more than 1 min. After adding 40 ml IMDM medium to stop lysis, cells were pelleted at 300 x *g* for 10 min. Splenocytes were then layered onto Lympholyte M (Cedarlane Laboratories, Hornby, Ontario, Canada) gradients and centrifuged at 1500 x *g* for 20 min to remove dead cells and debris essentially as described by the manufacturer. Purified splenocytes were washed in IMDM supplemented with 10 % heat inactivated foetal calf serum (FCS), 100 U/ml Pen-strep, 2 mM L-glutamine and 50 µM 2-mercaptoethanol (complete IMDM) and centrifuged for 10 min at 800 x *g*.

Cells were resuspended in chilled MACS buffer [0.5 % bovine serum albumin (BSA) and 2 mM EDTA in phosphate-buffered saline (PBS)] and the number of splenocytes was determined using a Coulter counter Z2 (Beckman Coulter, High Wycombe, UK) at an upper threshold of 15 µm and a lower threshold of 5 µm.

2.1.2 Isolation of splenic cell types by magnetic-activated cell sorting

Specific cell populations were enriched from total splenocytes by sequential magnetic-activated cell sorting (MACS) using antibody-coated magnetic microbeads (Miltenyi Biotech Ltd, Surrey, UK) as depicted in **figure 2.1**. To block unwanted binding of antibodies to cells expressing Fc receptors (FcR), splenocytes were suspended at a concentration 2×10^8 cells/ml MACS buffer and incubated with 25 µl FcR blocking reagent (Miltenyi Biotech Ltd, Surrey, UK) per 10^8 cells. Cells were magnetically labelled, essentially as specified by the manufacturer (Miltenyi Biotech Ltd, Surrey, UK) using the following microbeads: CD11c for dendritic cells (DC), mPDCA-1 for plasmacytoid DCs (pDC), CD11b for myeloid cells, CD49b for natural killer (NK) cells and NK-T cells, CD19 for B cells and CD90 for T cells. Since CD11b antigens are expressed on both macrophages ($CD11c^-$ $CD11b^+$) and mDCs ($CD11c^+$ $CD11b^+$), we did two positive rounds of selection with CD11c microbeads before isolating $CD11b^+$ macrophages. Macrophages were purified by fluorescence-activated cell sorting (FACS) using a MoFlo cell sorter (Dako, Cambridgeshire, UK). Briefly, MACS-isolated $CD11b^+$ cells were incubated for 30 min on ice with FITC-conjugated anti-CD11c (clone HL3, 1:100) and PE-conjugated anti-CD11b (clone M1/70, 1:50) (BD Biosciences, Oxford, UK) and $CD11c^-$ $CD11b^+$ cells were sorted at a concentration of $5\text{-}10 \times 10^6$ cells per ml. Isolated cells were counted with a Coulter Counter (Beckman Coulter, High Wycombe, UK) and stored at -80 °C until further processing.

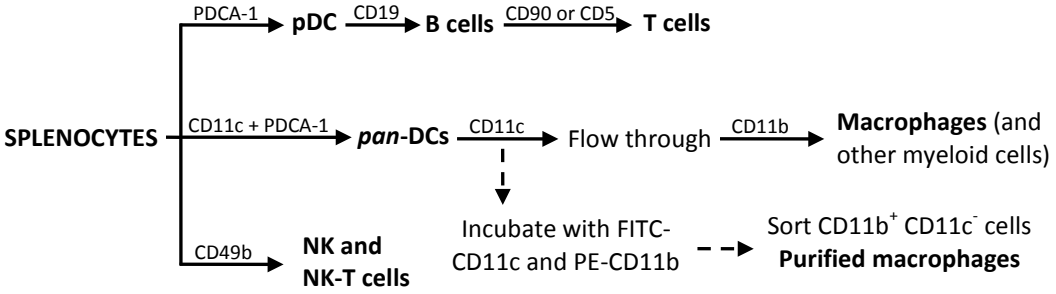

Figure 2.1 Standard isolation procedures of splenic cells by MACS. Splenocytes were released by repeated collagenase digestion, followed by removal of red blood cells and purification splenocytes on lympholyte gradients. Specific cell types were isolated by MACS using microbeads (Miltenyi Biotech Ltd, Surrey, UK) as indicated. Alternatively, macrophages were purified by FACS as $CD11c^-$ $CD11b^+$ cells.

Isolation of plasmacytoid dendritic cells and lymphocytes from blood

Whole blood was obtained from euthanized mice by cardiac puncture and collected in 4 mM EDTA used as anticoagulant. Blood samples were further diluted into MACS buffer, layered onto Lympholyte M and centrifuged for 20 min at 1500 x *g* at 22 °C. Cells from the interface were collected and erythrocytes removed as described before. After washing, blood cells were resuspended in MACS buffer and pDCs and lymphocytes were isolated by MACS as described above.

2.1.3 Isolation of follicular dendritic cell clusters

Follicular dendritic cell (FDC) clusters were separated by four successive sedimentations at unit gravity as previously described (Wekerle *et al.*, 1980; Tsunoda *et al.*, 1990). Before the enzymatic digestion of spleen tissue, the majority of lymphocytes were eliminated by flushing spleens repeatedly with IMDM 10 % FCS medium. The remaining tissue was minced and digested as described above. Pooled cells were pelleted at 200 x *g* for 5 min, resuspended in MACS buffer and subjected to 1 x *g* sedimentation in FCS for 20 min on ice. Cells from the serum layer were collected and

washed in MACS buffer. Pellets were resuspended in MACS buffer and layered onto FCS for three further sedimentation cycles (**figure 2.2**). To remove macrophages and fibroblasts, cell clusters were cultured for 30 min in tissue culture dishes at 37 °C and 5 % CO_2. Non-adherent FDC clusters were collected and counted in a Coulter counter at an upper threshold of 39 µm and a lower threshold of 19 µm.

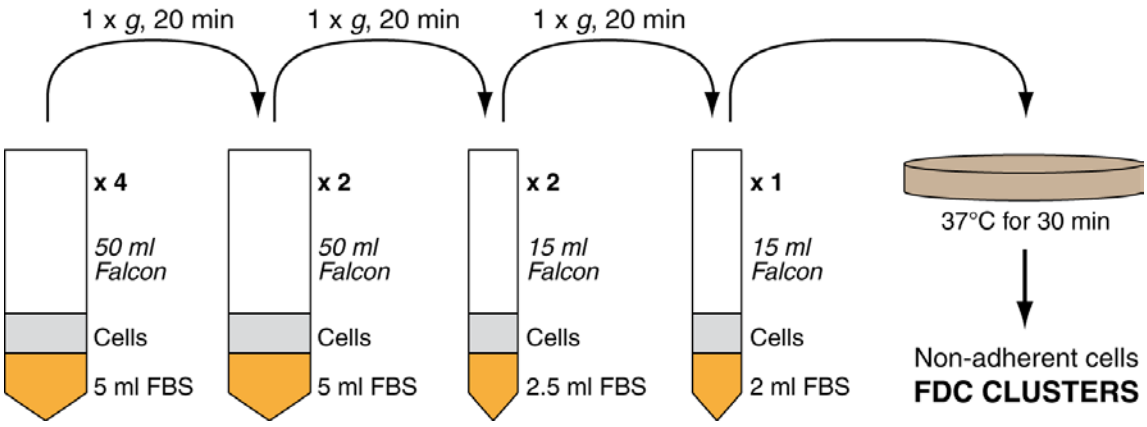

Figure 2.2 Purification of follicular dendritic cell clusters by a four step 1 x *g* sedimentation procedure. FDC/B cell clusters sediment at a faster rate than single cells and were recovered in the lower fraction of the gradients. Recovered cell clusters were incubated on plastic dishes for 30 min to allow adherence of macrophages, fibroblasts. Non-adherent cells containing mainly FDC clusters were collected.

2.2 Cell culture

All tissue culture work was performed in a class II or laminar flow tissue culture hood, using sterile techniques. All cell culture incubations were carried out at 37 °C in a humidified 5 % CO_2 atmosphere.

2.2.1 Short-term primary cultures of splenic cells

B cells, T cells and DCs were isolated by MACS and cultured at a concentration of 1-4 x 10^6 cells/ml in complete IMDM medium. To remove exosomes from serum, heat

inactivated FCS was spun at 100,000 x *g* for 2 h in an Optima XL-100K Beckman ultracentrifuge with a rotor SW70 before use. Freshly isolated splenic cells were stimulated with LPS (1 µg/ml, Sigma-Aldrich, Dorset, UK), IL-4 (10 ng/ml, AbD Serotec, Kidlington, UK) and GM-CSF (200 U/ml, gift from Dr Pichlmaier). Cells were cultured in complete IMDM medium at 37 °C and atmospheric CO_2 undergo rapid necrosis and were used as passive leakage controls. After 38 h in culture, supernatants from different cell types at various culture conditions were harvested for the isolation of exosomes. The viability of the cells was assessed using 7-Aminoactinomycin D (7-AAD) exclusion (BD Biosciences, Oxford, UK).

2.2.2 Long-term stroma cell cultures

Following enzymatic digestion of spleens, released cells were counted and separated by density gradient centrifugation. Two-layer Percoll (GE Healthcare, Buckinghamshire, UK) gradients were prepared by layering 4 ml of a 18 % Percoll solution (1.03 g/ml) over 6 ml of a 56 % Percoll (1.08 g/ml) diluted in 0.15 M NaCl. Aliquots of 500 µl containing 2 x 10^8 cells were loaded per gradient and centrifuged at 8500 x *g* (Beckman ultracentrifuge, rotor 70.1 Ti) for 40 min at 22 °C. Low density cells as indicated in **figure 2.3** were collected in complete IMDM medium and centrifuged at 800 x *g* to remove Percoll.

Cells were cultured at a concentration of 1-4 Mio/ml complete IMDM. After 24 h, non-adherent cells were removed and fresh medium was added to the cultures. Cells were passaged twice weekly.

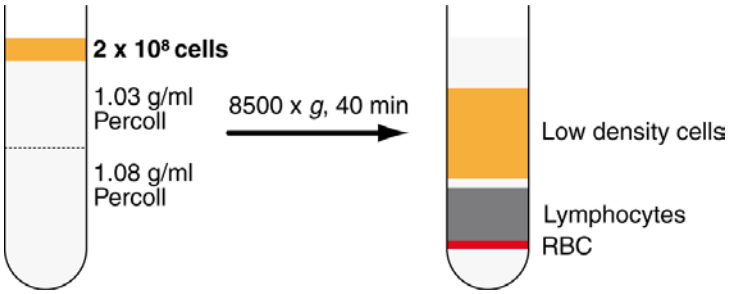

Figure 2.3 Separation of low density cells using a Percoll gradient. About 2 x 10^8 collagenase released splenic cells were loaded per gradient and spun at 8500 x *g* for 40 min at 22 °C with no brake. Lymphocytes and red blood cells (RBC) are readily separated accordingly to their buoyant densities.

2.2.3 Culture and maintenance of neuroblastoma N2a cells

Highly prion-susceptible neuroblastoma cells, subclone N2aPK1-2 cells were used for infectivity assays. Cells were cultured in OptiMEM (Invitrogen, Paisley, UK), supplemented with 10 % γ-irradiated FCS (Invitrogen, Paisley, UK) and 1 % Pen-step (Invitrogen, Paisley, UK) (OFCS). Since prolonged cell passages are known to affect prion susceptibility of cells (Klohn *et al.*, 2003), all experiments were performed with freshly thawed cells. PK1-2 cells were quickly thawed in a 37 °C water bath and pre-warmed gro*wt*h medium was added slowly at 5 min intervals. Cells were then centrifuged at 300 x *g* for 4 min, resuspended in 1 ml medium and transferred to a 10 cm tissue culture plate (VWR, West Sussex, UK). Gro*wt*h medium was regularly changed and cells were split 1:10 (1:8) into 15 cm plates (VWR, West Sussex, UK) every 3-4 days.

2.3 Isolation of exosome-enriched membrane fractions and analysis by electron microscopy

Exosomes were isolated by differential centrifugation as previously described (Johnstone *et al.*, 1987; Thery *et al.*, 1999; Wolfers *et al.*, 2001). Briefly, supernatants

from cell cultures of splenic cell types were retrieved after 38 h, sequentially centrifuged at 300 x *g* for 10 min and 5000 x *g* for 20 min and ultracentrifuged at 10,000 x *g* for 30 min and 100,000 x *g* for 2 h with a SW70 rotor (Beckman Coulter, High Wycombe, UK)as shown in **figure 2.4**. The pellet was resuspended in PBS and used immediately or stored at -70 °C until further use.

For analysis by electron microscopy 3 µl aliquots of 1:10 diluted resuspended pellets were adsorbed onto glow-discharged carbon-coated grids and negatively stained with 1 % uranyl acetate. Grids were examined by electron microscopy at the Bloomsbury Centre for Structural Biology (Birkbeck College, London, UK) by Dr Howard Tattum (MRC Prion Unit, London, UK). To determine the number of exosome-like membrane particles 20 random images taken at a magnification of x 10,000 were recorded per condition and the number of particles was counted in a blinded manner.

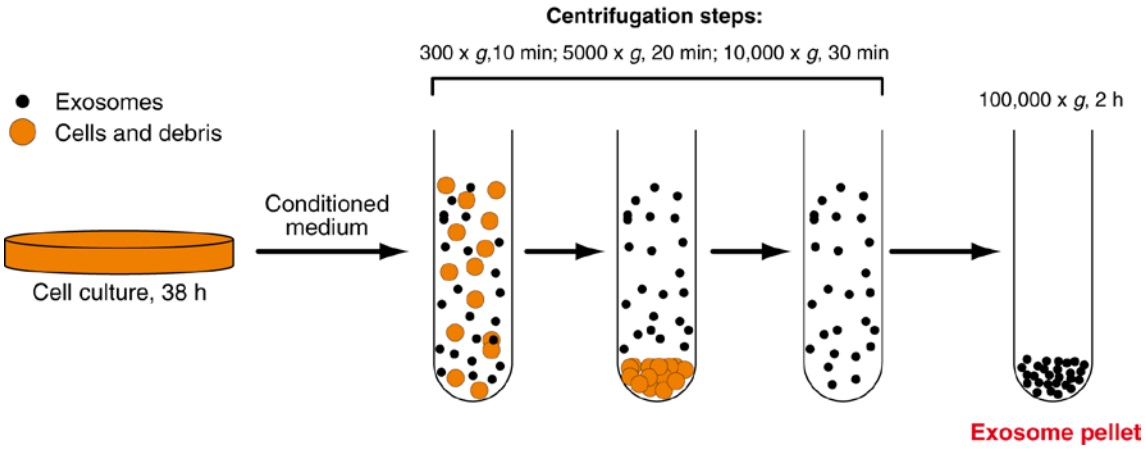

Figure 2.4 Isolation of exosomes from primary cultures of splenic cells. After 30 h culture of splenic cells, conditioned medium was collected and serially centrifuged to remove cell and debris. Exosomes were pelleted at 100,000 x *g* for 2 h. Adapted from Brain Res. Rev., Agnati *et al.*, 2010, Vol. 64, pp 137-159 (Agnati *et al.*, 2010).

2.4 Protein determination

Where cell counts could not be accurately determined (e.g. FDC clusters, stroma cells) infectious titres were expressed per µg protein. For this purpose, cell aliquots were spun at high speed and pellets stored at -70 °C. Pellets were resuspended in 100-200 µl lysis buffer (150 mM NaCl, 0.1 % Triton, 0.1 % sodium deoxycholate) for 15 min on ice. Total protein concentration was determined by Bio-Rad Bradford assay. Cell lysates were spun at high speed for 1 min and diluted 1:10 or 1:20 in PBS before loading 25 µl per well of a 96-well plate. Protein standards from 0 to 500 µg were prepared fresh from a BSA standard (Thermo Fischer Scientific, West Sussex, UK). BSA standard and samples were transferred in triplicates into plates before adding 200 µl of diluted dye reagent (Bio-Rad, Bath, UK) according to manufacturer instructions. Absorbance was measured at 595 nm on a Tecan plate reader (Sunrise, Reading, UK). Protein concentrations were determined in the linear range of standard dilution series.

2.5 *In vivo* depletion of plasmacytoid dendritic cells and RML inoculation

PDCs were depleted *in vivo* as previously described (Bailey-Bucktrout *et al.*, 2008). Four mice were injected i.p. with 250 µg of anti-mPDCA-1 antibody (Miltenyi Biotech Ltd, Surrey, UK) every 2-3 days for a total number of eight injections. Four control mice received the same amount of purified rat IgG_{2b} (eBioscience, Hatfield, UK) as isotype-matched control antibody. One day after the second injection of antibodies, mice were inoculated i.p. with a 1 % dilution of RML I6200 (see next section). Animals were culled at 19 dpi and spleens and mesenteric lymph nodes were collected for titre determination.

2.6 Infectivity measurements

2.6.1 Animals and scrapie inoculation

RML prion-infected brain homogenate (I6200) [10 % (w/v)] and normal CD1 brain homogenate (I8402) [10 % (w/v)] were prepared as previously described (Cronier *et al.*, 2008). After thawing, aliquots of RML or normal brain homogenates [10 % (w/v)] were ribolyzed or passed through needles with increasing gauge to break up any particulate matter before dilution into 1 % normal CD1 brain homogenate.

Six to eight week old female 129/Sv x C57BL/6 mice were purchased from Harlan Ltd., Oxfordshire, UK). *Prnp*$^{-/-}$ mice used here were derived from the original Zurich I mice (Bueler *et al.*, 1992) and crossed onto the FVB/N background for 10 generations (Isaacs *et al.*, 2008). Mice were inoculated intraperitoneally (i.p.) with 100 µl of 1 % RML or 1 % uninfected CD1 brain homogenate and culled at early stages of prion disease prior to the manifestation of neurological symptoms. Where prion titres were determined by bioassay, mice were inoculated intracerebrally (i.c.) with 30 µl inoculum and the incubation time until manifestation of neurological signs of scrapie was recorded. All mice were observed daily for indications of ill-health. All experimental procedures were conducted in compliance with Home Office regulation.

2.6.2 Preparation of samples for infectivity testing

Preparation of the RML standards

RML standards for infectivity assays were prepared by serial 10-fold dilutions (from 10^{-2} to 10^{-9}) of 10 % RML homogenate into 10 % normal CD1 brain and further diluted 1:10 in 1 % normal CD1 for tg20 inoculation or 1:1000 in OFCS for the infection of cells.

Preparation of tissue homogenates and cell homogenates

To determine infectious titres of tissue samples, spleens and mesenteric lymph nodes from scrapie-infected and control mice were minced and transferred into 2 ml microtubes (Sarstedt Ltd., Leicester, UK) containing zirconium beads. Ten percent homogenates (w/v) were prepared in PBS-buffered sucrose (0.32 M) in presence of 1× dilution of Protease Inhibitor Cocktail Set I (100×, Pierce, Leicestershire, UK) and 25-50 U benzonase (Novagen, Madison, WI) using a Ribolyser (Hybaid, Cambridge, UK) at maximum speed for two cycles of 45 s. Homogenates were cooled on ice between homogenisation rounds and before serial dilutions.

Aliquots of MACS-isolated splenic cells were ribolyzed at a concentration of typically 2×10^7 cells/ml complete medium, supplemented with protease inhibitors as described before. All homogenates were kept on ice until further processing. Where sonication was used to homogenise the cells, aliquots of MACS-isolated cells were transferred into 0.2 ml Thermo tubes (Thermo Fischer Scientific, West Sussex, UK) and placed beneath the sonication probe in ice water. Cells were homogenised in five cycles of 30 s at 30 % power using a Status 200 sonicator (Philip Harris Scientific, Hyde, UK). Neat homogenates were cooled on ice and serially diluted in OFCS or 1 % uninfected CD-1 brain for the determination of infectivity by *in-vitro* testing or the mouse bioassay, respectively. Dilutions were done in a way that the 10^{-1} dilution corresponded to 2×10^6 cell equivalent/ml, that is 6×10^5 cells in 300 µl per well of a 96-well plate or 6×10^4 cells in 30 µl inoculated i.c. in tg20 mice. Where aliquots $< 10^7$ cells were ribolyzed uninfected splenocytes (5×10^6 cells/ml in OFCS) were added to avoid loss by binding to plastic surfaces.

Infectivity of exosome pellets

Exosome pellets obtained by high speed centrifugation of conditioned medium were resuspended in 500 µl OFCS and serially diluted in OFCS for infectivity determination.

Prion titres were referred to the initial number of cells that formed the cell cultures and expressed per 10^6 cell equivalent.

2.6.3 Infectivity assays

Scrapie Cell Assay in End Point format

Infectious titres were determined by the Scrapie Cell Assay in End Point format (SCEPA) as described previously (Klohn *et al.*, 2003; Mahal *et al.*, 2008) with minor modifications. Briefly, 2×10^4 PK1-2 cells in OFCS were plated into wells of 96-well plates. After 16 h cells were incubated with 300 µl aliquots of serially diluted homogenates. Three days later cells were initially split twice 1:2 and once 1:3 every other day. Prior to resuspending cells, half the medium was replaced with fresh OFCS for all previous cell passages. After three days cells were split 1:6 every 3-4 d. Aliquots of 25,000 cells were transferred onto Elispot plates after the sixth and seventh split (MultiScreen HTS-IP Filter Plate, Millipore, Watford, UK) and dried at 50 °C for at least 1 h. PrP^{Sc}-positive cells were detected by enzyme-linked immunosorbent assay (ELISA). Briefly, plates were incubated with Proteinase K (PK) (Roche Diagnostics Limited, West Sussex, UK) 1:10,000 in lysis buffer (50 mM Tris.HCl, pH 8.0, 150 mM NaCl, 0.5 % Na deoxycholate, 0.5 % Triton-X) for 1 h at 37 °C. After inactivating PK with 1 mM phenylmethylsulfonyl fluoride (PMSF) for 10 min, samples were denatured with 3 M guanadinium thiocyanate in 1 M Tris.HCl (pH 8.0) for 10 min and washed excessively, incubated with superblock (Pierce) and labeled with 0.6 µg/ml of anti-PrP antibody ICSM18 in TBST (10 mM Tris.HCl, pH 8.0, 150 mM NaCl, 0.1 % Tween-20) and 1 % milk powder. After 1 h plates were washed 5 times with TBST and incubated with alkaline phosphatase (AP) conjugated anti-IgG1 (Southern Biotech, Cambridge, UK) 1:6000 in TBST/1 % milk for another hour. After washing with TBST, plates were incubated with AP substrate (Bio-Rad, Bath, UK) for 30-40 min. Plates were then washed twice with dH_2O, air-dried and stored at -20 °C. PrP^{Sc} positive cells were counted using a Zeiss KS

ELISPOT system (Stemi 2000-C stereo microscope equipped with a Hitachi HV-C20A color camera and a KL 1500 CD scanner and WellScan software from Imaging Associates). Using the training feature of the WellScan software, the detection of PrP^{Sc}-positive cells was optimised to yield maximal signal-to-noise ratios.

Bioassay with Tg20 indicator mice

To determine prion titres by bioassays, groups of 6 Tg20 mice (Fischer *et al.*, 1996) were inoculated i.c. with 30 µl of serial dilutions of cell homogenates (pDCs and B cells) and RML brain homogenates.

Calculation of infectious titres

The ratio of PrP^{Sc}-negative wells per dilution was determined. Wells were scored positive if the spot number exceeded the background level, defined as the mean spot number in control (uninfected) wells plus 6 times the standard deviation. Infectious titres were estimated by statistical modelling using generalized linear models in cooperation with the Dept. Statistical Science, UCL. For comparative purposes, the effective median dose, dilution leading to 50 % scrapie sick mice or PrP^{Sc}-positive wells, and standard errors were determined by the Spearman-Karber formula (Dougherty, 1964).

2.6.4 Detection of PrP^{Sc}

Spleens from scrapie infected mice were dissected at 3, 7, 14 and 30 days post inoculation (dpi) to determine the levels of PrP^{Sc} by western blotting (WB). Ten percent (w/v) homogenates were prepared for immunoblotting by ribolyzation.

NaPTA precipitation and immuno-detection of PrP^{Sc} by western blot

Sodium phosphotungstic acid (NaPTA) precipitation was performed as previously described (Wadsworth *et al.*, 2001). All incubations were performed at 37 °C under

constant agitation at 800 rpm (Eppedorf Thermomixer). Briefly, 250 µl aliquots of 10 % spleen homogenate were mixed with 250 µl of 4 % sarkosyl (laurylsarcosine sodium salt) and incubated for 10 min. Samples were then treated with 1 µl benzonase and further incubated another 30 min. After centrifugation at 1000 rpm for 1 min, supernatant was collected and incubated for 30 min with 40.5 µl of a pre-warmed NaPTA-stock solution (4 % NaPTA + 170 mM $MgCl_2$, pH 7.4) to give a final concentration of 0.3 % NaPTA. Following centrifugation at 14,000 rpm for 30 min, pellets resuspended in 20 µl of 0.1 % sarkosyl and digested for 1 h with 50 µg/ml PK.

After PK digestion (50 µg/ml at 37 °C for 1 h), pellets were mixed 1:1 with 2× reducing sample buffer [125 mM Tris.HCl (pH 6.8), 20 % glycerol, 4 % SDS, 4 % 2-ME and 0.02 % Bromophenol Blue] and boiled at 100 °C for 10 min. Pre-stained Seeblue Protein Standard (Invitrogen, Paisley, UK) as molecular weight marker together with the various samples were loaded onto 16 % Tris-Glycine gels (Invitrogen, Paisley, UK) and electrophoresed for 80 min at 200 mV. Gels were blotted overnight onto PVDF membranes (Millipore, Watford, UK) pre-soaked in 100 % methanol at 15 V. Blotted membranes were blocked for 1 h in PBST (PBS + 0.05 % Tween-20) and 5 % milk powder and then incubated for 2 h at room temperature (RT) with ICSM35 (1 mg/ml) diluted 1:500 in PBST. Secondary detection consisted of 1 h incubation at RT with alkaline-phosphatase-conjugated anti-mouse IgG (Sigma-Aldrich Company Ltd., Dorset, UK) diluted 1:10,000 in PBST. After each antibody incubation, membranes were washed 6 times in PBST for at least 1 h. Bound antibody was detected using the chemiluminescent substrate CPD-Star (Tropix, Bedford, MA, USA) as previously described (Wadsworth *et al.*, 2001); membranes were washed twice for 5 min in Tropix Assay buffer (20 mM Tris pH 9.8, 1 mM $MgCl_2$), incubated for 2 min in CDP start, transferred to the photographic cassettes and visualized on Biomax MR film (Kodak, Hertfordshire, UK).

2.7 Fluorescence techniques

2.7.1 Flow cytometry

Isolated cell types were characterised by flow cytometry with fluorescence conjugated antibodies against specific cell surface markers. Briefly, aliquots of 1-2 Mio cells were resuspended in 100 µl MACS buffer and incubated with FcR blocking reagent (1:20, Miltenyi Biotech Ltd, Surrey, UK) for 15 min on ice to prevent non-specific binding. Samples were then stained with directly conjugated antibodies on ice for 30 min and washed in MACS buffer to remove unbound antibody. Antibody specifications, including target cells and dilutions used, are detailed in **table 2.1**. Unconjugated and biotinylated antibodies (e.g. FDC-M1 & M2) required secondary staining with PE anti-rat IgG kappa (clone MRK1, BD Biosciences, Oxford, UK) and PE streptavidin (ebiosciences, Hatfield, UK), respectively. Cell viability of splenic cells after 40 h in culture was assessed by incubation with 7-AAD (BD Biosciences Biosciences, Oxford, UK, 1:20 dilution) for 15 min before analysis.

Cells were gated according to their forward and side scatter properties to exclude dead cells and debris. Unlabeled or isotype controls were used to locate the negative cells in the first quadrant, single labeled controls were used for compensation to minimize overlap of emission spectra. Data acquisition and analysis were performed using a FACS calibur and CellQuest software (BD Biosciences, Oxford, UK); alternatively, data analysis was done using the WinMDI v2.8 software.

Name	Flurochrome	Clone	Isotype	Target cell	Company	Dilution
B220/CD45R	FITC, PE	RA3-6B	rat IgG_{2a}	B cells, pDCs	BD Biosciences	1:100
CD90/Thy1.2	PE	30-H12	rat IgG_{2b}, *k*	T cells	BD Biosciences	1:1000
CD3	FITC	K3T	rat IgG_{2a}	T cells	AbD Serotec	1:50
CD11b	PE	M1/70	rat IgG_{2b}	Macrop, mDCs	eBioscience	1:50
CD11c	FITC	HL3	arm ham IgG_1	DC	BD Biosciences	1:100
CD49b	PE	DX5	rat IgM, *k*	NK, NK-T cells	eBioscience	1:50
Podoplanin/gp38	PE	8.1.1	syr ham IgG	Fibroblasts	Biolegend	1:250
FDC-M1	purified	FDC-M1	rat IgG_{2c}, *k*	FDC	Gift Prof. Kosko	
FDC-M2	purified, biotin	FDC-M2	rat IgG_{2a}	FDC	ImmunoKontact	
CD21/CD35	FITC	76G	rat IgG_{2b}	B cells, FDC	BD Biosciences	1:100
CD23/FcεRII	PE	B3B4	rat IgG_{2a}, *k*	B cells, macrop	BD Biosciences	1:100
CD86	PE	GL1	rat IgG_{2a}, *k*	DC maturation marker	BD Biosciences	1:100
ICSM35	Biotin		ms IgG_{2b}			
mPDCA-1	purified	JF05-1C2.4.1	rat IgG_{2b}	pDCs	Miltenyi Biotec	

Isotype controls: (purchased from eBioscience)	
FITC Arm Ham IgG isotype control	PE Rat IgG_{2b} Isotype control
Biotin Rat IgG_{2a} Isotype control	PE Rat IgG_{2a} Isotype control
FITC Rat IgG_{2b} Isotype control	Biotin Mouse IgG_1, κ Isotype control
Rat $IgG2_b$ Isotype control	

Table 2.1 List of primary antibodies and isotype controls used for cell characterization.

Immune complex labeling

The use of immune complexes (IC) to label FDCs was previously described by Sukumar *et al.*, and it is based on the fact that FDCs retain ICs on their surfaces for long periods via FcR (Sukumar *et al.*, 2008). Pre-complexed ICs were prepared by a 30 min incubation at 37 °C of chicken ovalbumin (OVA) (Sigma-Aldrich Ltd, Dorset, UK) and rabbit anti-chicken OVA (Sigma-Aldrich Ltd, Dorset, UK) at a ratio 6:1 prepared in PBS. Cells were then incubated in medium with pre-formed ICs (200 ng IgG / 1.2 µg OVA)

for 2 h on ice water. After thorough washing, half of the cells were transferred to a 37 °C water bath for 30 min to favour internalisation, while the rest were kept on ice water at all times. ICs retained on the cell surface were labeled with Alx488 anti-rabbit IgG (Invitrogen, Paisley, UK) used at a 1:1000 dilution for 30 min on ice water.

2.7.2 Fluorescence microscopy

FDCs clusters were grown overnight on 13 mm round glass coverslips (VWR, West Sussex, UK) and stained with 10 ng/µl FDC-M1 or anti-rat IgG_{2b} isotype control and 2 ng/µl PE-conjugated anti-rat IgG kappa as secondary antibody. Following overnight incubation clusters were fixed onto the coverslips with 2 % paraformalhdehide (PFA) for 15 min at RT and incubated in superblock (Pierce, Leicestershire, UK) for 40 min. Primary and secondary antibody staining was done in MACS 0.5 % milk powder for 30 min at RT. Clusters were washed three times between staining and analyzed in an Axioplan 2 fluorescent microscope (Carl Zeiss, UK).

CHAPTER 3

RESULTS

KINETICS OF PRION ACCUMULATION IN SPLENIC CELL TYPES OF MICE

In most transmissible spongiform encephalopathies (TSEs), prions accumulate in the lymphoreticular system (LRS) at early stages of the disease. This early replicative phase in the LRS is considered to be essential and to precede neuroinvasion (Eklund *et al.*, 1967; Kimberlin and Walker, 1989b). In the past two decades research focused on identifying the main cell types supporting replication and transport of prions from the periphery to the brain. Seminal work using immuno-deficient and $PrP^{0/0}$ mice showed that both haematopoietic and stroma cells play fundamental roles in prion pathogenesis; follicular dendritic cells (FDC), B cells, macrophages and dendritic cells (DC) have been associated to different aspects of lympho-invasion including replication, dissemination and the clearance of prions (Klein *et al.*, 1998; Beringue *et al.*, 2000; Mabbott *et al.*, 2000; Aucouturier *et al.*, 2001; Kaeser *et al.*, 2001; Prinz *et al.*, 2002). The existence of the critical cell type that mediates neuroinvasion does not seem to hold true given the failure to fully prevent neuroinvasion in mouse models with specific immuno-deficiencies. Instead, it is generally accepted that prion propagation in the LRS is a dynamic process that depends on the interaction and contribution of different cell types (Aucouturier and Carnaud, 2002; Aguzzi *et al.*, 2008).

A comprehensive study to compare infectious titres in candidate cells has not been preformed to date, mainly due to limitations in the scope of *in-vivo* infectivity assays where prohibitively high numbers of mice are required. Developed a few years ago, the Scrapie Cell Assay (SCA), a cell-based infectivity assay greatly improves the titre determination; it is faster, cheaper and has a sensitivity comparable to the bioassay (Klohn *et al.*, 2003).

Using sequential magnetic sorting and *in-vitro* infectivity testing, we here established a method to determine the rate of prion accumulation in representative cell populations of the spleen and investigated whether these cells release infectivity (i.e. exosomes) which could contribute to the dissemination of prions. We also aimed to address the contribution of the stroma compartment to prion titres in lymphoid organs.

3.1 Quantification of infectious titres using a generalized linear model

A reliable determination of prion titres is fundamental to the study of prion diseases where differences in titres may be critical to assess the efficacy of a therapeutic intervention or the outcome of an *in-vitro* perturbation on prion propagation. The SCA and its more sensitive format SCEPA are based on the microscopic detection of single PrP^{Sc}-positive cells that are formed *de-novo* by prion propagation after infection with prion-containing samples. In the standard assay (SCA), the proportion of PrP^{Sc}-positive cells is a function of the prion titre calculated from standard curves of brain homogenates of known titre. In SCEPA titres are determined at limiting dilutions of infectivity by the ratio of infected to total wells (Klohn *et al.*, 2003; Mahal *et al.*, 2008). The determination of titres by SCEPA is based on the assumption that the distribution of infected cells follows a Poisson distribution, but the validity of this assumption has not been verified previously. We now tested this assumption and propose a generalized linear model (GLM) to quantify prion titres.

3.1.1 Validation of a GLM for the estimation of infectious titres by SCEPA[2]

In the SCEPA prion titres are determined by the ratio of infected to total wells. At limiting dilution of infectivity the number of positive wells in n_j independent infections at the j^{th} dilution follows a binomial distribution with parameters n_j and P_j where P_j is the proportion of positive wells. If the number of scrapie-infected cells is assumed to have a Poisson distribution then the proportion of negative wells ($1- P_j$) is equal to e^{-mcj} where m is the mean number of infectious units per volume and c_j the dilution. A complementary log-log transformation converts this equation to:

$$\text{Log}\,(-\log\,(1- P_j)) = \log m + \log c_j \qquad (\mathbf{1})$$

Thus, if the experimental data follows a Poisson distribution then a complementary log-log transformation is linear with a slope of one.

To check this hypothesis we prepared multiple dilution series of brain homogenate, infected susceptible cells and determined the number of negative wells. The brain homogenate RML I6200 was serially diluted 1:3 from 10^{-7} to 10^{-9} and cell layers of 12 wells per dilution were infected using eight technical repeats per dilution (see appendices, **table A1**). Linear regression analysis resulted in an estimate of the slope of 1.06 ± 0.20 (**figure 3.1**), in agreement with the assumption of an underlying Poisson distribution for the number of positive wells.

[2] Statistical modelling to determine the relationship between the number of scrapie-infected cells and the infectious dose to calculate mean infectious units and variance was performed in cooperation with Professor Trevor Sweeting (Dept. Statistical Science, UCL).

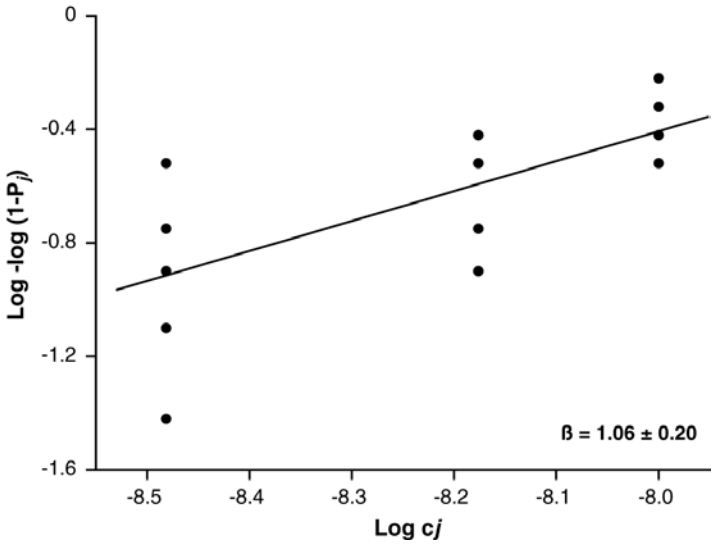

Figure 3.1 Initial validation of Poisson distribution. To test whether the experimental data from *in-vitro* endpoint titrations follows a Poisson distribution, serial 1:3 dilutions of RML brain homogenate from 10^{-7} to 10^{-9} were prepared and cell layers of 12 wells per dilution were infected. Complementary log-log transformed proportions of negative wells ($1\text{-}P_j$) *vs.* log dilutions of RML ($\log c_j$) are shown for eight technical assay repeats. Only data sets with proportions < 12 and > 0 positive wells were used for linear regression analysis, i.e. dilutions 10^{-8}, 6.6×10^{-9} and 3.3×10^{-9} (see appendices, **table A1**). If the distribution of infected cells follows a Poisson distribution, the slope β is expected to be 1.

This prompted us to calculate infectious titres using generalized linear model (GLM) regression, a statistical method first formulated by Nelder and Wedderburn (Nelder and Wedderburn, 1972) that unifies a wide range of probability distributions, comprising normal, binomial, Poisson, gamma, and others, generally known as 'exponential family distributions' by the use of a common method for computing maximum likelihood estimates (see **appendix 1**). Ordinary regression analysis is based on normally distributed error components with constant variance and could lead to severe errors in the estimation of the outcome variable in case of non-normal distributions. GLM, however, permits the analysis of the linear relationship between the predictor and response variables, even when it is not reasonable to assume that the data is normally distributed.

Using the GLM approach, the proportion of positive wells (P_j) can be fitted by the regression model (**1**). This can be written as

$$g(P_j) = \alpha + \beta x_j \quad (\mathbf{2})$$

where *g* is the link function, a complementary log-log transformation, α the log mean infectious units, β the regression slope and x_j the log dose. The link transformed proportions of positive wells using GLM were plotted in **figure 3.2** and overlap with the linear regression analysis in **figure 3.1**.

Parametres α and β are estimated by the maximum likelihood method (see **appendix 2**). An estimated value for β of 0.9608 ± 0.0969 is consistent with the hypothesis of an underlying Poisson distribution for the number of infected wells and the model provides a good fit to the data as estimated by an analysis of deviance (see **appendix 2**). An estimated titre (α) of 8.63 ± 0.03 log TCIU/g brain for eight technical repeats of serially diluted RML I6200 brain homogenate demonstrates the accuracy of the SCEPA.

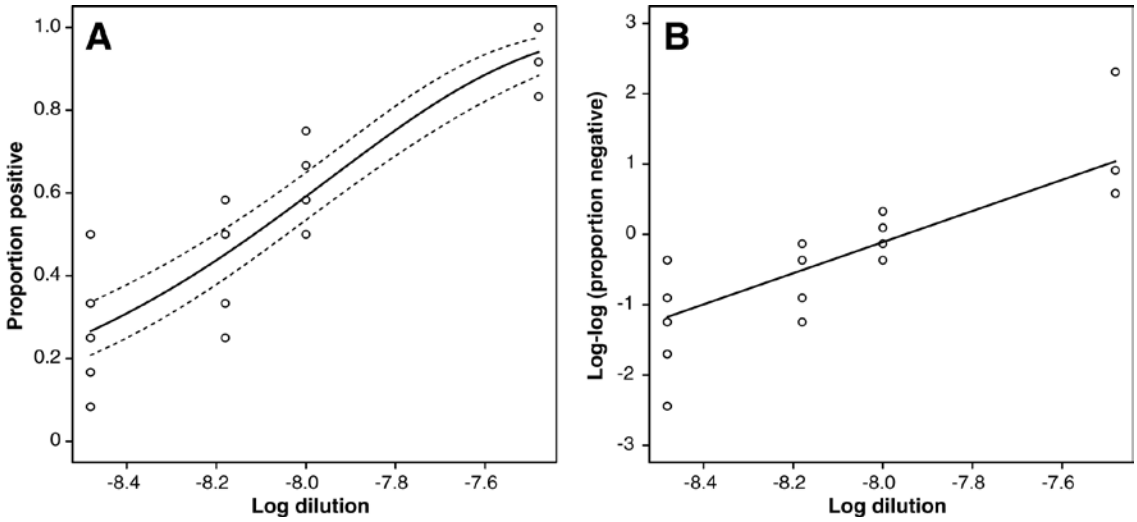

Figure 3.2 Regression analysis of SCEPA endpoint titration assay by GLM. For the estimation of prion titres by SCEPA, prion-susceptible cells were infected with serially diluted RML I6200 brain homogenate and the proportions of scrapie-positive wells were analysed using a GLM with binomial family and complementary log-log link. (**A**) Observed and estimated proportions of scrapie-positive wells with 95 % confidence intervals. (**B**) Link-transformed proportions of scrapie-positive wells: $g(P_j) = \log(-\log(1-P_j))$. Data represent eight technical assay repeats of serially diluted RML I6200 brain homogenate. The four zero values at dilution 3.3×10^{-8} or -7.5 log dilution (see **appendices**, **table A1**) were replaced by 0.5 in order to plot the observed loglog values.

3.1.2 Determination of the sensitivity of SCEPA

Having established a GLM for the estimation of infectious titres, we applied this model to determine the sensitivity of SCEPA and aimed to establish a GML for bioassays to compare the sensitivity of both assays. Endpoint titrations of RML brain homogenate (I6200) by SCEPA using the highly susceptible PK1-2 subclone and mouse bioassay were performed in parallel experiments. Titres from eight independent *in vitro* assays were highly reproducible and yielded an estimated titre of 8.71 ± 0.04 by GLM (**table 3.1**). As a first estimate to compare sensitivities we calculated the median infectious titres using the Spearman-Karber method (Dougherty, 1964). Eight independent cell-based assays

yielded a titre of 8.70 ± 0.19 log LD_{50}/g brain and the combined two independent bioassays a titre of 9.14 ± 0.28, in agreement with previously published titres for I6200 (Cronier *et al.*, 2008) (**table 3.1**).

To implement a GLM for bioassay, data from five independent bioassays with RML I6200 (from Dr Malin Sandberg MRC Prion unit, London) were fitted by GLM using a complementary log-log or a probit transformation as link functions (see **appendix 1**). The link-transformed proportions of scrapie-sick mice by both models were plotted in **figure 3.3**. A probit model yielded a titre of 8.71 ± 0.53 log LD_{50} units/g brain and the complementary log-log model a titre of 8.54 ± 0.54 log LD_{50} units /g brain. Using the Spearman-Karber method a corresponding titre of 8.66 ± 0.80 log LD_{50} units/g brain was determined. The obtained titres for RML I6200 are unexpectedly lower compared to data of **table 3.1** and previously published data (Cronier *et al.*, 2008). The observed variations of infectious titres between brain homogenates is most likely results from differences in the dispersion state of homogenates, an issue that will be addressed in the next section, or multiple freezing-thawing cycles (Properzi *et al.*, unpublished).

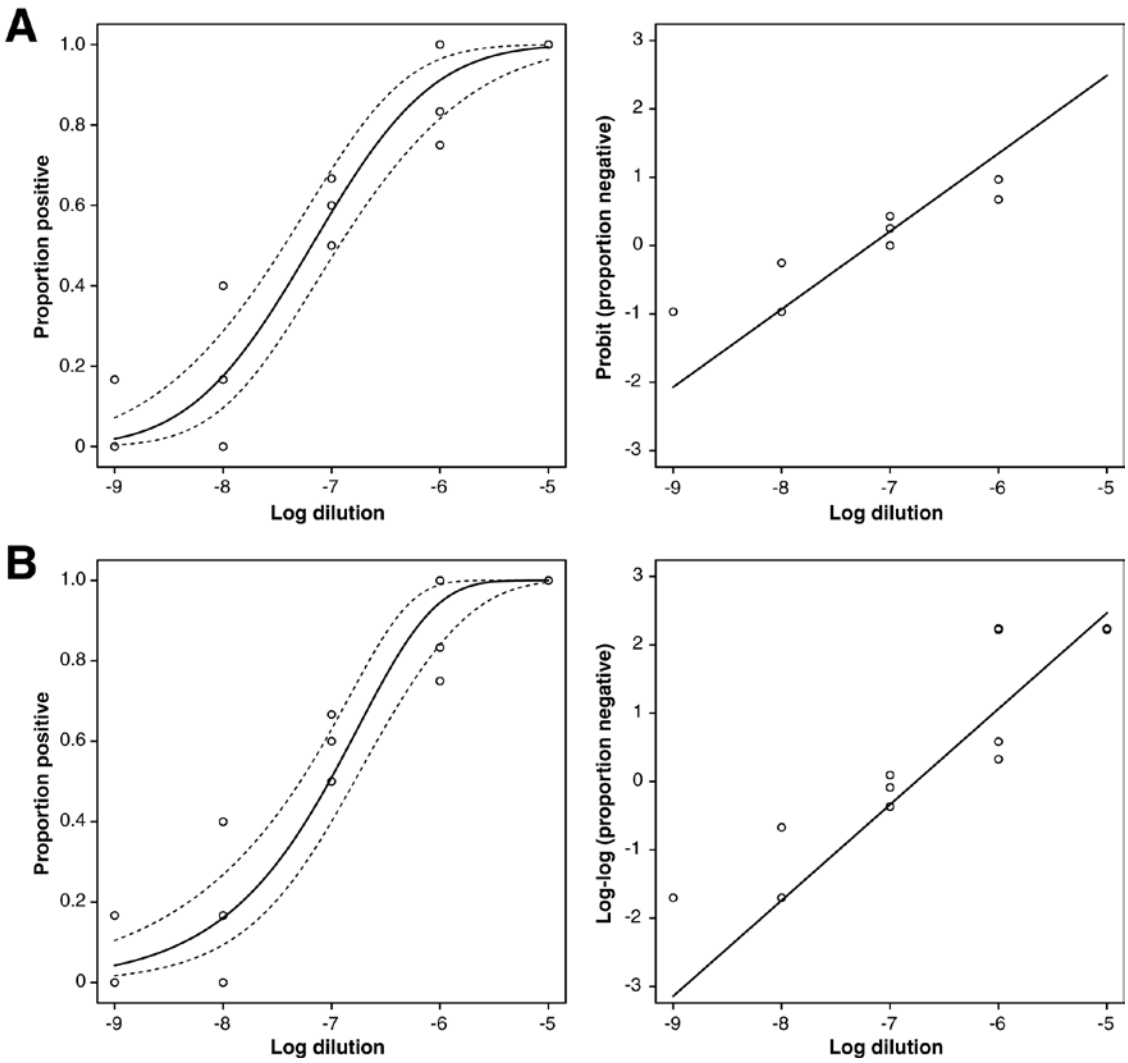

Figure 3.3 Regression analysis of mouse bioassay data by GLM. Data from five independent bioassays with RML I6200 was analysed by a GLM with binomial family complementary log-log (**A**) and probit (**B**) link functions. The *left* graphs represent the observed and estimated proportions of scrapie-sick mice with 95 % confidence intervals. The *right* graphs show the linearised link-transformed proportions of scrapie-sick mice.

By using GLM and comparing sensitivities of the infectivity assays in parallel experiments (**table 3.1**) we conclude that the sensitivity for prion detection by SCEPA (8.71 ± 0.04 log TCIU/g) was not significantly different from the combined mouse bioassay data (9.02 ± 0.23 LD_{50} units/g) given the high inter- and intra-assay variability of the bioassay. The high standard error in titre estimations from bioassays compromises a direct comparison between *in-vitro* and *in-vivo* assays. Despite the lack of statistical significance the bioassay seems to be more sensitive than SCEPA as shown in subsequent experiments (**table 3.2**). While the SCEPA outperforms the mouse bioassay in terms of statistical robustness, low cost and fast infectivity testing, the bioassay will be indispensable where prion titres are below the detection limit of the SCEPA (2 LD_{50}/g brain or spleen homogenates and 1-5 $LD_{50}/10^6$ cells, respectively, based on infectious titres determined at clinical end-stage). In addition, N2a derived cells are permissive to prion strains RML and 22L only, but not to other mouse adapted prion-strains like ME7, 22A and 301C. It should noted, though, that the sensitivity of the SCEPA is cell-type dependent.

RML input in LD_{50} units[#]	SCEPA[*] PrP^{Sc}-positive /total wells	Mouse bioassay 1		Mouse bioassay 2	
		Sick/ total	Incub.time, days ± SD	Sick/ total	Incub.time, days ± SD
$6x10^{3}$	n.d	5/5	75.8 ± 1.2	n.d	n.d
$6x10^{2}$	n.d	5/5	83.2 ± 3.6	5/5	86.2 ± 2.8
$6x10^{1}$	24/24	6/6	106.5 ± 6.4	5/5	112.6 ± 5.9
$6x10^{0}$	15/24	3/4	110.3 ± 4.0	3/5	122.3 ± 6.3
$6x10^{-1}$	2/24	1/5	116	1/5	104
$6x10^{-2}$	0/24	2/6	159.5 ± 1.0	1/6	136
$6x10^{-3}$	n.d	0/6	>200	0/6	>200
Infectious titres	*Log TCIU/g ± SE*	*Log LD_{50}/g ± SE*		*Log LD_{50}/g ± SE*	
Spearman-Karber	8.71± 0.19	9.31 ± 0.42		8.99 ± 0.41	
GLM	8.71 ± 0.04	9.02 ± 0.23[‡]			

[#] Prion infectivity of input (RML I6200) is based on a previous endpoint titration (Cronier *et al.*, 2008).

[*] The ratio between PrP^{Sc}-positive and total wells is shown for one representative out of eight experiments.

[‡] Infectious titres were estimated for the combined two bioassays using a GLM regression with probit link function and expressed as log LD_{50} units/g brain.

Table 3.1 Sensitivity for prion detection of SCEPA and mouse bioassay. The sensitivity for prion detection of SCEPA and mouse bioassay was determined by end-point titration using RML mouse brain homogenate I6200. Aliquots of 10 % (w/v) I6200 (9.3 logLD_{50}/g brain, Cronier *et al.*, 2008) were serially diluted 1:10 into uninfected CD1 brain homogenate (10 %, w/v) in a range between 10^{-4} and 10^{-10}. For mouse bioassay, groups of six Tga20 mice were inoculated intracerebrally with 30 µl of 1 % (w/v) homogenates and attack rates and scrapie incubation times were determined. In parallel experiments, brain homogenates were diluted 1:1000 into OFCS and cell layers of highly prion susceptible N_2aPK1-2 cells were infected with 300 µl aliquots. The input of RML infectivity for bioassay and SCEPA is expressed as LD_{50} units and was calculated from previous published titre (Cronier *et al.*, 2008) for each dilution and volume used in the infection, e.g. a 10^{-7} dilution of I6200 corresponds to 200 LD_{50} units/ml or $6x10^{0}$ LD_{50} units per 30 µl inoculum for the bioassay and $6x10^{1}$ LD_{50} units per 300 µl per well for SCEPA, respectively. Infectious titres for SCEPA and bioassay were determined using both Spearman-Karber and GLM and expressed as log TCIU/g brain ± SE of 8 independent experiments and log LD_{50} units/g brain ± SE for 2 independent bioassays, respectively.

3.2 Validation of a homogenization method for cell titre determination by SCEPA

The dispersion state of the homogenate is a critical parameter for titre determination by endpoint titration, since an increase in the dispersion of infectious brain homogenate results in an apparent increase of infectivity at limiting dilutions. The determination of infectious titres by the standard SCA has been validated for scrapie-infected brain homogenates, but not for homogenates of splenic cell isolates. We therefore aimed to establish a standardised method for tissue cell homogenisation and confirmed its suitability for prion determination by SCEPA.

Homogenisation by shear force with needles, a method broadly used to generate tissue homogenates, failed to homogenise splenocytes as indicated by a high percentage of Trypan blue-negative viable cells. We therefore tested two alternative homogenisation methods, sonication and ribolysation which both led to a complete disruption of cells. To determine infectious titres for isolated immune cells from scrapie-infected mice whole cells or cell homogenates were inoculated previously (Raeber *et al.*, 1999a; Aucouturier *et al.*, 2001). The uptake of infectious particles by susceptible cells may also depend on the particle size of the infectious entity and the number of infectious particles per volume. Preliminary experiments showed a significant difference between the infectious titres of MACS-isolated plasmacytoid DCs (pDC) and B cells. We therefore assessed the suitability of cell homogenisation methods using both cell types by determining infectious titres using mouse bioassay and SCEPA (**table 3.2**).

Infectious titres of B cells determined by mouse bioassay at 30 dpi were in agreement with previously published data from a similar experiment with RML and the same mouse strain (Raeber *et al.*, 1999a). Cell titres were about one log higher in the bioassay as compared to SCEPA, consistent with a reduced sensitivity of SCEPA. No significant differences in infectious titres were observed between the two

homogenisation methods for both cell types using SCEPA and bioassay, respectively. Remarkably, titres for pDCs were consistently higher than those of B cells, irrespective of the homogenisation method and the infectivity assay used. Estimates by GLM showed that titres of pDCs were significantly higher ($p < 0.005$) than those of B cells when assayed by SCEPA. Although similar estimates of the prion titre were calculated by either Spearman-Karber formula or GLM, higher variances were associated to Spearman-Karber estimations as compared to the GLM.

For all subsequent experiments ribolyzation was used as preferred homogenisation method to exclude the risk of cross-contamination during sonication of prion-infected samples (Barria *et al.*, 2009) .

(A) SONICATION

Cell Types	Cell number equivalents‡	SCEPA PrP^{Sc}-positive /total wells	Mouse bioassay Attack rate	Mouse bioassay Incub.time, days ± SD
pDC	$6x10^3$	12/12	5/5	89 ± 1
	$6x10^2$	5/12	5/5	117 ± 9
	$6x10^1$	1/12	2/6	131 ± 17
	$6x10^0$	0/12	0/6	> 200
control	$6x10^3$	0/12	0/6	> 200
Infectious titres		*Log TCIU/10^6 cells ± SE*	*Log LD_{50}/10^6 cells ± SE*	
Spearman-Karber		3.21 ± 0.08	4.06 ± 0.25	
GLM		3.13 ± 0.04 ($p < 0.005$)*	-	
B cells	$6x10^4$	12/12	5/5	92 ± 4
	$6x10^3$	8/12	6/6	99 ± 2
	$6x10^2$	2/12	5/6	124 ± 7
	$6x10^1$	0/12	1/6	171
Control	$6x10^4$	0/12	0/4	> 200
Infectious titres		*Log TCIU/10^6 cells ± SE*	*Log LD_{50}/10^6 cells ± SE*	
Spearman-Karber		2.61 ± 0.19	3.72 ± 0.30	
GLM		2.53 ± 0.03	-	

(B) RIBOLYZATION

Cell Types	Cell number equivalents‡	SCEPA PrP^{Sc}-positive /total wells	Mouse bioassay Attack rate	Mouse bioassay Incub.time, days ± SD
pDC	$6x10^3$	12/12	4/4	85 ± 1
	$6x10^2$	6/12	5/6	105 ± 5
	$6x10^1$	1/12	4/6	108 ± 8
	$6x10^0$	0/12	0/6	> 200
Control	$6x10^3$	0/12	0/4	> 200
Infectious titres		*Log TCIU/10^6 cells ± SE*	*Log LD_{50}/10^6 cells ± SE*	
Spearman-Karber		3.31 ± 0.15	4.22 ± 0.33	
GLM		3.24 ± 0.04 ($p < 0.005$)*	-	
B cells	$6x10^4$	12/12	6/6	88 ± 3
	$6x10^3$	9/12	5/5	100 ± 5
	$6x10^2$	2/12	5/5	107 ± 12
	$6x10^1$	0/12	1/5	174
Control	$6x10^4$	0/12	0/3	> 200
Infectious titres		*Log TCIU/10^6 cells ± SE*	*Log LD_{50}/10^6 cells ± SE*	
Spearman-Karber		2.70 ± 0.15	3.92 ± 0.29	
GLM		2.53 ± 0.03	-	

‡Inputs of infectious cell homogenates are expressed as cell number equivalents.

*Level of significance for maximum likelihood estimates (GLM) between infectious titres of pDCs versus B cells as determined by SCEPA.

Table 3.2 Infectious titres of MACS-isolated cells after homogenization by ribolyzation and sonication. Four 129/Sv x C57BL/6 mice were inoculated i.p. with 100 µl 1 % RML infected brain and uninfected CD1 brain homogenate (control), respectively. At 30 dpi spleens were dissected and pDCs and B cells isolated by MACS according to Figure 2.1 (section 2.1.1). Aliquots of 2×10^7 cells/ml OFCS, supplemented with protease inhibitors were homogenised by sonication ***(A)*** or ribolysation ***(B)*** according to material and methods (**section 2.2.2**). To determine infectious titres, cell homogenates were serially diluted 1:10 and inoculated intracerebrally into Tga20 mice or transferred onto layers of susceptible PK1-2 cells in parallel experiments. A 10^{-2} dilution of cell homogenates corresponds to 2×10^5 cell equivalents/ml or 6×10^3 cell equivalents per 30 µl inoculum for mouse bioassay and 6×10^4 cell equivalents per 300 µl per well for SCEPA. Infectious titres were determined by non-parametric statistical analysis for bioassay (Spearman-Karber) and GLM for SCEPA and expressed as log LD_{50} units/10^6 cells and log TCIU/10^6 cells, respectively.

3.3 Sequential isolation of splenic cell types by magnetic-activated cell sorting

To address the contribution of specific cell types to prion accumulation in the spleen we designed and optimized a cell separation protocol based on sequential rounds of positive selection using antibody-coated magnetic microbeads that enables the isolation of B cells, T cells, DCs, pDCs, macrophages and natural killer (NK) cells from the same pool of splenocytes, and determined infectious titres subsequently. Using this approach sufficient numbers of cells for infectivity testing can be isolated from spleens of scrapie-infected mice with high purities and within a reasonable time. For the isolation of DCs, for example, 4×10^8 splenocytes were processed in about an hour with an average yield of 3-4 % i.e. 12-16 Mio cells (**table 3.3**), and magnetic isolation of up to 6 different cell types was performed in about five hours.

From a mixed population of cells released by enzymatic digestion of freshly dissected spleens, individual cell subsets were purified in sequential rounds of positive selection with magnetic beads directed against specific surface markers in the target cells according to the sorting strategy depicted in **figure 2.1**, material and methods. Isolation

protocols were optimised against cell yields and purities aiming to reduce experimentation times as possible, e.g. rare populations such DCs and NK cells were isolated first to minimize cell losses associated to successive positive selections. During the implementation of a sorting strategy we also considered cases where a surface marker was expressed at low levels or on more than one cell type. For example, three main subsets of DCs in murine spleens can be distinguished by means of their surface markers: $CD11c^{+}CD11b^{+}$ myeloid DCs (mDC), $CD11c^{+}$ $CD8^{+}$ lymphoid DCs (lDC) and $CD11c^{low}$ $B220^{+}$ pDCs (Bjorck, 2001). Since low expression levels of CD11c on pDCs may compromise their quantitative isolation with CD11c microbeads, we used microbeads coated with murine plasmacytoid dendritic cell antigen-1 (mPDCA-1) which is specifically expressed on pDCs of murine spleen (Krug *et al.*, 2004). Accordingly, *pan*-DCs were isolated using a 2:1 mixture of CD11c and mPDCA-1 microbeads to ensure that all DC subsets were equally represented in the *pan*-DC fraction. Highly purified cell fractions with purities from about 87 % for rare cells (DCs and pDCs) to more than 95 % purity for lymphocytes subsets (B cells, T cells and NK cells) were obtained using this isolation strategy (**figure 3.4**).

Widely used for the isolation of macrophages, CD11b surface antigen is expressed not only on macrophages but also on mDCs ($CD11c^{+}$ $CD11b^{+}$). In an effort to avoid an enrrichment of mDC contaminants in the macrophage fraction, we proposed two positive selection rounds with CD11c microbeads to deplete DCs before the isolation of macrophages (**figure 2.1,** material and methods). However, this did not suffice to deplete mDCs that were still capture for CD11b beads (**figure 3.4 F**). A depletion strategy using Miltenyi depletion columns and CD11c microbeads, although gave better results (data not shown), was not considered since it would increase the number of mice needed and the costs of the cell sorting with MACS reagents considerably. Instead, we used fluorescence-activated cell sorting (FACS) to obtain a highly purified $CD11c^{-}$ $CD11b^{+}$ macrophage cell population (**figure 3.5**).

Spleen weight	72 ± 9 mg
Splenocytes	116 ± 9 x 10^6 cells per spleen

Cell types	**Microbeads**	**Yield**	**Surface marker**	**Purity**
pDCs	mPDCA-1	3.8 %	$CD11c^+$ $B220^+$	87 %
pan DCs	CD11c + mPDCA-1	3.3 %	$CD11c^+$	90 %
Macrophages	CD11b	1.9 %	$CD11c^-$ $CD11b^+$	74 %
B cells	CD19	33 %	$B220^+$	99 %
T cells	CD90	13 %	$CD3^+$	98 %
NK	CD49b	3 %	$CD49b^+$	97 %

Table 3.3 Summary of yields and purities of isolated splenic cell types. The number of cells was estimated from 3 to 6 independent counts using a Coulter counter Z2 (Beckman Coulter, High Wycombe, UK) and expressed as % yields (=number of sorted cells/number of total cells). The purity of the fractions was evaluated by flow cytometry using monoclonal antibodies (mAbs) against to CD11c (clone HL3), CD11b (clone M1/70), B220 (clone RA3-6B), CD49b (clone DX5) and CD3 (clone KT3). Data is representative of at least 5 experiments.

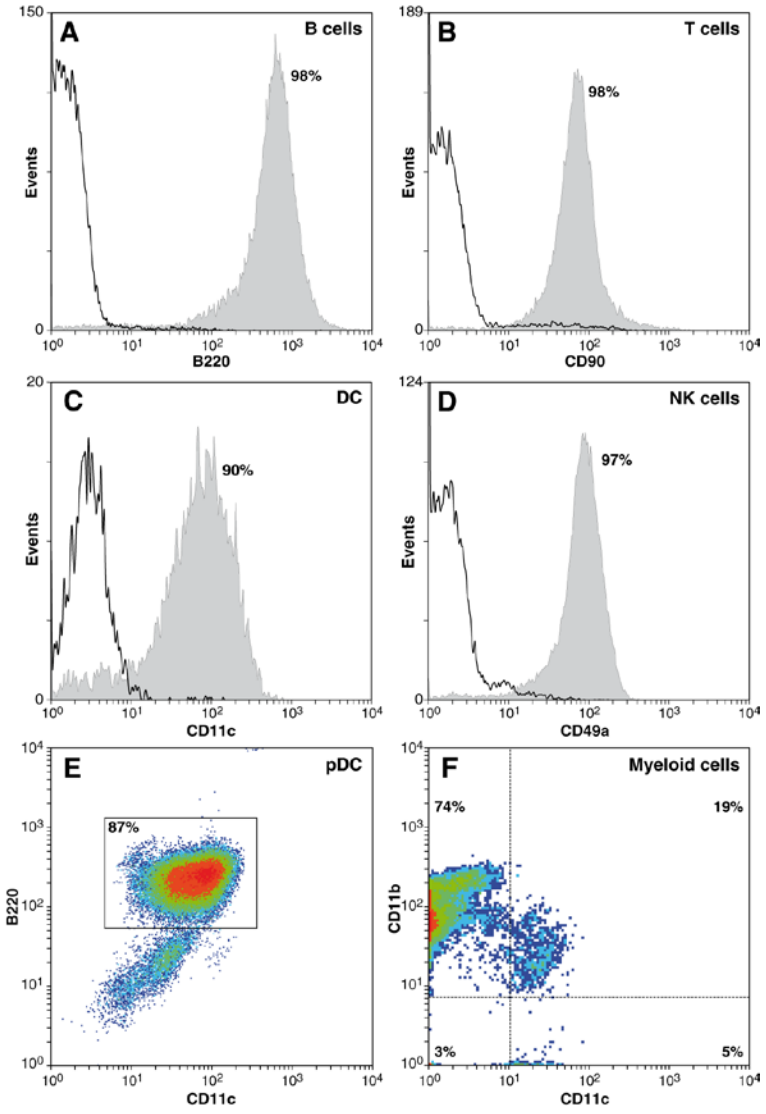

Figure 3.4 Flow cytometric analyses of isolated splenic cell types. Different splenic cell populations were isolated by sequential MACS as described in material and methods (**section 2.1.2**). Purities of the isolated cell fractions were assessed by flow cytometry in a FACScalibur (BD Biosciences, Oxford, UK) using the following monoclonal antibodies (mAbs): (**A**) anti-B220 for B cells, (**B**) anti-CD90 for T cells, (**C**) anti-CD11c for DCs and (**D**) anti-CD49a for NK and NK-T cells. Shaded histograms represent cell-specific mAbs, open histograms negative controls. (**E**) PDCs isolated with mPDCA-1 microbeads are $CD11c^{+}$ $B220^{+}$ with purities of 87 %. (**F**) $CD11b^{+}$ $CD11c^{-}$ Macrophages isolated with CD11b microbeads after depletion of $CD11c^{+}$ cells in the upper-left quadrant have a purity of 74 %, the macrophage-enriched fraction also contained about 19 % mDC contaminants. Representative results of at least three experiments are shown. The percentage of positive cells is indicated in each of the graphs.

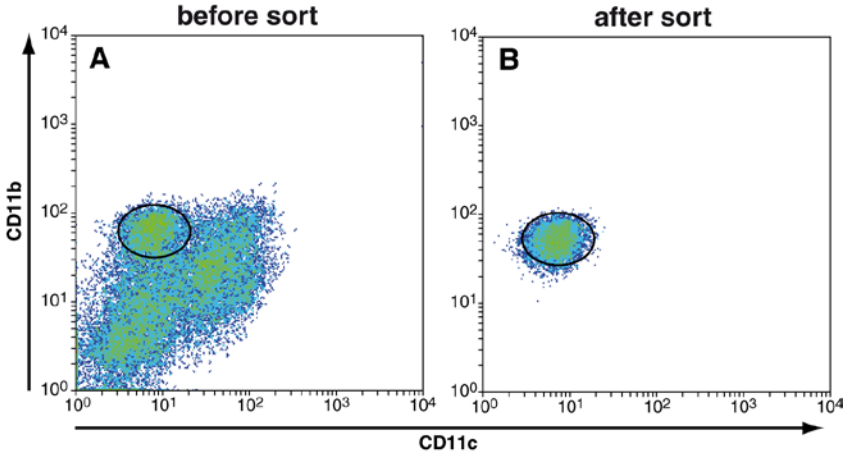

Figure 3.5 Purification of macrophages by fluorescent activated cell sorting. (**A**) $CD11b^+$ myeloid cells, containing $CD11b^+$ $CD11c^-$ macrophages and $CD11b^+$ $CD11c^+$ mDCs were isolated from total splenocytes by magnetic cell sorting with CD11b microbeads. (**B**) Macrophages were sorted by flow cytometry in a MoFlo (Dako, Cambridgeshire, UK) with mAbs against CD11c and CD11b. Sorted $CD11c^-$ $CD11b^+$ macrophages are shown in 3.2 A.

3.4 Prion accumulation in the lymphoreticular system at early stages of prion disease

Early studies have addressed the evolution of prion titers in different lymphoid organs after inoculation by different routes and showed that prions accumulate and replicate in spleen and lymphoid nodes reaching plateau levels early after inoculation (Eklund *et al.*, 1967; Kimberlin and Walker, 1979; Millson *et al.*, 1979). However, the contribution of specific immune cells to prion titres in the LRS is not well characterised as previous studies were restricted to single time points and a few cell subsets. We here examined the kinetics of prion accumulation in tissue and cells of the LRS during the rapid replication phase before maximum titres are reached (i.e. 30 dpi).

To assess the rate of prion accumulation in lymphoid tissues, prion titres in spleen and mesenteric lymph nodes (MLN) of 129Sv-C57/BL6 *wid-type* and *Prnp*$^{-/-}$ mice were

measured over the first month post inoculation. Groups of ten mice were inoculated intraperitoneally with 1 % RML corresponding to an infectious dose of 5.7 log LD_{50} units (**table 3.1**) and culled at 3, 7, 14 and 30 dpi. Ten percent homogenates (w/v) were prepared by ribolysation (see materials and methods, **section 2.5.2**) and analysed for infectivity. Prion replication in spleen was evident as early as 3 dpi, where 5.4 log TCIU/g spleen were detected in *wt* mice as compared to 2.5 log TCIU/g spleen in *Prnp*$^{-/-}$ mice, corresponding to an 800-fold difference in titres (**figure 3.6 A**). Accumulation of prions in MLN was delayed as compared to spleen in accordance to previous reports (Kimberlin and Walker, 1989b). No infectivity was detected in MLN at 3 dpi at the range of dilutions tested (< 2.5 log TCIU/g) and prion titres were consistently lower as compared to spleens throughout the studied time period (**figure 3.6 A**). In contrast to the *in-vitro* determination of infectivity by SCEPA, PrP^{Sc} was not detectable on Western blot at time points prior to 14 dpi corresponding to titres of 6.5 log TCIU/g (**figure 3.6 B**), highlighting the limitations of PrP^{Sc} detection for diagnostic purposes. Infectivity reached 7.2 log TCIU/g and 6.7 log TCIU/g tissue at 30 dpi in spleen and MLN, respectively.

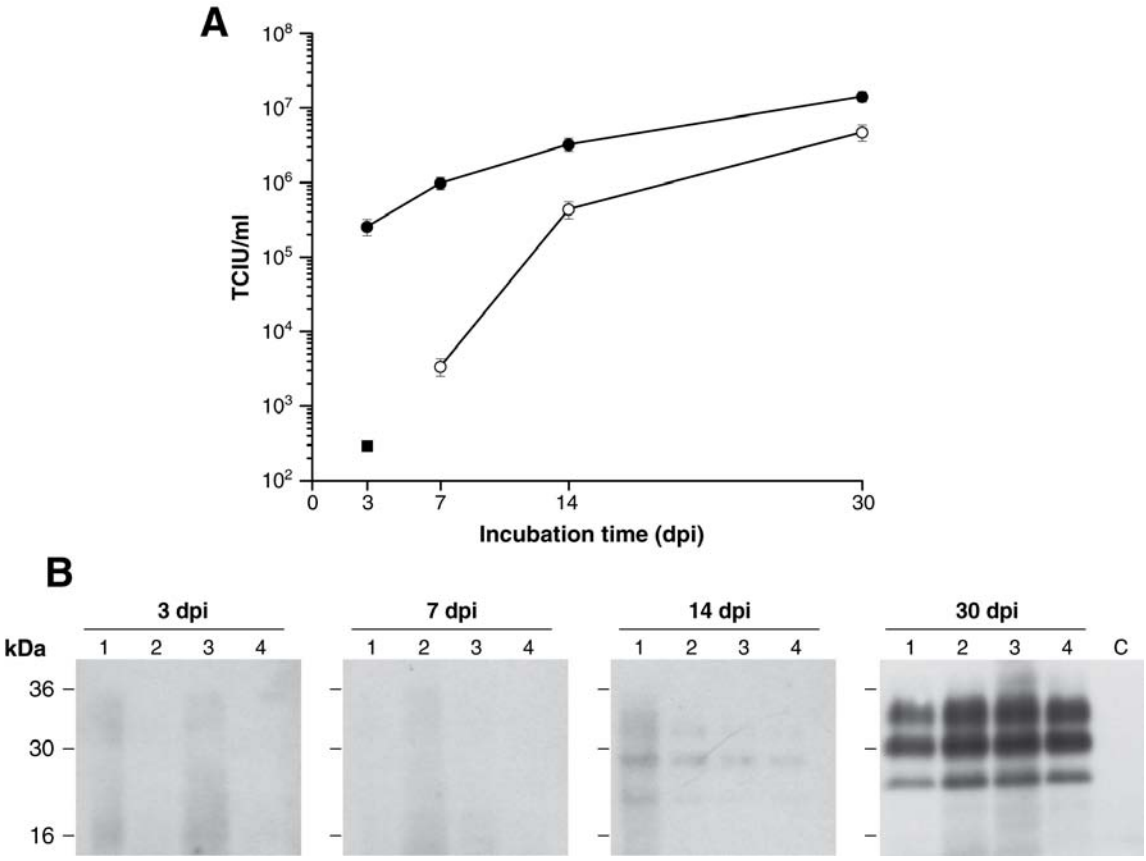

Figure 3.6 Kinetics of prion accumulation in spleen and mesenteric lymph nodes. (**A**) *Wild-type* and *Prnp*$^{-/-}$ mice were inoculated i.p. with 5.7 log TCIU RML prions and culled at 3, 7, 14 and 30 dpi to retrieve spleens and mesenteric lymph nodes (MLN). Infectious titres of tissue homogenates, determined by SCEPA were analyzed by a GLM. Dark circles: spleen tissue; empty circles: MLN tissue; black square: spleen tissue of *Prnp*$^{-/-}$ mice. (**B**) Samples from four spleens (1-4) were analyzed for PrP^{Sc} at each time point. An equivalent to 25 mg wet weight of tissue was precipitated with NaPTA, digested with PK (50 µg/ml at 37 °C for 1 h), and immunoblotted with the monoclonal anti-PrP antibody ICSM35 as described in material and methods (**section 2.5.4**).

Upon i.p inoculation of *Prnp*$^{-/-}$ mice with 100 µl 1 % RML I6200 (5.7 log TCIU, **table 3.1**), about 1.2 log TCIU/spleen were detected at 3 dpi at an average weight of 72 ± 9 mg. In contrast, no infectivity was detected in MLN of *Prnp*$^{-/-}$ mice, suggesting that following i.p inoculation prions are transported first to the spleen. We next investigated whether

infectivity from the inoculum was associated to specific splenic cells (**table 3.4**). Titres reached the detection limit of SCEPA, infectivity seemed to be associated primarily to antigen presenting cells (APC), i.e. macrophages, DCs, and lymphocytes. This is consistent with a role of APCs in prion sequestration.

Cell Types	TCIU/10^6 cells ± SE[#] 3 dpi
Pan DC	0.23 ± 0.09
Myeloid cells[‡]	0.47 ± 0.17
B cells	0.06 ± 0.06
T cells	0.06 ± 0.06

[‡]Myeloid cells contained mainly macrophages ($CD11b^+$ $CD11c^-$) and about 20 % myeloid DC ($CD11c^+$ $CD11b^+$) contaminants.
[#]Infectious titres calculated by the GLM are represented as mean values ± SE for at least three independent experiments.

Table 3.4 Infectious titres of different splenic cell types in the absence of prion replication at 3 dpi. Different cell types were isolated by magnetic sorting from spleens of *Prnp*$^{-/-}$ mice three days after intraperitoneal inoculation with RML prions. Infectious titres were determined by SCEPA and analyzed by GLM.

We next determined infectious titres of major splenic cell types and their rates of prion accumulation. Infectivity was detectable in all cell types as early as 3 dpi and increased rapidly over time. In splenocytes a 50-fold increase in cellular titres was determined on average between 3 and 30 dpi (**table 3.5**), consistent with the increase of infectious titres in spleen during the same time interval (**figure 3.6 A**).

Cell Types	Infectious titres: TCIU/10^6 cells ± SE (95 % confidence interval)[#]			
	3 dpi	7 dpi	14 dpi	30 dpi
Splenocytes	11	30	265 ± 64 (147,480)	544 ± 124 (311,952)
Pan DC	23	62 ± 14 (36,107)	265 ± 64 (147,480)	677 ± 87 (518,858)
pDC	41	106	370 ± 85 (211,650)	1798 ± 298 (1252,2579)
Myeloid cells[‡]	1	37 ± 9 (23,62)	127 ± 34 (67,244)	472 ± 57 (365,609)
Macrophages[†]	n.d	n.d	n.d	243 ± 49 (157,375)
B cells	9	26 ± 6 (16,43)	130 ± 35 (68,249)	262 ± 28 (210,328)
T cells	9	25 ± 6 (15,42)	135 ± 36 (71,260)	208 ± 28 (156,279)
NK/T cells[*]	n.d	n.d	183	721 ± 120 (491,1059)
pDC (blood)	n.d	n.d	n.d	< 6

[‡]Myeloid cells were isolated with CD11b magnetic microbeads after partial depletion of $CD11c^+$ DCs, it consisted mainly of macrophages ($CD11b^+CD11c^-$) and around 20 % myeloid DC ($CD11c^+CD11b^+$) contaminants (see **figure 3.5**).

[†]$CD11b^+$ macrophages devoid of mDCs were isolated by FACS (see **figure 3.4**).

[*]NK and NK-T cells were isolated with CD49b magnetic beads.

[#]Infectious titres are represented as mean values ± SE, and as lower and upper limits of 95 % confidence intervals.

Table 3.5 Time dependent accumulation of prion infectivity in isolated splenic cell types. Groups of ten 129Sv x C57/BL6 mice, inoculated i.p. with 100 µl aliquots of 1 % (w/v) RML brain homogenate I6200 were culled at various time points after inoculation. Splenocytes and splenic cell types were isolated from spleens by MACS after collagenase digestion and lympholyte purification. Infectious titres were determined by SCEPA using a GLM.

Whilst prions were detectable in all cell types, including lymphocytes, NK cells, DCs and macrophages, highest infectious titres were determined in two cell types that have previously not been associated to prion pathogenesis, pDC and NK cells. At 30 dpi, pDCs were 7-8 fold more infectious than lymphocytes and macrophages, and 2-fold more infectious than NK cells. Prion titres of NK cells were also significantly higher ($p < 0.05$)

than those of lymphocytes and purified macrophages. In addition to pDCs, *pan* DCs accumulated high prion titres (**figure 3.7**).

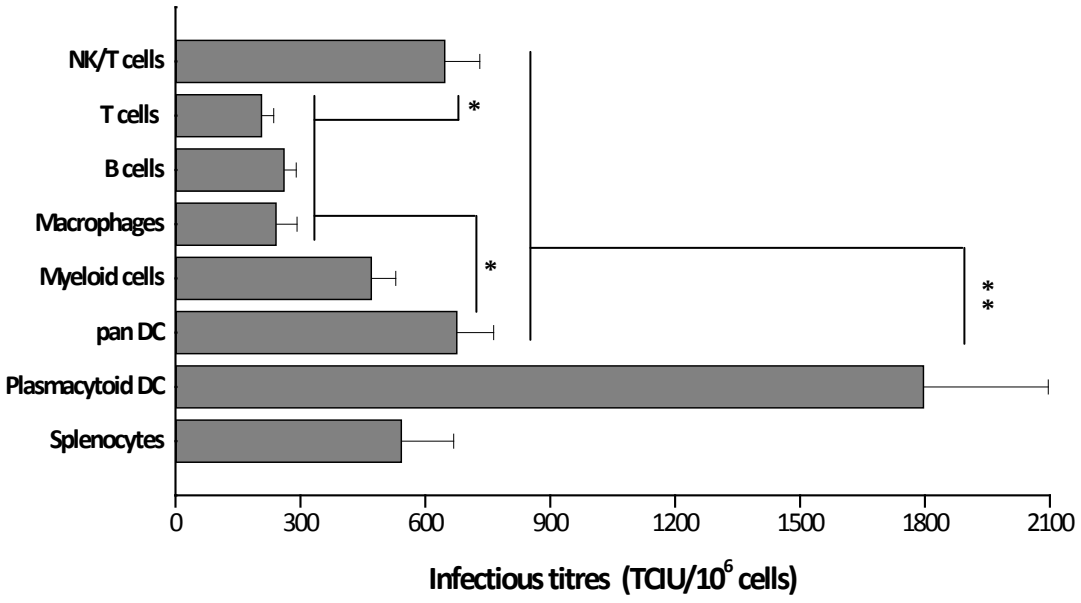

Figure 3.7 Distribution of infectivity in splenic cell types at 30 dpi. Infectious titres at 30 dpi from **table 3.4** were re-plotted for clarity. Significant differences between pDCs, *pan*DCs and NK/T cells and B cells, macrophages and T cells are indicated (* for a $p < 0.05$ or ** for a $p < 0.001$).

In an attempt to understand the participation of highly infectious pDCs on prion colonisation of the LRS, we examined the effect of pDC depletion on prion titres in spleen and MLNs. Previous studies have shown that administration of anti-mPDCA-1 can efficiently deplete pDCs *in vivo* (Krug *et al.*, 2004; Bailey-Bucktrout *et al.*, 2008). Groups of four mice were injected i.p. with 250 µg anti-mPDCA-1 or an isotype control before and after i.p. inoculation with prions. Injections were done every 2-3 days to a total of 8 injections covering most of the incubation period until the animals were culled at 19 dpi. Of note, the experiment was not controlled for the level of pDC depletion during the assayed period and can only be considered as preliminary.

Nevertheless, prion titres of MLNs were reduced by one log in pDC-depleted mice as compared to isotype control antibody-treated mice (**table 3.6**) suggesting that pDCs may somehow contribute to the prion titres in lymph nodes. No effect, however, was detected on splenic prion titres (**table 3.6**).

129Sv x C57B/6 mice	Spleen		Mesesenteric lymph nodes	
	Control (log TCIU/g)	**Treated** (log TCIU/g)	**Control** (log TCIU/g)	**Treated** (log TCIU/g)
1	7.04	6.37	5.29	4.33
2	6.78	6.76	4.86	4.42
3	6.25	7.25	5.78	3.46
4	6.13	6.47	5.20	4.66
Mean titre ± SD	6.70 ± 0.28	6.86 ± 0.30	5.41 ± 0.28	4.38 ± 0.24

Table 3.6 Effects of *in vivo* depletion of pDCs on prion titres of spleen and mesenteric lymph nodes. Before and after i.p inoculation with RML prions four mice per group were treated either with mPDCA-1 antibodies *(treated)* showed to deplete pDCs *in vivo*, or with the appropriated isotype control *(control)* as described in the main text. Animals were culled at 28 dpi to determine infectious titres of MLNs and spleens.

The high infectious titres of pDCs prompted us to investigate whether pDCs fulfil the criterion for prion-propagating cells. The expression of PrP^C, a pre-requisite for prion replication, was reportedly undetectable (del Hoyo *et al.*, 2006) or lower (Rybner-Barnier *et al.*, 2006) in pDCs as compared to other DCs in C57BL/6 mice. To exclude mouse strain-dependent differences in PrP^C expression levels, we determined the levels of PrP^C expression on pDCs. In agreement with previous reports (del Hoyo *et al.*, 2000), PrP^C expression was undetectable arguing against a direct role of pDCs in prion replication (**figure 3.8**).

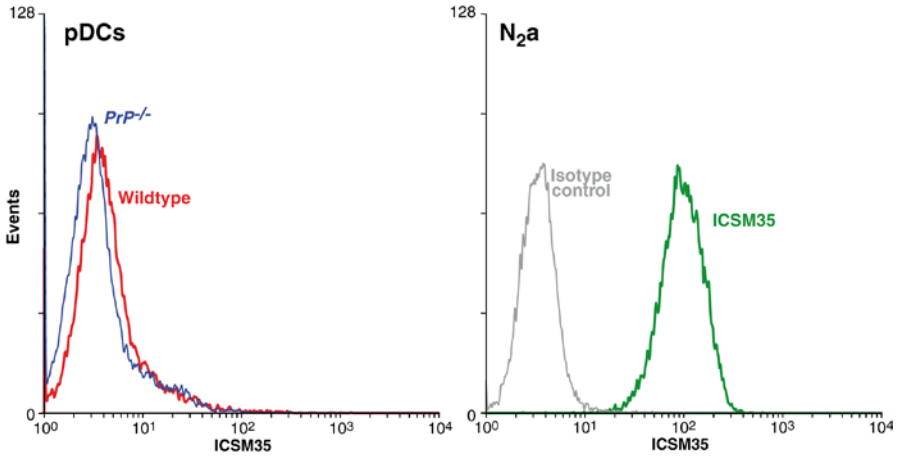

Figure 3.8 PrP^C expression of splenic pDCs. PDCs isolated from spleens of uninfected 129/Sv x C57BL/6, or *Prnp*$^{-/-}$ mice used as control, were analyzed by flow cytometry for PrP^C expression with biotinylated anti-PrP monoclonal antibody ICSM35. Allophycocyanin (APC)-conjugated streptavidin was used as secondary label. As a control for PrP^c expression mouse neuroblastoma cells (N2a) were labeled with biotinylated ICSM35 and biotinylated mouse IgG2b isotype control.

Prion infectivity was detected at extremely low titres in blood of rodents at presymptomatic and symptomatic stages and were associated with plasma and buffy coat fractions (Brown *et al.*, 1998; Castilla *et al.*, 2005a; Tattum *et al.*, 2010). In a previous report infectivity was not detected in peripheral blood leukocytes in 129/Sv x C57BL/6 mice at early stages of disease regardless of relatively high titres in B and T lymphocytes of the spleen (Raeber *et al.*, 1999a). Given the high infectious titres of DCs and pDCs we examined whether prion infectivity is associated to pDCs in blood. Although recirculation of DCs is greatly limited as compared to lymphocytes, evidence for recirculation under steady-state condition has been reported (Bonasio and von Andrian, 2006). The migratory pattern of pDCs greatly varies from convectional DCs, most reports support the view that pDCs enter the lymph nodes via the bloodstream (Randolph *et al.*, 2008). To determine whether prion infectivity is associated to pDCs in the blood we isolated pDCs from EDTA-treated whole blood. However, no infectivity

was associated with pDCs (**table 3.5**), lymphocytes and DCs (data not shown) from blood at 30 dpi under our experimental conditions.

Despite lymphocytes actively recirculate in steady-state conditions, no infectivity was detected lymphocytes isolated from blood (Raeber *et al.*, 1999a; our own observation) suggesting prion infected B cells are somehow confined in lymphoid organs. Interestingly, a recent study showed an abnormal germinal centre reaction in the spleen of scrapie-infected mice which was associated with increased maturation and numbers of B lymphocytes and hypertrophy of FDC dendrites in at 70 dpi and endstage (McGovern *et al.*, 2004). To examine whether prion related changes in splenic B cell subsets were detectable at preclinical stages, groups of three age-matched mice were inoculated i.p. with 1 % RML infected or uninfected CD1 brain homogenate and culled at 30, 80 and 100 dpi. Splenocytes were analysed by three-color FACS for CD19, CD21 and CD23. However, no changes were detected in the ratios of marginal zone B cells ($CD21^{hi}$ $CD23^{-}$) and follicular B cells ($CD21^{int}$ $CD23^{hi}$) (**figure 3.9**).

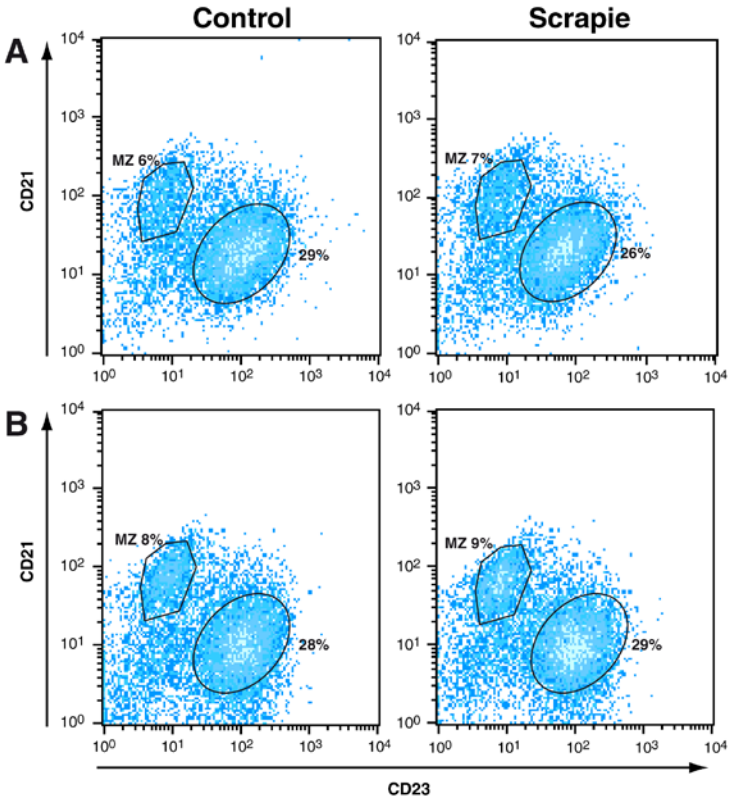

Figure 3.9 No abnormalities of splenic B cell subsets at preclinical disease. 129Sv x C57BL/6 mice were inoculated i.p. with 100 µl 1 % RML I6200 or 100 µl 1 % uninfected CD1 homogenate and culled at 80 dpi (**A**) and 100 dpi (**B**). Splenocytes were isolated according to materials and methods (**section 2.1.1**). To analyse B cell subsets splenocytes were labelled with mAbs against anti-CD19, anti-CD23 and anti-CD21. The CD19-gated B cell population was examined for CD21/35 and CD23 expression. Figures are representative of three independent experiments.

3.5 Contribution of the stromal compartment

A wealth of evidence indicates that stromal cells play a fundamental role in prion pathogenesis (Clarke and Kimberlin, 1984; Fraser and Farquhar, 1987; Fischer *et al.*, 1996). In particular, follicular dendritic cells (FDC) are considered prime candidates for prion replication in the LRS as inferred from studies where temporal depletion of FDCs abolished prion accumulation in the spleen and prolonged incubation times (Mabbott

et al., 2000; Montrasio *et al.*, 2000). Other stromal cell types, presumably fibroblastic reticular cells were shown to support prion replication when FDCs are absent, as shown for granulomas (Heikenwalder *et al.*, 2008). Macrophages that accumulate abnormal PrP in TNFR1$^{-/-}$ lymph nodes were also suggested alternative replication sites (Prinz *et al.*, 2002).

The contribution of the stromal compartment to prion replication has been addressed previously. In these studies the separation of splenic pulp from the stromal tissue was achieved by forcing spleens through a mesh and by repeatedly flushing out pulp cells using a syringe, respectively (Clarke and Kimberlin, 1984; Raeber *et al.*, 1999a; Kaeser *et al.*, 2001). Clarke and Kimberlin showed that about ten-fold higher titres were associated to the stromal, as compared to the pulp fraction of the spleen (Clarke and Kimberlin, 1984). The accumulation of disease-specific PrP was detected extracellularly on FDC membranes (Kitamoto *et al.*, 1991; Jeffrey *et al.*, 2000), suggesting that infectivity in the stromal compartment is most likely associated with these cells. However, infectious titres have not been determined for FDCs.

Whilst in the previous section we determined the contribution of the haematopoietic cell types to total prion titres in spleen, we now aimed to determine the titres of stromal FDCs in *wt* and *Prnp*$^{-/-}$ mice. In addition, we established an *in-vitro* model to study the involvement of the stromal compartment in prion pathogenesis by setting up heterogeneous stromal cultures from spleens of scrapie-infected mice and investigated their propensity to propagate prions.

3.5.1 Isolation of follicular dendritic cells

"I have not failed. I've just found 10,000 ways that won't work." Thomas A. Edison

The isolation of FDCs for the determination of infectious titres poses major challenges. FDCs are rare (1 in 10,000 cells) and highly connected cells with long dendritic processes, tightly anchored to reticular fibres. They are intimately associated with

B cells to form FDC-B clusters (Schnizlein *et al.*, 1985). Standard isolation methods for FDCs include immunization and sublethal irradiation of mice to boost the number of germinal centres and to deplete lymphocytes, respectively (Kosco-Vilbois *et al.*, 1993). However, we refrained from adapting these protocols, since these are likely to have profound effects on prion titres (Dickinson *et al.*, 1978; Fraser and Farquhar, 1987).

A critical step to successfully isolate FDCs is the gentle and complete disaggregation of stroma tissue by enzymatic digestion (Schnizlein *et al.*, 1985). Once released from tissue FDCs were enriched on a density gradients (FDCs float at densities around 1.06-1.05 g/ml), followed by the removal of fibroblasts and myeloid contaminants by adhesion to plastic (Schnizlein *et al.*, 1985). Alternative protocols for the enrichment of FDCs exploit the formation of clusters between FDCs and lymphocytes immediately after isolation (Kosco *et al.*, 1992). The separation of FDC clusters from single cells can be achieved by consecutive 1 x *g* sedimentations (Tsunoda *et al.*, 1990). MACS isolation was used as a more specific method to isolate FDCs (Schmitz *et al.*, 1993; Sukumar *et al.*, 2006). A purity of up to 90 % was reported for the isolation of murine FDCs by MACS when used in combination with immunization and irradiation protocols (Sukumar *et al.*, 2006).

Based on established protocols, we attempted to isolate FDCs from spleens of non-immunized, non-irradiated mice as depicted in **figure 3.10 A**. After extensive enzymatic digestion of spleen tissue, released cells were loaded onto discontinuous gradients. Low-density cells contained high numbers of cell clusters as confirmed by microscopy (**figure 3.10 C**). Low-density cells labelled with mAbs anti-FDC-M1 and anti-FDC-M2 were only marginally more positive than unlabelled cells used as controls in this case (**figure 3.10 B**). Incubation of cells on Petri dishes at 37 °C for 40 min only partly removed myeloid contaminants (**figure 3.10 D**). We next attempted to isolate FDCs by MACS using a modified protocol from Sukumar *et al.* (Sukumar *et al.*, 2006). Briefly, cells were labeled for 1 h with 0.64 µg/ml anti-FDC-M1, followed by 30 min

incubation with 5 µg/ml PE-conjugated mouse anti-rat Ig κ as secondary antibody. PE-conjugated mouse anti-rat Ig κ labelled cells were isolated using PE-microbeads. However, isolated cells with a yield < 1 % were negative for FDC-M1 and FDC-M2 as analyzed by flow cytometry (data not shown). To test the specificity of the pull down, we sorted cells in presence and absence of FDC-M1, which demonstrated that the sort with mAbs against FDC-M1 was unspecific (**figure 3.10 E**). The use of FcR blocking reagent or 10 % mouse serum to block unspecific binding did not improve the experimental outcome.

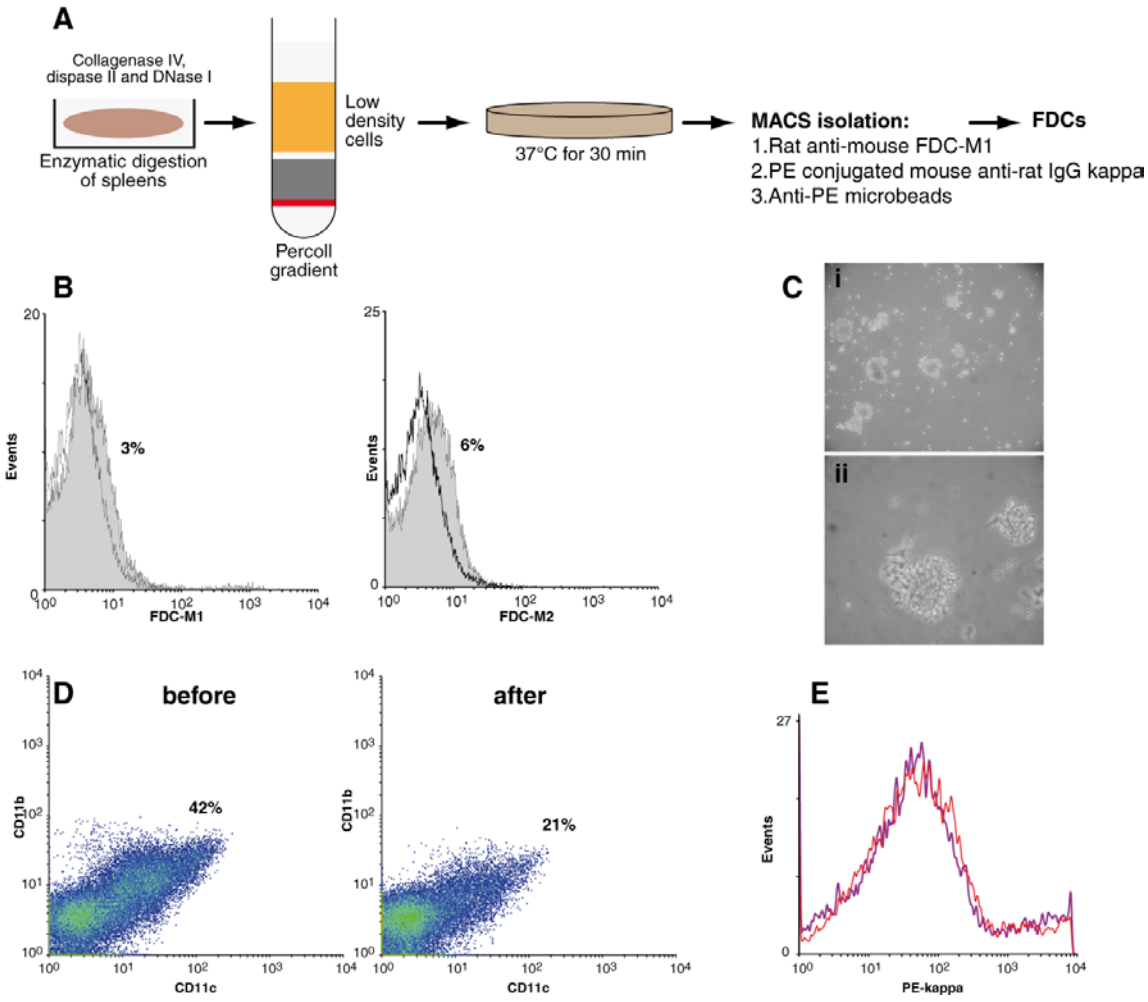

Figure 3.10 Summary of FDC isolation from spleen tissue. (**A**) Experimental procedure for FDC isolation. After collagenase digestion released cells were separated by density gradient centrifugation. Cells from the upper band of the low density population were retrieved and incubated in a Petri dish at 37 °C for 40 min. Non-adherent cells were harvested and used subsequently to isolate FDC-M1^{+} cells by MACS. Low density cells isolated in a Percoll gradient contained FDC-clusters as shown by direct microscopic observation (**B**) and were weakly positive for FDC-M1 and FDC-M2 (**C**). Empty histograms correspond to the unlabelled controls. Myeloid contaminants were partially removed after a 40 min adherence step in medium at 37 °C and 5 % CO_2 (**D**). Low density cells were magnetic sorted with PE-conjugated mouse anti-rat IgG κ in the presence (*red*) and absence (*purple*) of FDC-M1 as a primary antibody. Overlay histogram of the two sorted populations (**E**).

Immune complex labelling

Since magnetic sorting failed to isolate FDCs we sought to establish alternative isolation methods. The retention of immune complexes (IC) on FcR and complement receptors is a hallmark of FDCs and has previously been used to determine the purity of FDC preparations (Sukumar *et al.*, 2008). While FDCs retained ICs on their surfaces, peritoneal macrophages and lymphocytes were shown to phagocytose and clear ICs. Internalised and surface exposed ICs were distinguished by secondary antibody labelling of exposed ICs (Sukumar *et al.*, 2006).

By exploiting the unique ability of FDCs to retain ICs surface-bound for long periods, we attempted to isolate FDCs from a mixed high density cell population containing B cells, DCs and macrophages by pulse-chase experiments. Importantly, 125I-labelled IgG complexes were rapidly internalised into mouse macrophages with half-time values (t ½) of less than 2 min (Mellman and Plutner, 1984). The question therefore arose whether conditions could be established to distinguish FDCs from macrophages, DCs and B cells by means of their biological propensity to retain ICs.

To test this approach isolated macrophages, DCs and B cells were labelled with ovalbumine ICs (OVA ICs) at 4 °C for 2 h. After washing excess OVA ICs, cells were kept in ice-water to prevent internalization, and then transferred to 37 °C at distinct time intervals (1 min, 5 min, 10 min, etc), followed by labelling with a secondary antibody.

Although ICs are internalised into DCs, B cells and macrophages during a 30 min incubation period the fluorescent signal was still very high, possibly due to the reappearance of processed IC fragments on the surface of cells or due to unspecific binding of OVA ICs (**figure 3.11**). OVA fluorescence was not significantly reduced by extending the incubation period to 1 h (data not shown). Under these conditions the identification by flow cytometry of low numbers of FDCs in the low density fraction after gradient centrifugation was not possible.

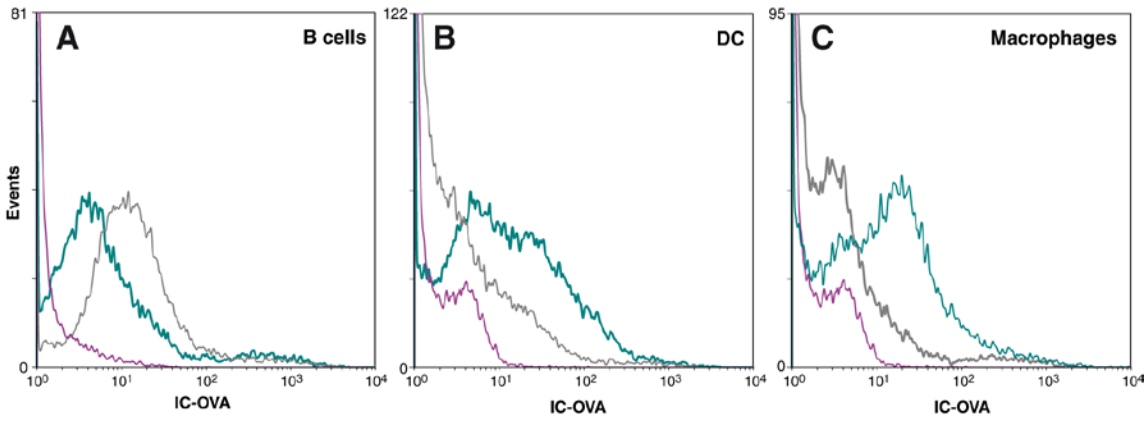

Figure 3.11 Internalization of OVA immune complexes by B cells **(A)**, DCs **(B)** and macrophages **(C)** after 30 min incubation at 37 °C. Cells were incubated with OVA/anti-OVA for 1 h and then placed into a water bath at 37 °C for 30 min *(grey)*. As a control cells were kept on ice throughout the experiment *(green)*. Unstained cells were used to locate the viable cells within the first log *(pink)*.

3.5.2 Infectious titres of follicular dendritic cell clusters

Due to the failed isolation of FDCs by MACS, we investigated whether the contribution of FDCs to spleen titres could be assessed using FDC clusters instead. Splenic FDC/B clusters isolated from *wt* and *Prnp*$^{-/-}$ mice that were inoculated with prions were isolated by successive sedimentations at 1 x *g* in FBS as described in material and methods (**section 2.2.1**). This method was favoured over density gradient centrifugation, since it yielded more cell clusters/single cells (*ca.* 150,000 clusters were isolated on average from 10 spleens). Isolated cell clusters were positive for FDC-M1, indicating the presence of FDCs (**figure 3.12**).

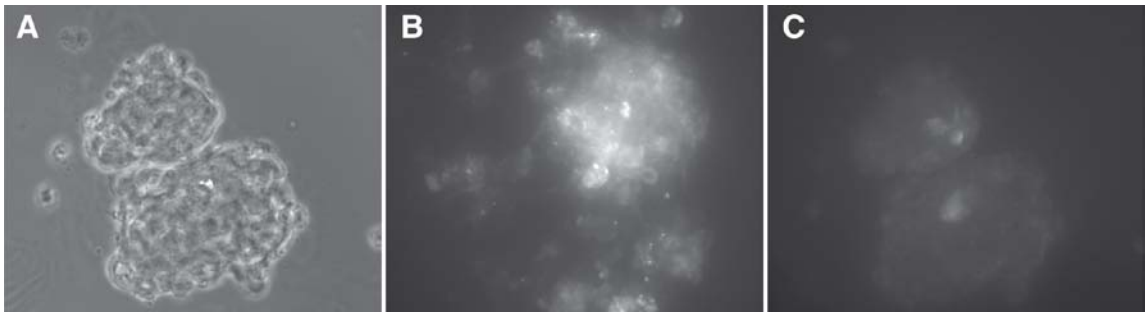

Figure 3.12 Characterization of follicular dendritic cell clusters. Following extensive collagenase digestion of spleen tissue, (**A**) cell clusters were isolated by 4 successive sedimentations at 1 x *g* in FBS. Isolated cells were cultured on coverslips and examined by fluorescence microscopy for FDC-M1 (**B**) and the corresponding isotype control (**C**). PE-anti-kappa was used as secondary antibody.

A typical FDC/B cell cluster is composed of 1 to 3 FDCs, 5 to 30 B cells and a few T cells attached (Kosco *et al.*, 1992; Liu *et al.*, 1996). To compare infectious titres of FDC clusters with previous data of single splenic cells, we determined the protein concentration of isolated cells and expressed titres as TCIU/mg of protein.

Prion titres of FDC clusters at 14 dpi and 30 dpi were compared to those of pDCs and NK cells. FDC clusters isolated at 14 dpi showed the highest prion titres and were as infectious as pDCs at 30 dpi (**table 3.7 A**). Of note, the data presented in **table 3.7** corresponds to a single experiment. Nonetheless, under these conditions titres of pDCs and NK cells were consistent with previous results.

Interestingly, infectivity could also be detected in FDC clusters at 3 dpi in the absence of prion replication (**table 3.7 B**).

A

Wild-type mice		
Cell types	**Log TCIU/mg protein**	
	14 dpi	**30 dpi**
pDC	2.8	3.6
NK cells	2.6	3.3
FDC clusters	3.4	3.6

B

Prnp$^{-/-}$ mice	
Cell types	**TCIU/mg protein**
	3 dpi
***Pan* DC**	8.3
B cells	u.d
FDC clusters	11.5

Table 3.7 Infectivity associated to FDC clusters in *wild-type* and *Prnp*$^{-/-}$ mice. Groups of 10 **(A)** *wt* or **(B)** *Prnp*$^{-/-}$ mice were inoculated i.p. with 1 % RML and culled at different time points after inoculation. Since accurate cell numbers cannot be obtained for FDC clusters, titres were calculated per mg protein. Each of the titres corresponded to one experiment. *u.d.* undetectable.

3.5.3 Stroma cultures isolated from spleens of scrapie-infected mice do not propagate prions *ex vivo*.

Stromal cells are considered the main players in prion pathogenesis possibly with a role in prion replication (Fraser and Farquhar, 1987; Brown *et al.*, 1999; Kaeser *et al.*, 2001). In the previous section we showed that isolated stroma tissue and FDC clusters were infectious (**table 3.7**). We now asked whether freshly isolated stromal cells were able to propagate prions *ex vivo*.

Long-term stromal cell cultures were established from spleens of adult *wild-type* mice. Following prolonged collagenase digestion of spleens, low density splenic cells were separated by density gradient centrifugation as described in material and methods (**section 2.2.2**). These cultures were very heterogeneous when newly established (**figure 3.13 C**), but lost heterogeneity with prolonged culture. At high passage numbers cells were mainly fibroblast-like. According to flow cytometric analysis stromal cultures contained mainly fibroblasts (podoplanin^{+}) and myeloid cells (CD11c^{+}CD11b^{+}), whereas no lymphocytes and NK cells were present (**figure 3.13 A**). Stromal cells were also shown to express PrP^{C} (**figure 3.13 B**).

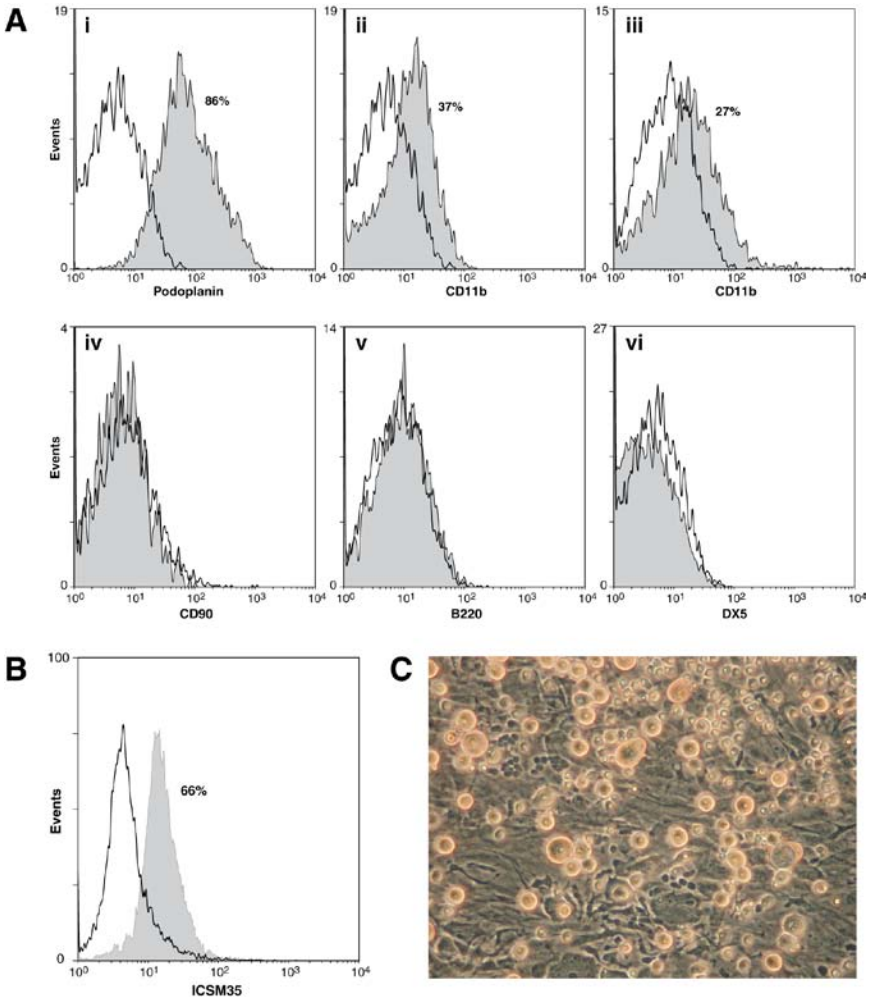

Figure 3.13 Characterization of stroma cultures. Low density cells, isolated by density centrifugation of splenic cells, were collected and cultured in sIMDM at 34 °C and 5 % CO_2. Cultures of stroma cells were established shortly after isolation. (**A**) Stroma cultures were characterised by flow cytometry with mAbs against podoplanin (fibroblasts), CD11c (DCs) and CD11b (macrophages); CD90, B220 and DX5 are specific for lymphocytes and NK cells (*i-vi*). (**B**) The expression levels of PrP^C were determined on fixed stroma cells using biotinylated ICSM35 and FITC-streptavidin as secondary staining. (**C**) Distinct functional areas can be identified in the stromal cultures. Attached to layers of fibroblastic cells myeloid cells are continuously formed.

To determine whether newly established splenic stroma cells replicate prions *ex vivo*, 129Sv x C57B/6 mice were inoculated i.p. with 1 % RML, culled at 50 dpi and spleens

used to generate the stromal cultures. Prion infectivity associated to confluent layers of stroma cells was measured by SCEPA at each 1:3 passage. However, infectivity rapidly declined during cell splits and no evidence for prion replication of RML prions was observed under these conditions (**figure 3.14**). A replication-competent stroma cell type, if present in these cultures, may not be detected in this model where the high cell division rates may dilute prions at a greater rate than they are formed and lead to its eventual clearance.

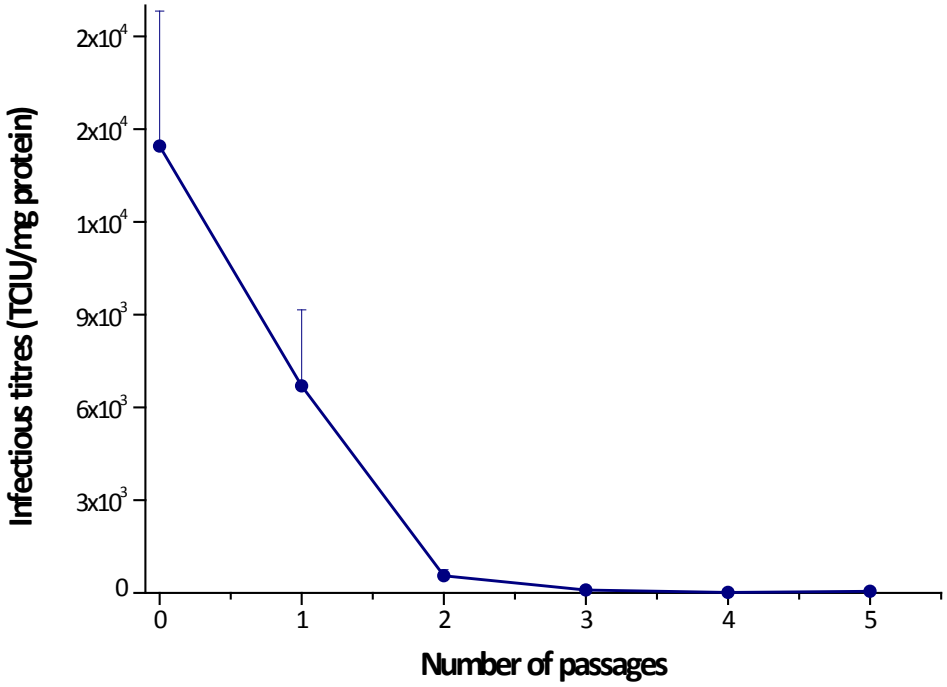

Figure 3.14 Infectivity of stroma cell cultures after splitting. Stromal cell cultures were established from *wild-type* 129Sv x C57B/6 mice inoculated i.p. with 100 µl of 1 % RML culled at 50 dpi. Infectious titres of confluent layer of stroma cells were measured overtime at different each 1:3 passages. Titres are expressed per mg protein.

3.5 *Ex-vivo* release of prions from scrapie-infected splenic cells

The molecular mechanisms involved in the dissemination of prions from the sites of infection to lymphoid organs and to peripheral nerves are poorly understood. Several immune cells including lymphocytes, DCs and macrophages accumulate prions early in the disease process, and extracellular deposits of disease-associated PrP were detected in conjunction to FDC membranes (Jeffrey *et al.*, 2000). Several mechanisms for the lateral spread of prions including direct cell-to-cell contact (Kanu *et al.*, 2002), prion transmission via membrane nanotubes (Gousset *et al.*, 2009) and the release of prions via exosomes (Fevrier *et al.*, 2004) have been suggested from several *in-vitro* studies. The *in-vivo* relevance of these processes has not been demonstrated and poses major experimental challenges.

Exosomes are small vesicles of endosomal origin secreted by all major immune cells, including lymphocytes and dendritic cells (reviewed in Thery *et al.*, 2002). Exosomes were detected attached to the surface of FDCs *in vivo* (Denzer *et al.*, 2000). Several cell lines secrete infectious exosomes (Fevrier *et al.*, 2004; Vella *et al.*, 2007; Alais *et al.*, 2008). To test whether the release of exosomes plays a role *in vivo* we investigated whether MACS-isolated immune cells from scrapie-infected animals secrete infectivity when cultured *ex vivo*.

Freshly isolated B cells, T cells and DCs from scrapie-infected mice were cultured for 38 h and culture supernatants were sequentially centrifuged according to protocols used for the isolation of exosomes (Johnstone *et al.*, 1987; Thery *et al.*, 1999; Wolfers *et al.*, 2001). After ultracentrifugation pellets were resuspended in medium and prion infectivity was determined by SCEPA. The limited survival of immune cells *ex vivo*, particularly of lymphocytes, may bias the determination of prion secretion where prions are released by passive leakage from necrotic cells. To account for the contribution of passive leakage of prions from dead cells we cultured cells at

atmospheric CO_2 at 37 °C in parallel experiments, a treatment that led to rapid necrosis of B and T lymphocytes (**figure 3.15**, **table 3.8**). In DCs exposure of cells to atmospheric CO_2 did not suffice to trigger rapid necrosis and we added Triton X-100 at low concentrations (0.01 % final) to the culture medium. Exosomes can be released both in a constitutive and in a regulated manner (Thery *et al.*, 2002). Exosome release upon B cell activation via CD40 and the IL-4 receptor have been reported, suggesting that exosome release might depend on external signalling from other immune cells (Saunderson *et al.*, 2008). We added IL-4 and LPS to the cultures, a treatment that leads to activation of lymphocytes and improved the viability of B cells (**figure 3.15**).

A more than 30-fold increase in infectious titres was detected in supernatants of B cells and DCs under basal conditions as compared to passive release controls, indicating that prions from scrapie infected cells are actively released (**table 3.8**). Supplementation of medium with IL-4, but not with LPS marginally increased prion titres of cell supernatants. The titres of released prions constitute about 1 % of the cellular infectivity of B cells and DCs. Similar values have been reported for the *in-vitro* release of PrP^{Sc} from cell lines using Western blot quantification (Fevrier *et al.*, 2004). To examine whether prion secretion in B cells is associated with exosome release we resuspended pellets from basal medium and atmospheric CO_2 in PBS after ultracentrifugation and absorbed aliquots of 3 µl onto EM grids for microscopic analysis (**figure 3.16**). The number of cup-shaped exosomes under basal conditions exceeded the number of exosomes during passive leakage by a factor of ten (1.7 ± 1.2 *vs.* 20.1 ± 5.7, $p < 0.001$). Microparticles shed by apoptotic or stimulated cells ranging from 200 to 1000 nm in diameter (Boulanger *et al.*, 2006; Kiama *et al.*, 2006; Schiller *et al.*, 2008; Beyer and Pisetsky, 2010) were infrequently detected under our experimental conditions with rates below 0.4 microparticles per count area of 2.82 μm^2 with no significant difference between basal medium and passive leakage control.

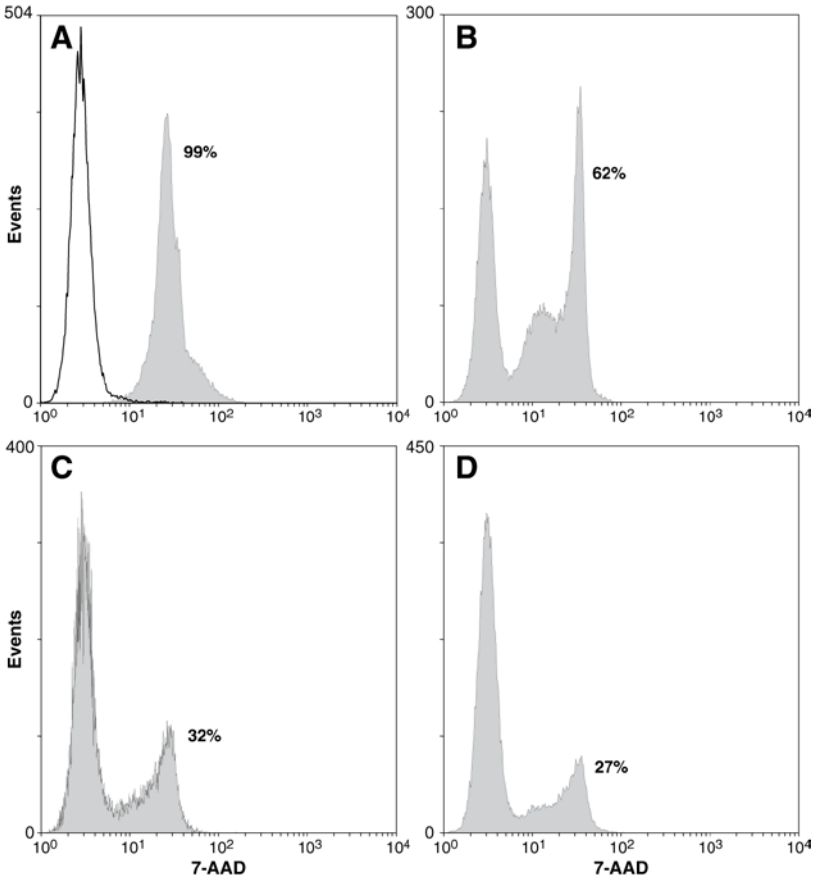

Figure 3.15 Effects of culture conditions on the viability of primary cultures of B lymphocytes. IMDM supplemented with 10 % FBS, 100 U/ml Pen-Strep, 2mM L-glutamine and 5 µM 2-ME was used as basal medium for all cell cultures. As a positive control for the unspecific release of infectivity, B lymphocytes were cultured at atmospheric CO_2 and 37 °C (**A**). Representative histograms for B cells, cultured at 5 % CO_2 and 37 °C in basal medium (**B**), in the presence of 10 ng/ml IL-4 (**C**) and with 50 µg/ml LPS (**D**) are shown. Cell viability was assessed by 7-AAD exclusion after 36 h culture. Empty histogram in **A** corresponded to unlabelled cells, this was not included in the other figures for simplicity as it was clear the position the unlabelled population.

Culture Conditions	B cells		T cells		‡Dendritic cells	
	Release (TCIU/10^6 cells ± SE)	Necrosis (%)	Release (TCIU/10^6 cells± SE)	Necrosis (%)	Release (TCIU/10^6 cells)	Necrosis (%)
atm. CO_2†	0.2 ± 0.3	100	< 0.1	100	0.2	100
Basal	5.6 ± 1.0	63	1.1 ± 0.3	48	6.8	51
basal + IL4	6.3 ± 1.2	34	1.9 ± 0.4	22	n.d.	n.d.
basal + LPS	4.4 ± 0.8	28	n.d.	n.d.	n.d.	n.d.
Cellular infectivity	227		188		898	

†Control incubations were performed in basal medium at atmospheric (atm.) CO_2 and 37 °C.

‡For dendritic cell cultures Triton X-100 was added to a final concentration of 0.01 % in basal medium.

n.d. = not determined

Table 3.8 Prions are actively released from scrapie-infected splenic cell cultures *ex vivo.* Fifteen 129Sv x C57BL/6 were inoculated i.p. with 100 µl RML I6200 and culled at 60 dpi (a time point at which infectivity should have been reached a plateau phase). MACS-isolated B and T lymphocytes were cultured at a concentration of 1 Mio/ml in basal medium (IMDM medium, 10 % FBS) in absence or presence of LPS (50 µg/ml) and IL-4 (10 ng/ml). After 36 h of culture conditioned medium was collected and centrifuged at 300 x g for 10 min, 5000 x g for 15 min and 10,000 x g for 30 min to remove cells and debris. The supernatant was then centrifuged for 2 h at 100,000 x g and the pellet resuspended in PBS, serially diluted and infectious titres were determined using the SCEPA. The detection limit of the SCEPA is 0.1 TCIU/Mio cells and corresponds to 1 positive well out of 12 wells. Titres were calculated by GLM as TCIU/10^6 cell equivalent ± SE of three independent experiments. Data for one single experiment is shown for the release of infectivity from DCs.

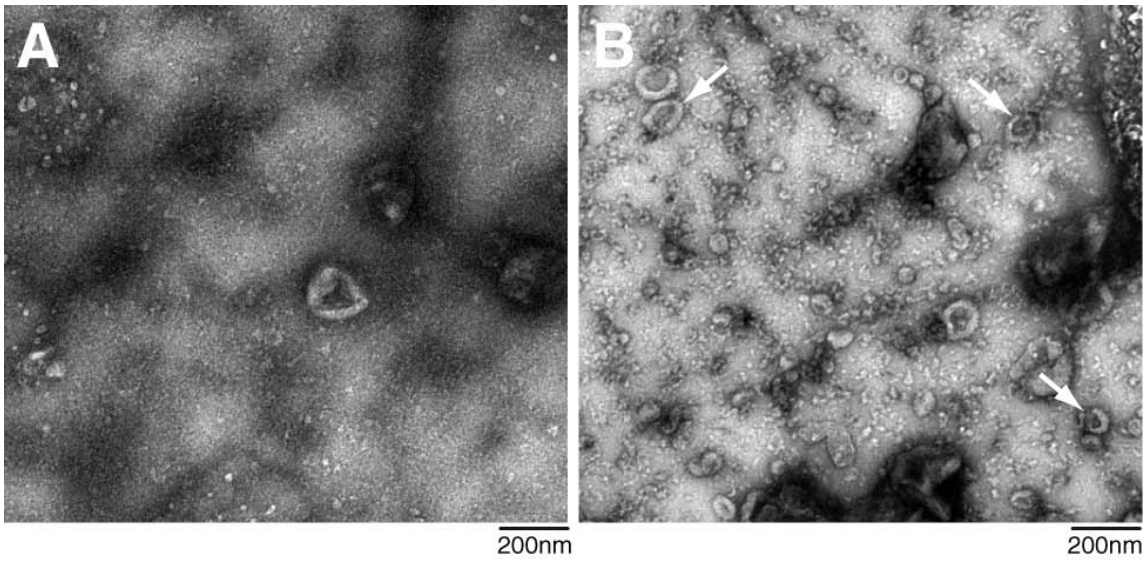

Figure 3.16 Exosomes are released from scrapie-infected B cells *ex vivo*. Spleens were dissected from 129/Sv x C57BL/6 mice 30 days after i.p. inoculation with 1 % (w/v) RML I6200. MACS-isolated B lymphocytes were cultured under passive leakage (**A**) and basal (**B**) conditions essentially as described in **table 3.8** and tissue culture supernatants were isolated by sequential centrifugation (see materials and methods, **section 2.3**). After centrifugation at 100,000 x g for 2 h pellets were resuspended in PBS, absorbed onto carbon-coated grids and negatively stained with 1 % uranyl acetate. Cup-shaped exosome-like membrane particles of different sizes (see arrows) are shown in (**B**). Twenty randomly recorded images (surface area: 2.82 μm^2) from each condition were counted and the number of exosome-like particles (1.7 ± 1.2 (A) and 22.8 ± 6.5 (B) per surface area, $p << 0.001$) determined in a blinded manner. Scale bar: 0.2 µm.

CHAPTER 4

DISCUSSION

DISCUSSION

Prion colonisation of the lymphoreticular system (LRS) is a hallmark of most prion diseases. Stromal and mobile haematopoietic cells participate in different aspects of lymphoinvasion, including replication and dissemination of prions. Prion propagation in the LRS is a dynamic process that is thought to depend on the interaction and contribution of different cell types. While most research focused on the identification of the sites of prion replication, in particular the role of follicular dendritic cells (FDC), little is known about the role of mobile haematopoietic cells in prion pathogenesis and the molecular underpinnings of prion dissemination.

4.1 Establishment of a method to determine infectious titres of splenic cell types involved in prion pathogenesis

By taking advantage of fast *in-vitro* infectivity testing (SCEPA) and magnetic activated cell sorting (MACS) we established a novel procedure to determine infectious titres of seven different cell types, including B cells, T cells, NK cells, DCs, the DC subset pDCs, FDC clusters and macrophages during the first weeks after inoculation with prions and addressed the dynamics of prion accumulation in the spleen.

Fluorescence-activated cell sorting (FACS) and MACS are commonly used cell separation techniques that yield highly purified cell populations. However, the comparatively low throughput of FACS (> 200-fold lower rates than MACS) limits its application when large numbers of cells are processed. Using high capacity cell sorting by MACS, we developed and optimised a procedure that uses sequential rounds of positive selection to isolate different cell types from a pool of splenocytes at high purities (**figure 3.4**) and reasonable processing times, i.e. six cell types were isolated in approximate 5 hours (**figure 2.1, table 3.3**).

Comprehensive studies to compare prion titres in candidate cell types at early stages of disease have not been performed due to limitations of traditional methods for infectivity testing. Animal bioassays, the principal method to determine infectious titres, are based on i.c. inoculation of infected samples into indicator mice. Generally, a minimum of four to six indicator mice are inoculated i.c. with serially diluted samples and infectious titres are calculated from the mortality data. Ethical and economical factors greatly limit the number of samples that can be processed by the bioassay. As an alternative, immunodetection of PrP^{Sc} by Western Blot, a fast *in-vitro* assay to characterise an infectious state, is most frequently used. Defined by its partial resistance to protease degradation, PrP^{Sc} is a surrogate marker for infectivity but PrP^{Sc} levels reportedly do not always correlate with prion titres (Sakaguchi *et al.*, 1993; Lasmezas *et al.*, 1997; Barron *et al.*, 2007). As a consequence, the bioassay is indispensable to confirm prion infectivity. Furthermore, the reduced sensitivity of PrP^{Sc} detection on Western Blot as compared to infectivity testing limits its use at early stages of disease when titres are low. In 129Sv x C57/BL6 mice PrP^{Sc} was not detected on Western Blot at 3 and 7 dpi in spleens, despite prion titres ranged between 5.4 to 6 log TCIU/g tissue (**figure 3.6**). The SCA, on the other hand, is a valuable alternative to the bioassay: it is sensitive, detects *de-novo* formed prions and greatly extends the scope of *in-vivo* assays. Still, the limited permissiveness of N2a cells to different prion strains renders animal bioassays yet indispensable. However, the identification of prion-susceptible cell lines with broader susceptibilities for mouse-adapted prion or natural scrapie strains is of great importance (Vorberg *et al.*, 2004; Mahal *et al.*, 2007; Neale *et al.*, 2010) and may further help to limit the requirement of bioassays.

A more sensitive version of the standard SCA, the SCEPA, was used in our studies to determine prion titres and is based on the observation that the proportion of infected cells greatly increases by altering the split ratio during passages. After exposure of prion-susceptible cells with limiting dilutions of prion-containing samples PrP^{Sc}-positive

cells could be detected after several passages (Klohn *et al.*, 2003). For example, a 10^{-9} dilution of RML (I6200, 9.3 log LD_{50} units/g brain) resulted in 2 positive wells out of 24, corresponding to a remarkable sensitivity of at least 2 LD_{50} units/ml (**table 3.1**). Given the technical and experimental advantages of the SCEPA, the important question arose how the sensitivity of SCEPA compares to that of the bioassay. Comparative endpoint titrations showed that the sensitivity of SCEPA was not significantly different from the bioassay given the high standard error of the bioassay (**table 3.1**). However, in experiments where prion titres of splenic cell types were determined, SCEPA was about one log less sensitive than the bioassay (**table 3.2**). The particle size of the infectious entity may be of particular importance for a cell-based assay, where infectious particles have to be internalised for propagation to resume. Differences in the dispersion state between homogenates or in the sensitivity to degradation by endogenous proteases might explain the reduced sensitivity of SCEPA for the estimation of cell titres as compared to tissue titres.

In conclusion, known advantages of SCEPA, like the short assay duration, the low costs and the increased experimental scope clearly outweigh the somewhat lower sensitivity levels for prion determination. High throughput prion determination by SCEPA therefore renders comparative studies to assess the contribution of specific cells types to prion accumulation in the LRS feasible.

The average number of infectious units in the SCEPA, termed tissue culture infectious units (TCIU) can be estimated by assuming that the number of PrP^{Sc} positive cells at a given dilution follows a Poisson distribution (Klohn *et al.*, 2003; Mahal *et al.*, 2008). Inherent to limiting dilution assays, however, the error variance may not be constant over the studied range of dilutions (**figure 3.1**) and thus violate premises of conventional linear regression analysis where normally distributed error components with constant variance are assumed. This may lead to large errors and compromise the estimation of precise infectious titres. To address this problem we here established a

generalised linear model (GLM) (Nelder and Wedderburn, 1972) for the estimation of robust infectious titres. GLM overcomes restrictions of ordinary regression models limited to normally distributed response variables and unify a wide range of probability distributions including normal, binomial and Poisson using a flexible iterative method for computing maximum likelihood estimates (see **appendices**). Alternatively, non-parametric test such Spearman-Karber or Reed-Muench can be used to determine prion titres when data is not normally distributed, for example in animal bioassays. Where the median lethal dose (LD_{50}) estimate may be a reasonable guess of the titre for an assay with no repeats, the corresponding standard error is comparatively high (**table 3.1** and **3.2**) and the more robust statistical method should be considered when possible. Nevertheless, the limited experimental scope of bioassays greatly restricts the use of statistics and although GLM framework can be equally applied to estimate prion titres from bioassays (**section 3.2.3**) we refrained from using statistical modelling for bioassay. The SCEPA yielded very low intra- and inter-assay variability which demonstrates the statistical robustness of the assay. The bioassay, on the other hand, clearly underperformed and intra- and inter-assay variability for independent assays of half to one log was estimated by GLM. However, since the limited experimental scope of bioassays greatly restricts the use of statistics we refrained from using statistical modelling for bioassay. Since a statistically reliable determination of prion titres is fundamental where differences in titres may be critical the SCEPA may be the assay of choice, given the cell lines are permissive to the investigated strains (Vorberg *et al.*, 2004; Mahal *et al.*, 2007; Neale *et al.*, 2010).

4.2 Role of antigen presenting cells in prion sequestration

The exceptional rate of prion propagation in lymphoid organs provides evidence of highly coordinated processes for the dissemination and replication of prions. In only 3 days after inoculation, infectivity increased by nearly 3 logs in spleens of *wt* mice as

compared to replication-deficient mice (**figure 3.6 A**). A titre of 2.5 log TCIU/g spleen was still detected in spleens of *Prnp*$^{-/-}$ at 3 dpi, indicating that PrP-independent mechanisms are involved in the sequestration and transport of prions from the sites of infection to lymphoid organs. A similar titre was found after i.c. inoculation of RML brain homogenate into *Prnp*$^{-/-}$ mice (Bueler *et al.*, 1993). Remarkably, in the absence of prion replication, infectivity accumulated preferentially in DCs and macrophages as compared to lymphocytes (**table 3.4**), thus supporting a role of antigen-presenting cells in prion sequestration. Macrophages and DCs are found in peripheral tissues and in strategic sites of lymphoid organs, the marginal zone and sinuses, where they can efficiently scavenge the lymphatic fluid, internalise and present antigens to T cells (Junt *et al.*, 2008) (see **figure 4.1**). Interestingly, in addition to macrophages and DCs, FDC clusters were also infectious in replication-deficient *Prnp*$^{-/-}$ mice (**table 3.7 B**). FDCs are immobile stromal cells confined to B cell follicles that retain antigens in the form of immune complexes at the plasma membrane (Batista and Harwood, 2009). Macrophages in the subcapsular sinus and medulla of lymph nodes were shown to capture and present antigens to B cells in the follicles (Carrasco and Batista, 2007; Junt *et al.*, 2007). The delivery of antigen to FDCs seems to be mediated by marginal and follicular B cells (Batista and Harwood, 2009). The presence of prions in FDC clusters in the absence of prion replication indicates that mechanisms for antigen delivery to FDCs are used by prions. B cells are indispensable for prion propagation irrespective of their PrP status (Klein *et al.*, 1998). In addition to their trophic support of FDCs via TNF/LT signalling, B cells may be involved in other mechanisms such as transfer of prions to FDCs. Migrating DCs mediate an active transport of antigens from the peripheral tissues into lymph nodes. Alternatively, antigens can be transported passively by lymph into lymph nodes, or by blood into the spleen, where large antigens require active transport by resident cells and small antigens (> 70 kDa) are transported directly to T cell areas in the lymphoid organs through the conduit system that consists of collagen fibres

enclosed by the stromal fibroblastic reticular cells and resident DCs scattered that sample the lymphatic fluid (Sixt *et al.*, 2005) (see **figure 4.1**).

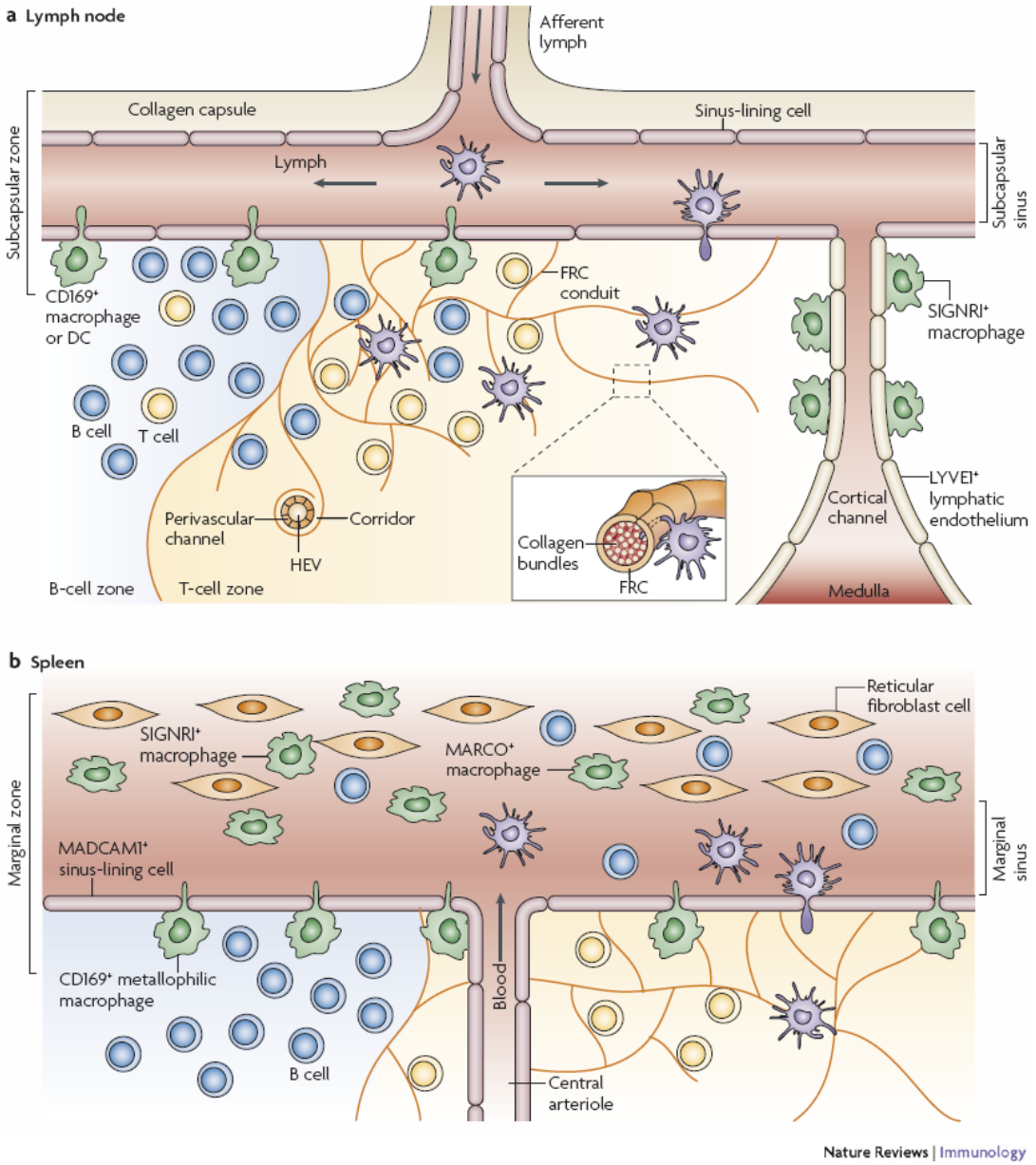

Figure 4.1 Areas of antigen encounter in lymphoid organs. Antigens are transported to the lymph nodes via afferent lymphatics (**A**) or to the spleen via blood (**B**) by cell-mediated or non cell-mediated mechanisms. Migrating DCs that capture antigen in peripheral tissues can enter the lymph nodes for antigen presentation to T cells. Soluble antigen can be captured by macrophages and DCs in the sinuses

or access the T cell areas directly through the FRC conduit in case it is smaller than 70 kDa. Reproduced from the Nature Reviews, Junt, T. *et al.*, 2008, Vol 8, pp 764-775 (Junt *et al.*, 2008).

Although several studies have addressed the time-dependent distribution of infectivity in different lymphoid organs following inoculation of prions, only a few studies determined the levels of infectivity attributable to different cell types (Eklund *et al.*, 1967; Kimberlin and Walker, 1979; Kimberlin and Walker, 1980; Kimberlin and Walker, 1989a). Early studies showed high infectious titres preferentially associated to cells with low buoyant densities, comprising enriched fractions of blast cells, macrophages and dendritic cells (Lavelle *et al.*, 1972; Kuroda *et al.*, 1983). More recently, high infectious titres have been detected in highly purified fractions of DCs (Aucouturier *et al.*, 2001) and lymphocytes (Raeber *et al.*, 1999a). Nonetheless, these studies are restricted to one or two cell types and a particular time point. We here characterised the time-dependent accumulation of prions in splenic cell types during the first month after inoculation, as prion titres reached plateau levels in the spleen.

Prions accumulated in all investigated cell types at 3 dpi and increased rapidly over time by about 20-50 fold between 3 and 30 dpi (**table 3.5**) consistent with an increase of infectivity in spleen tissue. The highest prion levels were determined in a subset of DCs, plasmacytoid DC (pDC) where prion titres exceeded the levels of B cells and T cells by about 7-fold. High titres were also associated to NK cells, a type of lymphocytes with about 3-fold higher infectious titres than conventional lymphocytes (**figure 3.7**).

High prion titres of DCs have previously been reported for the 139A prion strain (Aucouturier *et al.*, 2001). DCs are specialized antigen presenting cells that form a heterogeneous group of cells with distinct highly regulated trafficking patterns and functions. Their contribution to prion pathogenesis to date is unknown. DCs were suggested as mobile carriers for prions from the gut to draining lymph nodes after oral inoculation of mice with prions (Huang *et al.*, 2002; Huang and MacPherson, 2004). A

role of DCs in neuroinvasion was inferred from studies showing that i.v. inoculation of prion-infected DCs into $Rag^{-/-}$ mice sufficed to transmit disease into the CNS (Aucouturier *et al.*, 2001). However, this observation was not confirmed by other experimental approaches (Rybner-Barnier *et al.*, 2006; Raymond *et al.*, 2007). DCs were detected in the CNS of mice inoculated i.p. with the mouse-adapted GSS strain (Rosicarelli *et al.*, 2005). Recent evidence suggests that DCs migrate into the CNS in other neuropathological conditions. PDCs, for example are the major CNS-infiltrating cells during experimental autoimmune encephalomyelitis (EAE) (Bailey-Bucktrout *et al.*, 2008). Of note, prion disease progression was accelerated by induction of EAE in scrapie infected mice (Friedman-Levi *et al.*, 2007).

PDCs are specialized DCs that produce natural type 1 inferferon (IFN-1) in response to a viral infection. They are clearly distinct from conventional DCs in regards to their localisation in the lymphoid organs, their antigen presenting properties, their migration pathways and physiological function. Together with NK cells, pDCs are essential mediators of the antiviral immune response via IFN-1 signalling (Villadangos and Young, 2008). The number of pDCs is highly variable among mouse strains, with the 129Sv strain showing several fold higher numbers than most other strains (Asselin-Paturel *et al.*, 2003). Reportedly less endocytotic than conventional DCs (Grouard *et al.*, 1997; Dalgaard *et al.*, 2005), pDCs were initially considered to have a minor role in antigen uptake and presentation. Nonetheless, it has been show that pDCs efficiently internalise soluble proteins such as OVA *in vivo* and *in vitro* (Villadangos and Young, 2008). Other reports showed that pDCs internalise latex-beads and apoptotic debris (Ochando *et al.*, 2006; Hoeffel *et al.*, 2007). Of interest, PrP^{Sc} was internalised by bone marrow derived pDCs *in vitro* (Rybner-Barnier *et al.*, 2006). Due to their high infectious titres we investigated whether pDCs are replication-competent. However, expression of PrP^{C}, a pre-requisite for the replication of prions (Bueler *et al.*, 1993), was not detected in freshly isolated splenic pDCs (**figure 3.8**). This result was in agreement with

previous reports where PrP^C expression in pDCs was undetectable or low as compared to conventional DCs (Rybner-Barnier *et al.*, 2006; del Hoyo *et al.*, 2006). Although prion replication-competence of cells cannot be predicted on the basis of its level of PrP expression (Vorberg *et al.*, 2004), pDCs seem *a priori* a poor candidate for a role in prion replication.

Further investigations will be required to elucidate why pDCs accrue prions more effectively than lymphocytes. Preliminary experiments showed that proteasomal degradation of prion-infected pDCs was not significantly different from uninfected control pDCs (data not shown). PDCs are located in the T cell rich areas of lymph nodes associated to high endothelial venules (HEV). In the spleen pDCs are found scattered in the T cells areas or periarteriolar lymphoid sheath (PALS), in the red pulp and rarely in the marginal zone. Their distribution differs from conventional DCs which are predominantly found in the marginal zone and outer PALS, but not in the red pulp of the spleen (Asselin-Paturel *et al.*, 2005). Interestingly, highly infectious NK cells are also found in areas of antigen entry to lymphoid organs, mostly in the red pulp of spleen and inside the blood sinuses together with macrophages. In the lymph nodes, NK cells are found in the paracortex with HEVs and in the medulla within lymphatic sinuses (Gregoire *et al.*, 2007). Whether the distinct localisation of pDCs and NK cells and their presence in the red pulp or in the paracortex is related to their high prion titres has to be further investigated. A bidirectional cross-talk between pDCs and NK cells has recently been shown to play a key role in host defence (Gerosa *et al.*, 2005; Lucas *et al.*, 2007).

Another important characteristic of pDCs that distinguishes them from conventional DCs are their migration pathways. While conventional DCs travel from the peripheral tissues via afferent lymphatics to draining lymph nodes, most reports support the notion that pDC enter the lymph nodes via the bloodstream through the high endothelial venules (HEV) (Randolph *et al.*, 2008). Albeit at low numbers, pDCs are

found in peripheral tissues, mainly in the intestine and kidneys, but are also found in skin and liver, under steady-state conditions (Villadangos and Young, 2008). Whether pDCs, like conventional DCs, actively transport antigens from the periphery to lymphoid organs is not clear, but it raises the possibility that prions could be transported by pDCs to lymph nodes via HEVs. In a preliminary experiment where pDCs are depleted by treatment with mPDCA-1 antibodies before and after inoculation with prions, lower prion titres were detected in mesenteric lymph nodes of pDC-depleted mice as compared to control mice while no differences were found in spleens (**table 3.6**). The entry of cells into lymph nodes via HEV is a highly regulated process that is mainly restricted to lymphocytes under steady-state conditions (Young, 1999). If the transport of prions into the lymph nodes via the haematogenous route was more efficient than via the lymph (e.g. depending on the inoculation route), the entry of infectious pDCs via HEVs could contribute to the titre in lymph nodes. However, no evidence for a predominant role of the haematogenous route was found, in agreement with previous reports (Raeber *et al.*, 1999a).

Despite high prion titres in the spleen at early stages of disease, only very low titres were reported in blood, mainly associated to buffy coat fractions and plasma (Brown *et al.*, 1998; Aguzzi and Glatzel, 2006). No infectivity was detected in peripheral blood leukocytes (PBL) (Raeber *et al.*, 1999a) or in our study in blood-borne pDCs (**table 3.5**), regardless of the relatively high prion titres associated to these cells in spleen tissue, indicating that recirculation of prion-infected cells is clearly restricted. Indeed, recirculation of cells between blood and tissues via efferent lymphatics is mainly limited to lymphocytes, in particular to T cells and to a lesser degree to B cells (25 % recirculate) (Young, 1999). Recirculation of NK cells is also restricted under steady-state conditions (Gregoire *et al.*, 2007). Although small numbers of DCs in the thoracic duct which drains into the vascular system gives evidence for DC recirculation, this is very infrequent under steady-state conditions (Bonasio and von Andrian, 2006). Even

though prion infectivity is detected in various tissues, including lung, liver, spleen, salivary glands and in blood as early as 30 min after i.p. inoculation (Millson *et al.*, 1979), prion propagation is restricted to the LRS. A rapid decrease of prion titres in non-permissive tissues may be a result of rapid degradation and transport to the LRS, respectively. The intriguing question why prions remain largely confined in replication-competent lymphoid organs remains unanswered, and the highly coordinated interactions between haematopoietic and stromal cells may hold the answer. A clear evidence for this hypothesis comes from chronic inflammatory conditions, like systemic lupus erythematosus, autoimmune diabetes, nephritis and pancreatitis where prions propagate in non-permissive tissues (Heikenwalder *et al.*, 2005). Under these conditions, a mobilisation of immune cells to sites of infection could also transport prion cargo from lymphoid to affected organs. Although it is generally accepted that misfolded PrP does not stimulate an immune response in the host (Kasper *et al.*, 1982), recent reports showed abnormal germinal centre reactions in the spleen of scrapie infected mice manifested by an increased maturation of follicular B cells observed at 70 dpi and endstage (McGovern *et al.*, 2004). Variations in the number of $CD21^{+}$ B cells in lymph nodes of prion-infected sheep as compared to controls were also reported (Eaton *et al.*, 2007; Eaton *et al.*, 2009). We therefore examined whether we could changes in splenic B cell subsets between scrapie and control mice are detectable at preclinical stages. However, the ratios of $CD21^{hi}$ $CD23^{-}$ marginal zone B cells and $CD21^{int}$ $CD23^{hi}$ follicular B cells were unchanged between scrapie-infected and mock-infected mice at 30, 80 and 100 dpi in the 3 spleen analysed per time point (**figure 3.9**).

In summary, a novel procedure to characterise the time-dependent accumulation of prions in the spleen showed that DCs, in particular pDCs, and the lymphocyte subset, NK cells, sequester prions efficiently. In $Prnp^{-/-}$ mice in the absence of prion replication highest titres were associated to FDC clusters, DCs and macrophages which highlights the ability of these cells to sequester prions independently of their PrP status. Most

challenging for a further progress in our understanding of lymphatic prion colonisation will be to better characterise the contribution of each cell type. With the method reported here changes in the cell tropism of prion after experimental interventions could be determined in a uniquely comprehensive manner. While most of the previous reports that addressed the role of specific cells by depletion experiments fell short of controlling and preventing a fast replenishment of depleted haematopoietic cell types by blood-borne precursors, it will be highly valuable to revisit experiments that focused on the depletion of pDCs (our study), the depletion of DCs (Raymond *et al.*, 2007; Cordier-Dirikoc and Chabry, 2008), macrophages (Beringue *et al.*, 2000) and FDCs (Mabbott *et al.*, 2000; Montrasio *et al.*, 2000) using the established procedures and investigate how specific cell types affect the cell tropism of prion accumulation and whether changes in prion titres of major splenic cell types are correlated to disease onset. Based on our experimental evidence for a role of DCs in prion sequestration, it will be interesting to revisit the activation of the innate immune system using specific toll-like receptors (TLR) agonist that showed a protective effect on prion disease (Sethi *et al.*, 2002). TLRs which are involved in the recognition of conserved features of a wide range of invading pathogens are expressed on different DC subtypes, e.g. TLR9 and TLR7 are expressed on pDCs whereas TLR2, TLR4, TLR7 and TLR8 are expressed in mDCs (Larsson *et al.*, 2004). The reported immunopathology after multi-dose regimen with CpG oligonucleotides in the Sethi study (Heikenwalder *et al.*, 2004a) greatly discouraged further attempts to stimulate the immune system. With the development of new generation adjuvants with reduced toxicity and increased potency like clinical approved “Monophosphoryl Lipid A” (MPL), a low-toxicity version of LPS (Mata-Haro *et al.*, 2007) or the TLR7 ligand “imiquimod” (Wang *et al.*, 2005), it may now be possible to revisit the stimulation of the innate immune system to assess the cell tropism of prion accumulation.

4.3 Contribution of the stroma compartment to prion pathogenesis

To complement the characterisation of the kinetics of prion accumulation in haematopoietic cell types during early pathogenesis, a major goal was to determine infectivity associated to the stromal compartment. FDCs have received the most attention of all stromal cell types and are discussed as main candidates for a role in prion replication (Mabbott and Bruce, 2002). Abnormal PrP deposits accumulate on the surface of FDCs (Jeffrey *et al.*, 2000), but infectious titres have not been reported yet. The isolation of a highly purified FDC fraction by magnetic sorting has been described previously (Sukumar *et al.*, 2006). Standard protocols for the isolation of FDCs include immunisation and irradiation of mice to boost the number of germinal centres and to deplete lymphocytes, respectively (Kosco-Vilbois *et al.*, 1993). Both procedures are likely to have an impact on prion titres (Dickinson *et al.*, 1978; Fraser and Farquhar, 1987) and were not considered for our purposes. Using SCEPA for titre determination and MACS for the specific isolation of FDCs we attempt to determine infectious titres of FDCs. However, under these conditions any attempt to isolate FDCs (e.g. cell enrichment in a Percoll gradient before MACS isolation) failed. Once the collagen matrix of spleen tissue is digested, FDCs readily form clusters that can be detected by microscopy after enrichment (**figure 3.10 C**). We suppose that major problems during MACS isolation of FDCs are related to the limited access of antibodies to epitopes on the surface of FDCs which may be buried by B cells or to the low expression levels of FDC-M1 in the non-activated state (Rao *et al.*, 2002). By diverting from standard protocols such as immunisation and irradiation of mice, the performance of FDC-M1 used in the MACS isolation may drop significantly. Alternative isolation strategies based on the unique ability of FDCs to retain immune complexes (IC) on their surfaces were envisaged. Although an internalisation of ICs by antigen presenting cells was observed after 30 min incubation, fluorescence did not decrease to control levels and therefore failed the identification of low numbers of positive FDCs (**figure 3.11**).

Given the failure to obtain purified FDCs, enrichment protocols for FDC/B cell clusters were used to determine infectious titres. FDC-M1^{+} FDC/B cell clusters were isolated based on their higher sedimentation rate at 1 x *g* in FBS as compared to single cells of a heterogeneous cell population (**figure 3.12**). Titres of FDC clusters were determined in *Prnp*$^{-/-}$ mice at 3 dpi and in *wt* mice at 14 and 30 dpi and compared to prion titres of other cell subsets from the same pool of cells (**table 3.7**). In the absence of prion replication FDC yielded a titre of 12 TCIU/mg protein and 8 TCIU/mg protein for *pan* DCS, whereas B cells were not infectious which clearly indicating that FDCs retain infectivity at early phases after inoculation (**table 3.7 B**). In *wt* mice FDC clusters were about 1 log more infectious than pDCs and NK cells at 14 dpi (**table 3.7 A**). However, since an unknown number of infectious B cells are aggregated with FDCs in *wt* mice the actual infectious titre of FDCs remains unknown.

Recent reports have suggested that other stromal cells, like mesenchymal and fibroblastic reticular cells could support prion propagation in the absence of FDCs (Heikenwalder *et al.*, 2008). Several fibroblastic cell lines were found to be prion-permissive and propagate prions at high rates (Vorberg *et al.*, 2004). In agreement with previous results (Clarke and Kimberlin, 1984), the stromal compartment of the spleen contains high prion titres about 7 logs/g tissue (**section 3.5.2**) and therefore the interesting question arose whether primary cultures of stroma cells isolated from scrapie-infected mice retain the ability of prion propagation *ex vivo*. Splenic stromal cell cultures can be readily generated within 4 days after isolation from *wt* mice and form a heterogeneous population of cells. Stromal cultures consisted mainly of podoplanin^{+} fibroblasts and expressed PrP^{C}, but also contained macrophages and DCs (**figure 3.13**).

However, evidence of prion replication was not observed in splenic stroma cultures and the endogenous infectivity decreased rapidly with subsequent passages (**figure 3.14**). The high rate of cell division of stroma cultures *ex vivo* may dilute out propagating prions by repeated cell division (Bosque and Prusiner, 2000) or activate pathways that

degrade prions as reported by for myeloid cells (Luhr *et al.*, 2002; Rybner-Barnier *et al.*, 2006).

4.4 *Ex-vivo* release of prions from scrapie-infected splenic cells

Prions colonise the LRS of 129Sv x C57BL/6 mice at very early stages of the disease at compelling rates. Infectivity is found in lymphocytes, macrophages, DCs and FDC clusters (**table 3.4** and **table 3.7**), indicating the existence of very efficient mechanisms for the lateral spread of prions. We here present the first evidence for an active secretion of prions from immune cells isolated from scrapie-infected mice (**table 3.8**). Infectivity released into the culture medium was pelleted by high speed centrifugation and pellets were highly enriched in exosome-like particles (**figure 3.16**).

Since the limited viability of immune cells in culture could bias the determination of an active prion secretion, we maximised passive leakage of infectivity in control cultures by incubating cells at atmospheric CO_2 (data shown for B cells in **figure 3.15**). We showed that infectious titres of cell culture supernatants of B cells and DCs exceeded those of passive leakage controls by about 30-fold, T cells also secreted infectivity although at lower amounts (**table 3.8**). Interestingly, the release of prions from scrapie-infected B cells was associated with the secretion of exosome-like vesicles (**figure 3.16**). The limited amount of infectivity released into the culture medium, i.e. 1-2 % of the cellular infectivity, hampered the characterisation on Western Blot of the 100,000 x *g* pellets for the presence of exosomal markers such as CD63, Tsg 101, Alix-1 or flotillin (Simons and Raposo, 2009). Still, exosomes can be distinguished from other secreted microvesicles or apoptotic blebs by their characteristic cup-shape morphology and smaller size 30-100 nm (Mathivanan *et al.*, 2010). Other mechanisms that such as cell-to-cell contact (Kanu *et al.*, 2002) or the recently proposed transfer of prions along nanotubes (Gousset *et al.*, 2009) could also contribute to the spread of prions.

While the exact site of prion replication is under debate, PrP^{Sc} can be detected on the plasma membrane, recycling endosomes, late endosomes and lysosomes (McKinley *et al.*, 1991; Arnold *et al.*, 1995; Marijanovic *et al.*, 2009). Exosomes are small vesicles of endosomal origin formed by invagination of the membrane of late endosomes or multivesicular bodies (MVB) (van Niel *et al.*, 2006). Fusion of MVBs with the plasma membrane release exosomes to the extracellular medium. The integration of prions into exosomes would enable the transfer of prion infectivity without the requirement for direct cell-to-cell contact and the question arises whether exosome secretion has a role for the spread of infectivity *in vivo*. Haematopoietic and stromal cells with a role in the propagation and dissemination of prions were shown to either secrete exosomes or act as recipients for exosomes. Macrophages, DCs, T cells and B cells were shown to secrete exosomes in culture (Thery *et al.*, 2002; Vella *et al.*, 2008b) and exosomes are found *in vivo* associated to the membrane of FDCs (Denzer *et al.*, 2000). Interestingly, studies showed that B cell-derived exosomes, but not those from other cell types, bind to FDCs surfaces *in vitro* (Denzer *et al.*, 2000). B cell exosomes might also bind to extracellular matrix (ECM) proteins (collagen I and fibronectin) and activated fibroblasts as suggested in other *in vitro* studies (Clayton *et al.*, 2004). In addition, reports for the secretion of PrP^{C} in primary cultures of cortical (Faure *et al.*, 2006) and PrP^{C} in exosomes isolated from the CSF from sheep (Vella *et al.*, 2008a), suggest that exosomes might also be implicated in the dissemination in the CNS.

The involvement of exosomes in pathological processes is not a new concept (Gould *et al.*, 2003). Retroviruses were shown to hijack the exosomal machinery to bud out of the cells, e.g. HIV-1 infected exosomes released into the medium by DCs mediated the infection of T cells (Wiley and Gummuluru, 2006). Interestingly, the release of prion-infected exosomes is enhanced by retroviral infection, suggesting that both pathogens use common pathways for exocytose the cells (Leblanc *et al.*, 2006). Exosome release has also been linked to other neurodegenerative diseases such

Alzheimer and Parkinson's diseases where Aβ peptides and α-synuclein can be secreted in exosomes (Rajendran *et al.*, 2006; Emmanouilidou *et al.*, 2010).

4.5 Concluding remarks

The work presented here forms the basis for a novel approach to the unresolved question of the mode of prion dissemination which I hope may inspire further attempts to investigate the dynamics of prion spread. The statistical power and short duration of *in-vitro* infectivity assays are convincing arguments to pursue and refine cell-based infectivity assays to better understand early stages of prion dissemination. High prion titres in pDCs, a cell type that so far has not caught the attention in the field due to undetectable levels of PrP^{C}, the substrate for protein misfolding may contribute to the appreciation of PrP-independent processes, like prion sequestration and dissemination. Where seminal work in the last two decades helped to elucidate the molecular mechanisms of prion replication in the LRS, the role of antigen-presenting cells remained dubious. A better characterisation of the migration pathways of antigen-presenting cells may be critical to understand prion colonisation of the LRS. The compelling rate of prion accumulation in the LRS at early stages after infection gives evidence to a complex network of interaction between a variety of cell types. Of importance the active release of prions by immune cells may represent the same molecular pathways that are usurped by viruses, and future experiments will show whether gene perturbation of members of the ESCRT complex which prevents the release of virions will also inhibit prion release. Give the important role of antigen-presenting cell in the innate immune system the stimulation of Toll-like receptors as postexposure prophylaxis is definitely an avenue worth pursuing.

REFERENCES

1. Agnati,LF, D Guidolin, M Guescini, S Genedani, K Fuxe, 2010, Understanding wiring and volume transmission: Brain Research Reviews, v. 64, p. 137-159.

2. Aguzzi,A, M Glatzel, 2006, Prion infections, blood and transfusions: Nature Clinical Practice Neurology, v. 2, p. 321-329.

3. Aguzzi,A, M Heikenwalder, 2005, Prions, cytokines, and chemokines: a meeting in lymphoid organs: Immunity., v. 22, p. 145-154.

4. Aguzzi,A, M Heikenwalder, 2006, Pathogenesis of prion diseases: current status and future outlook: Nat Rev Microbiol, v. 4, p. 765-775.

5. Aguzzi,A, M Polymenidou, 2004, Mammalian prion biology: One century of evolving concepts: Cell, v. 116, p. 313-327.

6. Aguzzi,A, C Sigurdson, M Heikenwaelder, 2008, Molecular mechanisms of prion pathogenesis: Annual Review of Pathology-Mechanisms of Disease, v. 3, p. 11-40.

7. Aguzzi,A, F Montrasio, P S Kaeser, 2001, Prions: health scare and biological challenge: Nat Rev Mol Cell Biol, v. 2, p. 118-126.

8. Alais,S, S Simoes, D Baas, S Lehmann, G Raposo, J L Darlix, P Leblanc, 2008, Mouse neuroblastoma cells release prion infectivity associated with exosomal vesicles: Biol Cell, v. 100, p. 603-615.

9. Alper,T, W A CRAMP, D A HAIG, M C CLARKE, 1967, Does the agent of scrapie replicate without nucleic acid?: Nature, v. 214, p. 764-766.

10. Alper,T, D A HAIG, M C CLARKE, 1978, Scrapie agent - Evidence against its dependence for replication on intrinsic nucleic acid: Journal of General Virology, v. 41, p. 503-516.

11. Andreoletti,O, P Berthon, D Marc, P Sarradin, J Grosclaude, L van Keulen, F Schelcher, J M Elsen, F Lantier, 2000, Early accumulation of PrP^{Sc} in gut-associated lymphoid and nervous tissues of susceptible sheep from a Romanov flock with natural scrapie: Journal of General Virology, v. 81, p. 3115-3126.

12. Arnold,JE, C Tipler, L Laszlo, J Hope, M Landon, R J Mayer, 1995, The abnormal isoform of the prion protein accumulates in late-endosome-like organelles in scrapie-infected mouse-brain: Journal of Pathology, v. 176, p. 403-411.

13. Ashok,A, R S Hegde, 2006, Prions and retroviruses: an endosomal rendezvous?: EMBO Rep., v. 7, p. 685-687.

14. Asselin-Paturel,C, G Brizard, K Chemin, A Boonstra, A O'Garra, A Vicari, G Trinchieri, 2005, Type I interferon dependence of plasmacytoid dendritic cell activation and migration: Journal of Experimental Medicine, v. 201, p. 1157-1167.

15. Asselin-Paturel,C, G Brizard, J J Pin, F Briere, G Trinchieri, 2003, Mouse strain differences in plasmacytoid dendritic cell frequency and function revealed by a novel monoclonal antibody: The Journal of Immunology, v. 171, p. 6466-6477.

16. Aucouturier,P, C Carnaud, 2002, The immune system and prion diseases: a relationship of complicity and blindness: J Leukoc Biol, v. 72, p. 1075-1083.

17. Aucouturier,P, F Geissmann, D Damotte, G P Saborio, H C Meeker, R Kascsak, R Kascsak, R I Carp, T Wisniewski, 2001, Infected splenic dendritic cells are sufficient for prion transmission to the CNS in mouse scrapie: J Clin Invest, v. 108, p. 703-708.

18. Bailey-Bucktrout,SL, S C Caulkins, G Goings, J A A Fischer, A Dzionek, S D Miller, 2008, Central nervous system plasmacytoid dendritic cells regulate the severity of relapsing experimental autoimmune encephalomyelitis: Journal of Immunology, v. 180, p. 6457-6461.

19. Baldauf,E, M Beekes, H Diringer, 1997, Evidence for an alternative direct route of access for the scrapie agent to the brain bypassing the spinal cord: Journal of General Virology, v. 78, p. 1187-1197.

20. Banchereau,J, F Briere, C Caux, J Davoust, S Lebecque, Y T Liu, B Pulendran, K Palucka, 2000, Immunobiology of dendritic cells: Annual Review of Immunology, v. 18, p. 767-811.

21. Barmada,SJ, D A Harris, 2005, Visualization of prion infection in transgenic mice expressing green fluorescent protein-tagged prion protein: Journal of Neuroscience, v. 25, p. 5824-5832.

22. Baron,GS, A C Magalhaes, M A Prado, B Caughey, 2006, Mouse-adapted scrapie infection of SN56 cells: greater efficiency with microsome-associated versus purified PrP-res: J Virol, v. 80, p. 2106-2117.

23. Barria,MA, A Mukherjee, D Gonzalez-Romero, R Morales, C Soto, 2009, De novo generation of infectious prions in vitro produces a new disease phenotype: PLoS Pathog., v. 5, p. e1000421.

24. Barron,RM, S L Campbell, D King, A Bellon, K E Chapman, R A Williamson, J C Manson, 2007, High titers of transmissible spongiform encephalopathy infectivity associated

with extremely low levels of PrP^{Sc} in vivo: Journal of Biological Chemistry, v. 282, p. 35878-35886.

25. Basler,K, B Oesch, M Scott, D Westaway, M Walchli, D F Groth, M P McKinley, S B Prusiner, C Weissmann, 1986, Scrapie and cellular PrP isoforms are encoded by the same chromosomal gene: Cell, v. 46, p. 417-428.

26. Batista,FD, N E Harwood, 2009, The who, how and where of antigen presentation to B cells: Nature Reviews Immunology, v. 9, p. 15-27.

27. Belay,ED, R A Maddox, E S Williams, M W Miller, P Gambetti, L B Schonberger, 2004, Chronic wasting disease and potential transmission to humans: Emerging Infectious Diseases, v. 10, p. 977-984.

28. Benestad,SL, J N Arsac, W Goldmann, M Noremark, 2008, Atypical/Nor98 scrapie: properties of the agent, genetics, and epidemiology: Vet.Res, v. 39, p. 19.

29. Beranger,F, A Mange, B Goud, S Lehmann, 2002, Stimulation of PrP^{C} retrograde transport toward the endoplasmic reticulum increases accumulation of PrP^{Sc} in prion-infected cells: Journal of Biological Chemistry, v. 277, p. 38972-38977.

30. Beringue,V, P Couvreur, D Dormont, 2002, Involvement of macrophages in the pathogenesis of transmissible spongiform encephalopathies: Dev Immunol, v. 9, p. 19-27.

31. Beringue,V, M Demoy, C I Lasmezas, B Gouritin, C Weingarten, J P Deslys, J P Andreux, P Couvreur, D Dormont, 2000, Role of spleen macrophages in the clearance of scrapie agent early in pathogenesis: J Pathol, v. 190, p. 495-502.

32. Bessen,RA, D A Kocisko, G J Raymond, S Nandan, P T Lansbury, B Caughey, 1995, Non-genetic propagation of strain-specific properties of scrapie prion protein: Nature, v. 375, p. 698-700.

33. Beyer,C, D S Pisetsky, 2010, The role of microparticles in the pathogenesis of rheumatic diseases: Nature Reviews Rheumatology, v. 6, p. 21-29.

34. Bjorck,P, 2001, Isolation and characterization of plasmacytoid dendritic cells from Flt3 ligand and granulocyte-macrophage colony-stimulating factor-treated mice: Blood, v. 98, p. 3520-3526.

35. Blattler,T, S Brandner, A J Raeber, M A Klein, T Voigtlander, C Weissmann, A Aguzzi, 1997, PrP-expressing tissue required for transfer of scrapie infectivity from spleen to brain: Nature, v. 389, p. 69-73.

36. Bolton,DC, M P McKinley, S B Prusiner, 1982, Identification of a protein that purifies with the scrapie prion: Science, v. 218, p. 1309-1311.

37. Bonasio,R, U H von Andrian, 2006, Generation, migration and function of circulating dendritic cells: Current Opinion in Immunology, v. 18, p. 503-511.

38. Borchelt,DR, A Taraboulos, S B Prusiner, 1992, Evidence for synthesis of scrapie prion proteins in the endocytic pathway: Journal of Biological Chemistry, v. 267, p. 16188-16199.

39. Bosque,PJ, S B Prusiner, 2000, Cultured cell sublines highly susceptible to prion infection: Journal of Virology, v. 74, p. 4377-4386.

40. Boulanger,CM, N Amabile, A Tedgui, 2006, Circulating microparticles - A potential prognostic marker for atherosclerotic vascular disease: Hypertension, v. 48, p. 180-186.

41. Brandner,S, A Raeber, A Sailer, T Blattler, M Fischer, C Weissmann, A Aguzzi, 1996a, Normal host prion protein (PrP^C) is required for scrapie spread within the central nervous system: Proceedings of the National Academy of Sciences of the United States of America, v. 93, p. 13148-13151.

42. Brandner,S, S Isenmann, A Raeber, M Fischer, A Sailer, Y Kobayashi, S Marino, C Weissmann, A Aguzzi, 1996b, Normal host prion protein necessary for scrapie-induced neurotoxicity: Nature, v. 379, p. 339-343.

43. Brown,KL, K Stewart, D L Ritchie, N A Mabbott, A Williams, H Fraser, W I Morrison, M E Bruce, 1999, Scrapie replication in lymphoid tissues depends on prion protein-expressing follicular dendritic cells: Nature Medicine, v. 5, p. 1308-1312.

44. Brown,P, R G Rohwer, B C Dunstan, C MacAuley, D C Gajdusek, W N Drohan, 1998, The distribution of infectivity in blood components and plasma derivatives in experimental models of transmissible spongiform encephalopathy: Transfusion, v. 38, p. 810-816.

45. Bruce,ME, I McConnell, R G Will, J W Ironside, 2001, Detection of variant Creutzfeldt-Jakob disease infectivity in extraneural tissues.: Lancet, v. 358, p. 208-209.

46. Bueler,H, A Aguzzi, A Sailer, R A Greiner, P Autenried, M Aguet, C Weissmann, 1993, Mice devoid of PrP are resistant to scrapie: Cell, v. 73, p. 1339-1347.

47. Bueler,H, M Fischer, Y Lang, H Bluethmann, H P Lipp, S J DeArmond, S B Prusiner, M Aguet, C Weissmann, 1992, Normal development and behaviour of mice lacking the neuronal cell-surface PrP protein: Nature, v. 356, p. 577-582.

48. Caby,MP, D Lankar, C Vincendeau-Scherrer, G Raposo, C Bonnerot, 2005, Exosomal-like vesicles are present in human blood plasma: International Immunology, v. 17, p. 879-887.

49. Campana,V, D Sarnataro, C Zurzolo, 2005, The highways and byways of prion protein trafficking: Trends in Cell Biology, v. 15, p. 102-111.

50. Carp,RI, S M Callahan, 1982, Effect of mouse peritoneal macrophages on scrapie infectivity during extended in vitro incubation: Intervirology, v. 17, p. 201-207.

51. Carp,RI, S M Callahan, B A Patrick, P D Mehta, 1994, Interaction of scrapie agent and cells of the lymphoreticular system: Arch Virol, v. 136, p. 255-268.

52. Carrasco,YR, F D Batista, 2007, B cells acquire particulate antigen in a macrophage-rich area at the boundary between the follicle and the subcapsular sinus of the lymph node: Immunity, v. 27, p. 160-171.

53. Castilla,J, P Saa, C Soto, 2005a, Detection of prions in blood: Nat Med, v. 11, p. 982-985.

54. Castilla,J, P Saa, C Hetz, C Soto, 2005b, In vitro generation of infectious scrapie prions: Cell, v. 121, p. 195-206.

55. Caughey,B, G S Baron, B Chesebro, M Jeffrey, 2009, Getting a grip on prions: oligomers, amyloids, and pathological membrane interactions: Annu Rev Biochem, v. 78, p. 117-204.

56. Caughey,BW, A Dong, K S Bhat, D Ernst, S F Hayes, W S Caughey, 1991, Secondary structure-analysis of the scrapie-associated protein PrP 27-30 in water by infrared-spectroscopy: Biochemistry, v. 30, p. 7672-7680.

57. Clarke,MC, R H Kimberlin, 1984, Pathogenesis of mouse scrapie: distribution of agent in the pulp and stroma of infected spleens: Vet.Microbiol, v. 9, p. 215-225.

58. Clayton,A, A Turkes, S Dewitt, R Steadman, M D Mason, M B Hallett, 2004, Adhesion and signaling by B cell-derived exosomes: the role of integrins: FASEB J, v. 18, p. 977-979.

59. Colby,DW, R Wain, I V Baskakov, G Legname, C G Palmer, H O Nguyen, A Lemus, F E Cohen, S J DeArmond, S B Prusiner, 2010, Protease-sensitive synthetic prions: PLoS Pathog, v. 6, p. e1000736.

60. Collinge,J, 2005, Molecular neurology of prion disease: Journal of Neurology Neurosurgery and Psychiatry, v. 76, p. 906-919.

61. Collinge,J, A R Clarke, 2007, A general model of prion strains and their pathogenicity: Science, v. 318, p. 930-936.

62. Come,JH, P E Fraser, P T Lansbury, 1993, A kinetic-model for amyloid formation in the prion diseases - importance of seeding: Proceedings of the National Academy of Sciences of the United States of America, v. 90, p. 5959-5963.

63. Cordier-Dirikoc,S, J Chabry, 2008, Temporary depletion of CD11c+ dendritic cells delays lymphoinvasion after intraperitonal scrapie infection: J Virol, v. 82, p. 8933-8936.

64. Couzin,J, 2005, Cell biology: The ins and outs of exosomes: Science, v. 308, p. 1862-1863.

65. Cronier,S, N Gros, M H Tattum, G S Jackson, A R Clarke, J Collinge, J D F Wadsworth, 2008, Detection and characterization of proteinase K-sensitive disease-related prion protein with thermolysin: Biochemical Journal, v. 416, p. 297-305.

66. Dalgaard,J, K J Beckstrom, F L Jahnsen, J E Brinchmann, 2005, Differential capability for phagocytosis of apoptotic and necrotic leukemia cells by human peripheral blood dendritic cell subsets: Journal of Leukocyte Biology, v. 77, p. 689-698.

67. Defaweux,V, G Dorban, C Demonceau, J Piret, O Jolois, O Thellin, C Thielen, E Heinen, N Antoine, 2005, Interfaces between dendritic cells, other immune cells, and nerve fibres in mouse Peyer's patches: Potential sites for neuroinvasion in prion diseases: Microscopy Research and Technique, v. 66, p. 1-9.

68. del Hoyo,GM, M Lopez-Bravo, P Metharom, C Ardavin, P Aucouturier, 2006, Prion protein expression by mouse dendritic cells is restricted to the nonplasmacytoid subsets and correlates with the maturation state: Journal of Immunology, v. 177, p. 6137-6142.

69. Denzer,K, M van Eijk, M J Kleijmeer, E Jakobson, C de Groot, H J Geuze, 2000, Follicular dendritic cells carry MHC class II-expressing microvesicles at their surface: Journal of Immunology, v. 165, p. 1259-1265.

70. Dickinson,AG, H Fraser, I McConnell, G W Outram, 1978, Mitogenic stimulation of the host enhances susceptibility to scrapie: Nature, v. 272, p. 54-55.

71. Dorban,G, V Defaweux, C Demonceau, S Flandroy, P B Van Lerberghe, N Falisse-Poirrier, J Piret, E Heinen, N Antoine, 2007, Interaction between dendritic cells and nerve fibres in lymphoid organs after oral scrapie exposure: Virchows Archiv, v. 451, p. 1057-1065.

72. Dougherty,RM, 1964, Animal virus titration techniques, in RJC Harris (ed), New York, Academic Press, p. 183-186.

73. Eaton,SL, M J Anderson, S Hamilton, L Gonzalez, J Sales, M Jeffrey, H W Reid, M S Rocchi, F Chianini, 2009, CD21 B cell populations are altered following subcutaneous scrapie inoculation in sheep: Veterinary Immunology and Immunopathology, v. 131, p. 105-109.

74. Eaton,SL, M Rocchi, L Gonzalez, S Hamilton, J Finlayson, J Sales, M Jeffrey, P J Steele, M P Dagleish, S M Rodger, H W Reid, F Chianini, 2007, Immunological differences between susceptible and resistant sheep during the preclinical phase of scrapie infection: Journal of General Virology, v. 88, p. 1384-1391.

75. Eklund,CM, R C Kennedy, W J Hadlow, 1967, Pathogenesis of scrapie virus infection in the mouse: J Infect.Dis, v. 117, p. 15-22.

76. Emmanouilidou,E, K Melachroinou, T Roumeliotis, S D Garbis, M Ntzouni, L H Margaritis, L Stefanis, K Vekrellis, 2010, Cell-produced α-synuclein is secreted in a calcium-dependent manner by exosomes and impacts neuronal survival: Journal of Neuroscience, v. 30, p. 6838-6851.

77. Everest,SJ, L Thorne, D A Barnicle, J C Edwards, H Elliott, R Jackman, J Hope, 2006, Atypical prion protein in sheep brain collected during the British scrapie-surveillance programme: J Gen Virol, v. 87, p. 471-477.

78. Faure,J, G Lachenal, M Court, J Hirrlinger, C Chatellard-Causse, B Blot, J Grange, G Schoehn, Y Goldberg, V Boyer, F Kirchhoff, G Raposo, J Garin, R Sadoul, 2006, Exosomes are released by cultured cortical neurones: Molecular and Cellular Neuroscience, v. 31, p. 642-648.

79. Fevrier,B, D Vilette, F Archer, D Loew, W Faigle, M Vidal, H Laude, G Raposo, 2004, Cells release prions in association with exosomes: Proceedings of the National Academy of Sciences of the United States of America, v. 101, p. 9683-9688.

80. Fischer,M, T Rulicke, A Raeber, A Sailer, M Moser, B Oesch, Brandner S, A Aguzzi, C Weissmann, 1996, Prion protein (PrP) with amino-proximal deletions restoring susceptibility of PrP knockout mice to scrapie: EMBO Journal, v. 15, p. 1255-1264.

81. Fivaz,M, F Vilbois, S Thurnheer, C Pasquali, L Abrami, P E Bickel, R G Parton, F G van der Goot, 2002, Differential sorting and fate of endocytosed GPI-anchored proteins: Embo Journal, v. 21, p. 3989-4000.

82. Flores-Langarica,A, Y Sebti, D A Mitchell, R B Sim, G G MacPherson, 2009, Scrapie pathogenesis: the role of complement C1q in scrapie agent uptake by conventional dendritic cells: J Immunol, v. 182, p. 1305-1313.

83. Fraser,H, K L Brown, K Stewart, I McConnell, P McBride, A Williams, 1996, Replication of scrapie in spleens of SCID mice follows reconstitution with wild-type mouse bone marrow: Journal of General Virology, v. 77, p. 1935-1940.

84. Fraser,H, A G Dickinson, 1970, Pathogenesis of scrapie in the mouse: the role of the spleen: Nature, v. 226, p. 462-463.

85. Fraser,H, C F Farquhar, 1987, Ionising radiation has no influence on scrapie incubation period in mice: Vet.Microbiol, v. 13, p. 211-223.

86. Friedman-Levi,Y, H Ovadia, R Hoftberger, O Einstein, O Abramsky, H Budka, R Gabizon, 2007, Fatal neurological disease in scrapie infected mice induced for Experimental Autoimmune Encephalopathy: J Virol., v. 81, p. 9942-9949.

87. Gabizon,R, M P McKinley, D Groth, S B Prusiner, 1988, Immunoaffinity purification and neutralization of scrapie prion infectivity: Proceedings of the National Academy of Sciences of the United States of America, v. 85, p. 6617-6621.

88. Gerdes,HH, 2009, Prions tunnel between cells: Nat Cell Biol, v. 11, p. 235-236.

89. Gerosa,F, A Gobbi, P Zorzi, S Burg, F Briere, G Carra, G Trinchieri, 2005, The reciprocal interaction of NK cells with plasmacytoid or myeloid dendritic cells profoundly affects innate resistance functions: The Journal of Immunology, v. 174, p. 727-734.

90. Glatzel,M, E Abela, M Maissen, A Aguzzi, 2003, Extraneural pathologic prion protein in sporadic Creutzfeldt-Jakob disease: N.Engl.J Med., v. 349, p. 1812-1820.

91. Glatzel,M, F L Heppner, K M Albers, A Aguzzi, 2001, Sympathetic innervation of lymphoreticular organs is rate limiting for prion neuroinvasion: Neuron, v. 31, p. 25-34.

92. Gould,SJ, A M Booth, J E K Hildreth, 2003, The Trojan exosome hypothesis: Proceedings of the NationalAcademy of Sciences of the United States of America, v. 100, p. 10592-10597.

93. Gousset,K, E Schiff, C Langevin, Z Marijanovic, A Caputo, D T Browman, N Chenouard, F de Chaumont, A Martino, J Enninga, J C Olivo-Marin, D Mannel, C Zurzolo, 2009, Prions hijack tunnelling nanotubes for intercellular spread: Nature Cell Biology, v. 11, p. 328-336.

94. Gregoire,C, L Chasson, C Luci, E Tomasello, F Geissmann, E Vivier, T Walzer, 2007, The trafficking of natural killer cells: Immunological Reviews, v. 220, p. 169-182.

95. Griffith,JS, 1967, Self-replication and Scrapie: Nature, v. 215, p. 1043-1044.

96. Grouard,G, M C Rissoan, L Filgueira, I Durand, J Banchereau, Y J Liu, 1997, The enigmatic plasmacytoid T cells develop into dendritic cells with interleukin (IL)-3 and CD40-ligand: J Exp Med, v. 185, p. 1101-1111.

97. Hadlow,WJ, R C Kennedy, R E Race, 1982, Natural infection of Suffolk sheep with scrapie virus: J Infect Dis., v. 146, p. 657-664.

98. Harris,DA, 2003, Trafficking, turnover and membrane topology of PrP: British Medical Bulletin, v. 66, p. 71-85.

99. Heikenwalder,M, C Federau, L V Boehmer, P Schwarz, M Wagner, N Zeller, J Haybaeck, M Prinz, B Becher, A Aguzzi, 2007, Germinal center B cells are dispensable in prion transport and neuroinvasion: J Neuroimmunol., v. 192, p. 113-123.

100. Heikenwalder,M, M Polymenidou, T Junt, C Sigurdson, H Wagner, S Akira, R Zinkernagel, A Aguzzi, 2004a, Lymphoid follicle destruction and immunosuppression

after repeated CpG oligodeoxynucleotide administration: Nature Medicine, v. 10, p. 187-192.

101. Heikenwalder,M, M Prinz, F L Heppner, A Aguzzi, 2004b, Current concepts and controversies in prion immunopathology: J Mol.Neurosci., v. 23, p. 3-12.

102. Heikenwalder,M, M O Kurrer, I Margalith, J Kranich, N Zeller, J Haybaeck, M Polymenidou, M Matter, J Bremer, W S Jackson, S Lindquist, C J Sigurdson, A Aguzzi, 2008, Lymphotoxin-dependent prion replication in inflammatory stromal cells of granulomas: Immunity, v. 29, p. 998-1008.

103. Heikenwalder,M, N Zeller, H Seeger, M Prinz, P C Klohn, P Schwarz, N H Ruddle, C Weissmann, A Aguzzi, 2005, Chronic Lymphocytic Inflammation Specifies the Organ Tropism of Prions: Science, v. 307, p. 1107-1110.

104. Heppner,FL, A D Christ, M A Klein, M Prinz, M Fried, J P Kraehenbuhl, A Aguzzi, 2001, Transepithelial prion transport by M cells: Nature Medicine, v. 7, p. 976-977.

105. Hill,AF, R J Butterworth, S Joiner, G Jackson, M N Rossor, D J Thomas, A Frosh, N Tolley, J E Bell, M Spencer, A King, S Al Sarraj, J W Ironside, P L Lantos, J Collinge, 1999, Investigation of variant Creutzfeldt-Jakob disease and other human prion diseases with tonsil biopsy samples: Lancet, v. 353, p. 183-189.

106. Hoeffel,G, A C Ripoche, D Matheoud, M Nascimbeni, N Escriou, P Lebon, F Heshmati, J G Guillet, M Gannage, S Caillat-Zucman, N Casartelli, O Schwartz, H De la Salle, D Hanau, A Hosmalin, C Maranon, 2007, Antigen crosspresentation by human plasmacytoid dendritic cells: Immunity, v. 27, p. 481-492.

107. Hooper,NM, 2002, Prion disease: close encounters of the cellular kind: Current Biology, v. 12, p. R248-R249.

108. Hsiao,K, S R Dlouhy, M R Farlow, C Cass, M Da Costa, P M Conneally, M E Hodes, B Ghetti, S B Prusiner, 1992, Mutant prion proteins in Gerstmann-Straussler-Scheinker disease with neurofibrillary tangles: Nat Genet, v. 1, p. 68-71.

109. Huang,FP, C F Farquhar, N A Mabbott, M E Bruce, G G MacPherson, 2002, Migrating intestinal dendritic cells transport PrP^{Sc} from the gut: J Gen.Virol., v. 83, p. 267-271.

110. Huang,FP, G G MacPherson, 2004, Dendritic cells and oral transmission of prion diseases: Advanced Drug Delivery Reviews, v. 56, p. 901-913.

111. Isaacs,JD, O A Garden, G Kaur, J Collinge, G S Jackson, D M Altmann, 2008, The cellular prion protein is preferentially expressed by CD4(+) CD25(+) Foxp3(+) regulatory T cells: Immunology, v. 125, p. 313-319.

112. Jarrett,JT, P T Lansbury, 1993, Seeding "one-dimensional crystallization" of amyloid: a pathogenic mechanism in Alzheimer's disease and scrapie?: Cell, v. 73, p. 1055-1058.

113. Jeffrey,M, G McGovern, C M Goodsir, K L Brown, M E Bruce, 2000, Sites of prion protein accumulation in scrapie-infected mouse spleen revealed by immuno-electron microscopy: J Pathol, v. 191, p. 323-332.

114. Johnstone,RM, M Adam, J R Hammond, L Orr, C Turbide, 1987, Vesicle formation during reticulocyte maturation. Association of plasma-membrane activities with released vesicles (exosomes): Journal of Biological Chemistry, v. 262, p. 9412-9420.

115. Junt,T, E A Moseman, M Iannacone, S Massberg, P A Lang, M Boes, K Fink, S E Henrickson, D M Shayakhmetov, N C Di Paolo, N Van Rooijen, T R Mempel, S P Whelan, U H von Andrian, 2007, Subcapsular sinus macrophages in lymph nodes clear lymph-borne viruses and present them to antiviral B cells: Nature, v. 450, p. 110-114.

116. Junt,T, E Scandella, B Ludewig, 2008, Form follows function: lymphoid tissue microarchitecture in antimicrobial immune defence: Nat Rev Immunol, v. 8, p. 764-775.

117. Kaeser,PS, M A Klein, P Schwarz, A Aguzzi, 2001, Efficient lymphoreticular prion propagation requires PrP^{C} in stromal and hematopoietic cells: J Virol, v. 75, p. 7097-7106.

118. Kanu,N, Y Imokawa, D N Drechsel, R A Williamson, C R Birkett, C J Bostock, J P Brockes, 2002, Transfer of scrapie prion infectivity by cell contact in culture: Current Biology, v. 12, p. 523-530.

119. Kasper,KC, D P Stites, K Bowman, H Panitch, S B Prusiner, 1982, Immunological studies of scrapie infection: J Neuroimmunol., v. 3, p. 187-201.

120. Khalili-Shirazi,A, L Summers, Linehan J, G Mallinson, D Anstee, S Hawke, Jackson GS, Collinge J, 2005, PrP glycoforms are associated in a strain-specific ratio in native PrP^{Sc}: Journal of General Virology, v. 86, p. 2635-2644.

121. Kiama,SG, D Dreher, L Cochand, M Kok, C Obregon, L Nicod, P Gehr, 2006, Host cell responses of *Salmonella typhimurium* infected human dendritic cells: Immunology and Cell Biology, v. 84, p. 475-481.

122. Kimberlin,RH, C A Walker, 1979, Pathogenesis of mouse scrapie: dynamics of agent replication in spleen, spinal cord and brain after infection by different routes: J Comp.Pathol, v. 89, p. 551-562.

123. Kimberlin,RH, C A Walker, 1980, Pathogenesis of mouse scrapie: evidence for neural spread of infection to the CNS: J Gen Virol, v. 51, p. 183-187.

124. Kimberlin,RH, C A Walker, 1989a, Pathogenesis of scrapie in mice after intragastric infection: Virus Research, v. 12, p. 213-220.

125. Kimberlin,RH, C A Walker, 1989b, The role of the spleen in the neuroinvasion of scrapie in mice: Virus Res, v. 12, p. 201-211.

126. Kitamoto,T, T Muramoto, S Mohri, K Doh-Ura, J Tateishi, 1991, Abnormal isoform of prion protein accumulates in follicular dendritic cells in mice with Creutzfeldt-Jakob disease: J Virol, v. 65, p. 6292-6295.

127. Klein,MA, R Frigg, E Flechsig, A J Raeber, U Kalinke, H Bluethmann, F Bootz, M Suter, R M Zinkernagel, A Aguzzi, 1997, A crucial role for B cells in neuroinvasive scrapie: Nature, v. 390, p. 687-690.

128. Klein,MA, R Frigg, A J Raeber, E Flechsig, I Hegyi, R M Zinkernagel, C Weissmann, A Aguzzi, 1998, PrP expression in B lymphocytes is not required for prion neuroinvasion: Nat Med, v. 4, p. 1429-1433.

129. Klein,MA, P S Kaeser, P Schwarz, H Weyd, I Xenarios, R M Zinkernagel, M C Carroll, J S Verbeek, M Botto, M J Walport, H Molina, U Kalinke, H Acha-Orbea, A Aguzzi, 2001, Complement facilitates early prion pathogenesis: Nature Medicine, v. 7, p. 488-492.

130. Klohn,PC, L Stoltze, E Flechsig, M Enari, C Weissmann, 2003, A quantitative, highly sensitive cell-based infectivity assay for mouse scrapie prions: Proceedings of the National Academy of Sciences of the United States of America, v. 100, p. 11666-11671.

131. Knepper,MA, T Pisitkun, 2007, Exosomes in urine: Who would have thought?: Kidney International, v. 72, p. 1043-1045.

132. Kocisko,DA, S A Priola, G J Raymond, B Chesebro, P T Lansbury, Jr., B Caughey, 1995, Species specificity in the cell-free conversion of prion protein to protease-resistant forms: a model for the scrapie species barrier: Proc Natl Acad Sci U S A, v. 92, p. 3923-3927.

133. Kocisko,DA, J H Come, S A Priola, B Chesebro, G J Raymond, P T Lansbury, B Caughey, 1994, Cell-free formation of protease-resistant prion protein: Nature, v. 370, p. 471-474.

134. Kosco,MH, E Pflugfelder, D Gray, 1992, Follicular dendritic cell-dependent adhesion and proliferation of B cells *in vitro*: Journal of Immunology, v. 148, p. 2331-2339.

135. Kosco-Vilbois,MH, D Gray, D Scheidegger, M Julius, 1993, Follicular dendritic cells help resting B cells to become effective antigen-presenting cells: induction of B7/BB1 and upregulation of major histocompatibility complex class II molecules: J Exp Med, v. 178, p. 2055-2066.

136. Kretzschmar,HA, 1993, Neuropathology of human prion diseases (spongiform encephalopathies): Developments in Biological Standardization, v. 80, p. 71-90.

137. Krug,A, A R French, W Barchet, J A A Fischer, A Dzionek, J T Pingel, M M Orihuela, S Akira, W M Yokoyama, M Colonna, 2004, TLR9-dependent recognition of MCMV by IPC and DC generates coordinated cytokine responses that activate antiviral NK cell function: Immunity, v. 21, p. 107-119.

138. Kuroda,Y, C J Gibbs, Jr., H L Amyx, D C Gajdusek, 1983, Creutzfeldt-Jakob disease in mice: persistent viremia and preferential replication of virus in low-density lymphocytes: Infect.Immun., v. 41, p. 154-161.

139. Larsson,M, A S Beignon, N Bhardwaj, 2004, DC-virus interplay: a double edged sword: Seminars in Immunology, v. 16, p. 147-161.

140. Lasmezas,CI, J P Deslys, O Robain, A Jaegly, V Beringue, J M Peyrin, J G Fournier, J J Hauw, J Rossier, D Dormont, 1997, Transmission of the BSE agent to mice in the absence of detectable abnormal prion protein: Science, v. 275, p. 402-405.

141. Lavelle,GC, L Sturman, W J Hadlow, 1972, Isolation from mouse spleen of cell populations with high specific infectivity for scrapie virus: Infect.Immun., v. 5, p. 319-323.

142. Leblanc,P, S Alais, I Porto-Carreiro, S Lehmann, J Grassi, G Raposo, J L Darlix, 2006, Retrovirus infection strongly enhances scrapie infectivity release in cell culture: EMBO J, v. 21, p. 2674-2685.

143. Levavasseur,E, P Metharom, G Dorban, H Nakano, T Kakiuchi, C Carnaud, P Sarradin, P Aucouturier, 2007, Experimental scrapie in 'plt' mice: an assessment of the role of dendritic-cell migration in the pathogenesis of prion diseases: J Gen Virol., v. 88, p. 2353-2360.

144. Linden,R, V R Martins, M A M Prado, M Cammarota, I Izquierdo, R R Brentani, 2008, Physiology of the Prion Protein: Physiological Reviews, v. 88, p. 673-728.

145. Liu,T, R Li, T Pan, D Liu, R B Petersen, B S Wong, P Gambetti, M S Sy, 2002, Intercellular transfer of the cellular prion protein: J.Biol.Chem., v. 277, p. 47671-47678.

146. Liu,YJ, G Grouard, O d Bouteiller, J Banchereau, 1996, Follicular Dendritic Cells and Germinal Centers, in WJ Kwang (ed), International Review of Cytology: Academic Press, p. 139-179.

147. Lotscher,M, M Recher, L Hunziker, M A Klein, 2003, Immunologically induced, complement-dependent up-regulation of the prion protein in the mouse spleen: follicular dendritic cells versus capsule and trabeculae: J Immunol., v. 170, p. 6040-6047.

148. Lucas,M, W Schachterle, K Oberle, P Aichele, A Diefenbach, 2007, Dendritic cells prime natural killer cells by trans-presenting interleukin 15: Immunity, v. 26, p. 503-517.

149. Luhr,KM, R P Wallin, H G Ljunggren, P Low, A Taraboulos, K Kristensson, 2002, Processing and degradation of exogenous prion protein by CD11c(+) myeloid dendritic cells in vitro: J Virol, v. 76, p. 12259-12264.

150. Mabbott,NA, 2004, The complement system in prion diseases: Curr.Opin.Immunol, v. 16, p. 587-593.

151. Mabbott,NA, M E Bruce, 2002, Follicular dendritic cells as targets for intervention in transmissible spongiform encephalopathies: Seminars in Immunology, v. 14, p. 285-293.

152. Mabbott,NA, M E Bruce, M Botto, M J Walport, M B Pepys, 2001, Temporary depletion of complement component C3 or genetic deficiency of C1q significantly delays onset of scrapie: Nature Medicine, v. 7, p. 485-487.

153. Mabbott,NA, F Mackay, F Minns, M E Bruce, 2000, Temporary inactivation of follicular dendritic cells delays neuroinvasion of scrapie: Nat Med, v. 6, p. 719-720.

154. Mabbott,NA, M E Bruce, 2001, The immunobiology of TSE diseases: Journal of General Virology, v. 82, p. 2307-2318.

155. Mahal,SP, C A Demczyk, E W Smith, Jr., P C Klohn, C Weissmann, 2008, Assaying prions in cell culture: The Standard Scrapie Cell Assay (SSCA) and the Scrapie Cell Assay in End Point Format (SCEPA): Methods Mol Biol, v. 459, p. 49-68.

156. Mahal,SP, C A Baker, C A Demczyk, E W Smith, C Julius, C Weissmann, 2007, Prion strain discrimination in cell culture: The cell panel assay: Proceedings of the National Academy of Sciences, v. 104, p. 20908-20913.

157. Maignien,T, M Shakweh, P Calvo, D Marce, N Sales, E Fattal, J P Deslys, P Couvreur, C I Lasmezas, 2005, Role of gut macrophages in mice orally contaminated with scrapie or BSE: International Journal of Pharmaceutics, v. 298, p. 293-304.

158. Mallucci,GR, S Ratte, E A Asante, J Linehan, I Gowland, J G R Jefferys, J Collinge, 2002, Post-natal knockout of prion protein alters hippocampal CA1 properties, but does not result in neurodegeneration: Embo Journal, v. 21, p. 202-210.

159. Manuelidis,L, I Zaitsev, P Koni, Z Y Lu, R A Flavell, W Fritch, 2000, Follicular dendritic cells and dissemination of Creutzfeldt-Jakob disease: Journal of Virology, v. 74, p. 8614-8622.

160. Marijanovic,Z, A Caputo, V Campana, C Zurzolo, 2009, Identification of an intracellular site of prion conversion: Plos Pathogens, v. 5, p. e100426.

161. Martins,VR, R Linden, M A M Prado, R Walz, A C Sakamoto, I Izquierdo, R R Brentani, 2002, Cellular prion protein: on the road for functions: Febs Letters, v. 512, p. 25-28.

162. Mata-Haro,V, C Cekic, M Martin, P M Chilton, C R Casella, T C Mitchell, 2007, The vaccine adjuvant Monophosphoryl lipid A as a TRIF-biased agonist of TLR4: Science, v. 316, p. 1628-1632.

163. Mathivanan,S, H Ji, R J Simpson, 2010, Exosomes: Extracellular organelles important in intercellular communication: Journal of Proteomics, v. 73, p. 1907-1920.

164. Maxfield,FR, T E Mcgraw, 2004, Endocytic recycling: Nature Reviews Molecular Cell Biology, v. 5, p. 121-132.

165. McBride,PA, M Beekes, 1999, Pathological PrP is abundant in sympathetic and sensory ganglia of hamsters fed with scrapie: Neuroscience Letters, v. 265, p. 135-138.

166. McBride,PA, W J Schulz-Schaeffer, M Donaldson, M Bruce, H Diringer, H A Kretzschmar, M Beekes, 2001, Early spread of scrapie from the gastrointestinal tract to the central nervous system involves autonomic fibers of the splanchnic and vagus nerves: Journal of Virology, v. 75, p. 9320-9327.

167. McGovern,G, K L Brown, M E Bruce, M Jeffrey, 2004, Murine scrapie infection causes an abnormal germinal centre reaction in the spleen: Journal of Comparative Pathology, v. 130, p. 181-194.

168. McGovern,G, M Jeffrey, 2007, Scrapie-specific pathology of sheep lymphoid tissues: PLoS ONE, v. 2, p. e1304.

169. McKinley,MP, A Taraboulos, L Kenaga, D Serban, A Stieber, S J DeArmond, S B Prusiner, N Gonatas, 1991, Ultrastructural-localization of scrapie prion proteins in cytoplasmic vesicles of infected cultured-cells: Laboratory Investigation, v. 65, p. 622-630.

170. Medof,ME, S Nagarajan, M L Tykocinski, 1996, Cell-surface engineering with GPI-anchored proteins: Faseb Journal, v. 10, p. 574-586.

171. Mellman,I, H Plutner, 1984, Internalization and degradation of macrophage Fc-receptors bound to polyvalent immune-complexes: Journal of Cell Biology, v. 98, p. 1170-1177.

172. Millson,GC, R H Kimberlin, E Jane Manning, S C Collis, 1979, Early distribution of radioactive liposomes and scrapie infectivity in mouse tissues following administration by different routes: Veterinary Microbiology, v. 4, p. 89-99.

173. Mohan,J, M E Bruce, N A Mabbott, 2005, Follicular dendritic cell dedifferentiation reduces scrapie susceptibility following inoculation via the skin: Immunology, v. 114, p. 225-234.

174. Mohri,S, S Handa, J Tateishi, 1987, Lack of effect of thymus and spleen on the incubation period of Creutzfeldt-Jakob disease in mice: J Gen.Virol., v. 68, p. 1187-1189.

175. Montrasio,F, A Cozzio, E Flechsig, D Rossi, M A Klein, T Rülicke, A J Raeber, C A J Vosshenrich, J Proft, A Aguzzi, C Weissmann, 2001, B lymphocyte-restricted expression of prion protein does not enable prion replication in prion protein knockout mice: Proceedings of the National Academy of Sciences of the United States of America, v. 98, p. 4034-4037.

176. Montrasio,F, R Frigg, M Glatzel, M A Klein, F Mackay, A Aguzzi, C Weissmann, 2000, Impaired prion replication in spleens of mice lacking functional follicular dendritic cells: Science, v. 288, p. 1257-1259.

177. Neale,MH, S J Mountjoy, J C Edwards, D Vilette, H Laude, O Windl, G C Saunders, 2010, Infection of cell lines with experimental and natural ovine scrapie agents: Journal of Virology, v. 84, p. 2444-2452.

178. Nelder,JA, R W Wedderburn, 1972, Generalized Linear Models: Journal of the Royal Statistical Society Series A-General, v. 135, p. 370-384.

179. O'Rourke,KI, T P Huff, C W Leathers, M M Robinson, J R Gorham, 1994, SCID mouse spleen does not support scrapie agent replication: Journal of General Virology, v. 75, p. 1511-1514.

180. Ochando,JC, C Homma, Y Yang, A Hidalgo, A Garin, F Tacke, V Angeli, Y Li, P Boros, Y Ding, R Jessberger, G Trinchieri, S A Lira, G J Randolph, J S Bromberg, 2006, Alloantigen-presenting plasmacytoid dendritic cells mediate tolerance to vascularized grafts: Nat Immunol, v. 7, p. 652-662.

181. Oesch,B, D Westaway, M Walchli, M P McKinley, S B H Kent, R Aebersold, R A Barry, P Tempst, D B Teplow, L E Hood, S B Prusiner, C Weissmann, 1985, A cellular gene encodes scrapie PrP 27-30 protein: Cell, v. 40, p. 735-746.

182. Oldstone,MB, R Race, D Thomas, H Lewicki, D Homann, S Smelt, A Holz, P Koni, D Lo, B Chesebro, R Flavell, 2002, Lymphotoxin-α and lymphotoxin-β-deficient mice differ in susceptibility to scrapie: evidence against dendritic cell involvement in neuroinvasion: The Journal of Virology, v. 76, p. 4357-4363.

183. Outram,GW, A G Dickinson, H Fraser, 1974, Reduced susceptibility to scrapie in mice after steroid administration: Nature, v. 249, p. 855-856.

184. Paquet,S, C Langevin, J Chapuis, Jackson GS, H Laude, D Vilette, 2007, Efficient dissemination of prions through preferential transmission to nearby cells: J Gen.Virol., v. 88, p. 706-713.

185. Peters,PJ, A Mironov, D Peretz, E van Donselaar, E Leclerc, S Erpel, S J DeArmond, D R Burton, R A Williamson, M Vey, S B Prusiner, 2003, Trafficking of prion proteins through a caveolae-mediated endosomal pathway: Journal of Cell Biology, v. 162, p. 703-717.

186. Piccardo,P, J C Manson, D King, B Ghetti, R M Barron, 2007, Accumulation of prion protein in the brain that is not associated with transmissible disease: Proc Natl Acad Sci U S A, v. 104, p. 4712-4717.

187. Pisitkun,T, R F Shen, M A Knepper, 2004, Identification and proteomic profiling of exosomes in human urine: Proceedings of the National Academy of Sciences of the United States of America, v. 101, p. 13368-13373.

188. Prado,MAM, J Alves-Silva, A C Magalhaes, V F Prado, R Linden, V R Martins, R R Brentani, 2004, PrPc on the road: trafficking of the cellular prion protein: Journal of Neurochemistry, v. 88, p. 769-781.

189. Prinz,M, M Heikenwalder, T Junt, P Schwarz, M Glatzel, F L Heppner, Y X Fu, M Lipp, A Aguzzi, 2003, Positioning of follicular dendritic cells within the spleen controls prion neuroinvasion: Nature, v. 425, p. 957-962.

190. Prinz,M, F Montrasio, M A Klein, P Schwarz, J Priller, B Odermatt, K Pfeffer, A Aguzzi, 2002, Lymph nodal prion replication and neuroinvasion in mice devoid of follicular dendritic cells: Proc Natl Acad Sci U S A, v. 99, p. 919-924.

191. Prusiner,SB, 1982, Novel proteinaceous infectious particles cause scrapie: Science, v. 216, p. 136-144.

192. Prusiner,SB, D C Bolton, D F Groth, K A Bowman, S P Cochran, M P McKinley, 1982, Further purification and characterization of scrapie prions: Biochemistry, v. 21, p. 6942-6950.

193. Raeber,AJ, M A Klein, R Frigg, E Flechsig, A Aguzzi, C Weissmann, 1999a, PrP-dependent association of prions with splenic but not circulating lymphocytes of scrapie-infected mice: Embo Journal, v. 18, p. 2702-2706.

194. Raeber,AJ, F Montrasio, I Hegyi, R Frigg, M A Klein, A Aguzzi, C Weissmann, 2001, Studies on prion replication in spleen: Dev.Immunol., v. 8, p. 291-304.

195. Raeber,AJ, A Sailer, I Hegyi, M A Klein, T Rulicke, M Fischer, S Brandner, A Aguzzi, C Weissmann, 1999b, Ectopic expression of prion protein (PrP) in T lymphocytes or hepatocytes of PrP knockout mice is insufficient to sustain prion replication: Proc Natl Acad Sci U S A, v. 96, p. 3987-3992.

196. Rajendran,L, M Honsho, T R Zahn, P Keller, K D Geiger, P Verkade, K Simons, 2006, Alzheimer's disease β-amyloid peptides are released in association with exosomes:

Proceedings of the National Academy of Sciences of the United States of America, v. 103, p. 11172-11177.

197. Randolph,GJ, J Ochando, S Partida-Sanchez, 2008, Migration of dendritic cell subsets and their precursors: Annual Review of Immunology, v. 26, p. 293-316.

198. Rao,SP, K A Vora, T Manser, 2002, Differential Expression of the Inhibitory IgG Fc Receptor FcϒRIIB on Germinal Center Cells: Implications for Selection of High-Affinity B Cells: The Journal of Immunology, v. 169, p. 1859-1868.

199. Raymond,CR, P Aucouturier, N A Mabbott, 2007, *In vivo* depletion of CD11c+ cells impairs scrapie agent neuroinvasion from the intestine: J Immunol, v. 179, p. 7758-7766.

200. Raymond,CR, N A Mabbott, 2007, Assessing the involvement of migratory dendritic cells in the transfer of the scrapie agent from the immune to peripheral nervous systems: J Neuroimmunol., v. 187, p. 114-125.

201. Richt,JA, R A Kunkle, D Alt, E M Nicholson, A N Hamir, S Czub, J Kluge, A J Davis, S M Hall, 2007, Identification and characterization of two bovine spongiform encephalopathy cases diagnosed in the United States: Journal of Veterinary Diagnostic Investigation, v. 19, p. 142-154.

202. Riek,R, S Hornemann, G Wider, R Glockshuber, K Wuthrich, 1997, NMR characterization of the full-length recombinant murine prion protein, mPrP(23-231): Febs Letters, v. 413, p. 282-288.

203. Rosicarelli,B, B Serafini, M Sbriccoli, M Lu, F Cardone, M Pocchiari, F Aloisi, 2005, Migration of dendritic cells into the brain in a mouse model of prion disease: Journal of Neuroimmunology, v. 165, p. 114-120.

204. Rubenstein,R, R I Carp, S M Callahan, 1984, *In vitro* replication of scrapie agent in a neuronal model: infection of PC12 cells: J Gen.Virol., v. 65, p. 2191-2198.

205. Rybner-Barnier,C, C Jacquemot, C Cuche, G Dore, L Majlessi, M M Gabellec, A Moris, O Schwartz, J Di Santo, A Cumano, C Leclerc, F Lazarini, 2006, Processing of the bovine spongiform encephalopathy-specific prion protein by dendritic cells: J Virol, v. 80, p. 4656-4663.

206. Safar,J, H Wille, V Itrri, D Groth, H Serban, M Torchia, F E Cohen, S B Prusiner, 1998, Eight prion strains have PrP^{Sc} molecules with different conformations: Nature Medicine, v. 4, p. 1157-1165.

207. Sakaguchi,S, S Katamine, K Yamanouchi, M Kishikawa, R Moriuchi, N Yasukawa, T Doi, T Miyamoto, 1993, Kinetics of infectivity are dissociated from PrP accumulation in

salivary glands of Creutzfeldt-Jakob-Disease agent-inoculated mice: Journal of General Virology, v. 74, p. 2117-2123.

208. Saunderson,SC, P C Schuberth, A C Dunn, L Miller, B D Hock, P A MacKay, N Koch, R W Jack, A D McLellan, 2008, Induction of exosome release in primary B cells stimulated via CD40 and the IL-4 receptor: J Immunol, v. 180, p. 8146-8152.

209. Schatzl,HM, L Laszlo, D M Holtzman, J Tatzelt, S J DeArmond, R I Weiner, W C Mobley, S B Prusiner, 1997, A hypothalamic neuronal cell line persistently infected with scrapie prions exhibits apoptosis: J Virol, v. 71, p. 8821-8831.

210. Schiller,M, I Bekeredjian-Ding, P Heyder, N Blank, A D Ho, H M Lorenz, 2008, Autoantigens are translocated into small apoptotic bodies during early stages of apoptosis: Cell Death and Differentiation, v. 15, p. 183-191.

211. Schmitz,J, S Petrasch, J Van Lunzen, P Racz, H D Kleine, F Hufert, P Kern, H Schmitz, K Tenner-Racz, 1993, Optimizing follicular dendritic cell isolation by discontinuous gradient centrifugation and use of the magnetic cell sorter (MACS): Journal of Immunological Methods, v. 159, p. 189-196.

212. Schnizlein,CT, M H Kosco, A K Szakal, J G Tew, 1985, Follicular dendritic cells in suspension: identification, enrichment, and initial characterization indicating immune complex trapping and lack of adherence and phagocytic activity: J Immunol, v. 134, p. 1360-1368.

213. Sethi,S, K M Kerksiek, T Brocker, H Kretzschmar, 2007, Role of the CD8+ dendritic cell subset in transmission of prions: J Virol., v. 81, p. 4877-4880.

214. Sethi,S, G Lipford, H Wagner, H Kretzschmar, 2002, Postexposure prophylaxis against prion disease with a stimulator of innate immunity: Lancet, v. 360, p. 229-230.

215. Shyng,SL, J E Heuser, D A Harris, 1994, A glycolipid-anchored prion protein is endocytosed via clathrin-coated pits: Journal of Cell Biology, v. 125, p. 1239-1250.

216. Shyng,SL, M T Huber, D A Harris, 1993, A prion protein cycles between the cell-surface and an endocytic compartment in cultured neuroblastoma-cells: Journal of Biological Chemistry, v. 268, p. 15922-15928.

217. Shyng,SL, K L Moulder, A Lesko, D A Harris, 1995, The N-terminal domain of a glycolipid-anchored prion protein is essential for its endocytosis via clathrin-coated pits: Journal of Biological Chemistry, v. 270, p. 14793-14800.

218. Sigurdson,CJ, C Barillas-Mury, M W Miller, B Oesch, L J van Keulen, J P Langeveld, E A Hoover, 2002, PrP^{CWD} lymphoid cell targets in early and advanced chronic wasting disease of mule deer: Journal of General Virology, v. 83, p. 2617-2628.

219. Silveira,JR, G J Raymond, A G Hughson, R E Race, V L Sim, S F Hayes, B Caughey, 2005, The most infectious prion protein particles: Nature, v. 437, p. 257-261.

220. Simons,M, G Raposo, 2009, Exosomes: vesicular carriers for intercellular communication: Current Opinion in Cell Biology, v. 21, p. 575-581.

221. Sixt,M, N Kanazawa, M Seig, T Samson, G Roos, D P Reinhardt, R Pabst, M B Lutz, L Sorokin, 2005, The conduit system transports soluble antigens from the afferent lymph to resident dendritic cells in the T cell area of the lymph node: Immunity, v. 22, p. 19-29.

222. Smith,BA, S Gartner, Y Liu, A S Perelson, N I Stilianakis, B F Keele, T M Kerkering, A Ferreira-Gonzalez, A K Szakal, J G Tew, G F Burton, 2001, Persistence of onfectious HIV on follicular dendritic cells: The Journal of Immunology, v. 166, p. 690-696.

223. Somerville,RA, C R Birkett, C F Farquhar, N Hunter, W Goldmann, J Dornan, D Grover, R M Hennion, C Percy, J Foster, M Jeffrey, 1997, Immunodetection of PrP^{Sc} in spleens of some scrapie-infected sheep but not BSE-infected cows: Journal of General Virology, v. 78, p. 2389-2396.

224. Stahl,N, D R Borchelt, K Hsiao, S B Prusiner, 1987, Scrapie prion protein contains a phosphatidylinositol glycolipid: Cell, v. 51, p. 229-240.

225. Stahl,N, S B Prusiner, 1991, Prions and Prion proteins: Faseb Journal, v. 5, p. 2799-2807.

226. Stoorvogel,W, M J Kleijmeer, H J Geuze, G Raposo, 2002, The biogenesis and functions of exosomes: Traffic, v. 3, p. 321-330.

227. Sukumar,S, M El Shikh, J Tew, A Szakal, 2008, Ultrastructural study of highly enriched follicular dendritic cells reveals their morphology and the periodicity of immune complex binding: Cell and Tissue Research, v. 332, p. 89-99.

228. Sukumar,S, A K Szakal, J G Tew, 2006, Isolation of functionally active murine follicular dendritic cells: Journal of Immunological Methods, v. 313, p. 81-95.

229. Sunyach,C, A Jen, J Deng, K T Fitzgerald, Y Frobert, J Grassi, M W McCaffrey, R Morris, 2003, The mechanism of internalization of glycosylphosphatidylinositol-anchored prion protein: Embo Journal, v. 22, p. 3591-3601.

230. Taraboulos,A, A J Raeber, D R Borchelt, D Serban, S B Prusiner, 1992, Synthesis and trafficking of prion proteins in cultured-cells: Molecular Biology of the Cell, v. 3, p. 851-863.

231. Tattum,MH, S Jones, S Pal, A Khalili-Shirazi, J Collinge, G S Jackson, 2010, A highly sensitive immunoassay for the detection of prion-infected material in whole human blood without the use of proteinase K: Transfusion, v. 50, p. 2619-2627.

232. Taylor,DR, N M Hooper, 2006, The prion protein and lipid rafts: Molecular Membrane Biology, v. 23, p. 89-99.

233. Thery,C, A Regnault, J Garin, J Wolfers, L Zitvogel, P Ricciardi-Castagnoli, G Raposo, S Amigorena, 1999, Molecular characterization of dendritic cell-derived exosomes. Selective accumulation of the heat shock protein hsc73: Journal of Cell Biology, v. 147, p. 599-610.

234. Thery,C, L Zitvogel, S Amigorena, 2002, Exosomes: composition, biogenesis and function: Nature Reviews Immunology, v. 2, p. 569-579.

235. Tsunoda,R, M Nakayama, K Onozaki, E Heinen, N Cormann, C Kinetdenoel, M Kojima, 1990, Isolation and long-term cultivation of human tonsil follicular dendritic cells: Virchows Archiv B-Cell Pathology Including Molecular Pathology, v. 59, p. 95-105.

236. Tzaban,S, G Friedlander, O Schonberger, L Horonchik, Y Yedidia, G Shaked, R Gabizon, A Taraboulos, 2002, Protease-sensitive scrapie prion protein in aggregates of heterogeneous sizes: Biochemistry, v. 41, p. 12868-12875.

237. van Keulen,LJM, B E C Schreuder, R H Meloen, G Mooij-Harkes, M E W Vromans, J P M Langeveld, 1996, Immunohistochemical detection of prion protein in lymphoid tissues of sheep with natural scrapie: Journal of Clinical Microbiology, v. 34, p. 1228-1231.

238. van Niel,G, I Porto-Carreiro, S Simoes, G Raposo, 2006, Exosomes: A common pathway for a specialized function: Journal of Biochemistry, v. 140, p. 13-21.

239. Vella,LJ, D L V Greenwood, R Cappai, J P Y Scheerlinck, A F Hill, 2008a, Enrichment of prion protein in exosomes derived from ovine cerebral spinal fluid: Veterinary Immunology and Immunopathology, v. 124, p. 385-393.

240. Vella,LJ, R A Sharples, V A Lawson, C L Masters, R Cappai, A F Hill, 2007, Packaging of prions into exosomes is associated with a novel pathway of PrP processing: J Pathol, v. 211, p. 582-590.

241. Vella,LJ, R A Sharples, R M Nisbet, R Cappai, A F Hill, 2008b, The role of exosomes in the processing of proteins associated with neurodegenerative diseases: Eur Biophys J, v. 37, p. 323-332.

242. Vey,M, S Pilkuhn, H Wille, R Nixon, S J DeArmond, E J Smart, R G W Anderson, A Taraboulos, S B Prusiner, 1996, Subcellular colocalization of the cellular and scrapie prion proteins in caveolae-like membranous domains: Proceedings of the National Academy of Sciences of the United States of America, v. 93, p. 14945-14949.

243. Villadangos,JA, L Young, 2008, Antigen-presentation properties of plasmacytoid dendritic cells: Immunity, v. 29, p. 352-361.

244. Vorberg,I, A Raines, B Story, S A Priola, 2004, Susceptibility of common fibroblast cell lines to transmissible spongiform encephalopathy agents: J Infect.Dis., v. 189, p. 431-439.

245. Wadsworth,JDF, S Joiner, A F Hill, T A Campbell, M Desbruslais, P J Luthert, J Collinge, 2001, Tissue distribution of protease resistant prion protein in variant Creutzfeldt-Jakob disease using a highly sensitive immunoblotting assay: The Lancet, v. 358, p. 171-180.

246. Wang,F, X H Wang, C G Yuan, J Y Ma, 2010, Generating a prion with bacterially expressed recombinant prion protein: Science, v. 327, p. 1132-1135.

247. Wang,Y, K Abel, K Lantz, A M Krieg, M B McChesney, C J Miller, 2005, The Toll-like receptor 7 (TLR7) agonist, Imiquimod, and the TLR9 agonist, CpG ODN, induce antiviral cytokines and chemokines but do not prevent vaginal transmission of Simian Immunodeficiency Virus when applied intravaginally to Rhesus macaques: The Journal of Virology, v. 79, p. 14355-14370.

248. Weissmann,C, 1991, The prion's progress: Nature, v. 349, p. 569-571.

249. Wekerle,H, U P Ketelsen, M Ernst, 1980, Thymic nurse cells. Lymphoepithelial cell complexes in murine thymuses: morphological and serological characterization: Journal of Experimental Medicine, v. 151, p. 925-944.

250. Wiley,RD, S Gummuluru, 2006, Immature dendritic cell-derived exosomes can mediate HIV-1 trans infection: Proceedings of the National Academy of Sciences of the United States of America, v. 103, p. 738-743.

251. Wolfers,J, A Lozier, G Raposo, A Regnault, C Thery, C Masurier, C Flament, S Pouzieux, F Faure, T Tursz, E Angevin, S Amigorena, L Zitvogel, 2001, Tumor-derived exosomes are a source of shared tumor rejection antigens for CTL cross-priming: Nature Medicine, v. 7, p. 297-303.

252. Wu,Q, Y Wang, J Wang, E O Hedgeman, J L Browning, Y X Fu, 1999, The requirement of membrane lymphotoxin for the presence of dendritic cells in lymphoid tissues: J Exp Med, v. 190, p. 629-638.

253. Young,AJ, 1999, The physiology of lymphocyte migration through the single lymph node *in vivo*: Seminars in Immunology, v. 11, p. 73-83.

254. Zabel,MD, M Heikenwalder, M Prinz, I Arrighi, P Schwarz, J Kranich, A von Teichman, K M Haas, N Zeller, T F Tedder, J H Weis, A Aguzzi, 2007, Stromal complement receptor CD21/35 facilitates lymphoid prion colonization and pathogenesis: J Immunol, v. 179, p. 6144-6152.

APPENDICES

1. Determination of infectious titres using a GLM regression

GLMs constitute a class of statistical models that relate observations to linear combinations of predictor variables. GLM regression can be applied to a wide range of probability distributions that belong to the 'exponential family' by the use of a common method for computing maximum likelihood estimates. In a standard linear model E [Y_j], the expected value of the j^{th} response Y_j, is equal to a linear combination of explanatory variables x_{j1}, $x_{j2, \ldots,}$ x_{jk}, termed the linear predictor η_j, thus:

$$E(Y_j) = \alpha + \beta_1 x_{j1} + \beta_2 x_{j2} + \ldots \beta_k x_{jk} + e_j = \eta_j + e_j \qquad e_j \sim \text{iid } N(\theta,\sigma^2) \qquad (\mathbf{1})$$

In a GLM the link function *g*, a monotone differentiable function, defines the relationship between the linear predictor η and the mean of the distribution, thus:

$$g(E(Y)) = \eta \qquad (\mathbf{2})$$

The inverse of the link function is $g^{-1}(\eta) = E(Y)$. For prion titre determinations by endpoint assays the response variable Y_j, the number of positive wells at the j^{th} dilution, is linked to the dilution by a complementary log-log transformation $g(P_j) = \log(-\log(1-P_j))$, where $P_j = E(Y_j/n_j)$ and n_j is the number of independent infections at the j^{th} dilution, via

$$g(P_j) = \alpha + \beta x_j \qquad (\mathbf{3})$$

where x_j is the j^{th} log dilution, α is the log mean number of infectious units and β is the slope parameter. Other link functions for the binomial model used for titre determination by bioassay are the logit function $g(P_j) = \log(P_j/(1-P_j))$ and the probit function $g(P_j) = \Phi^{-1}(P_j)$. The probit function is the inverse cumulative distribution

function of the standard normal distribution. These three common link functions and their inverses are summarised below:

	g (**P**)	g^{-1} (η)
Complementary log-log	Log (-log (**P**))	1-exp [-exp(η)]
Logit	Log (**P**/(1–**P**)	1/(1+exp(-η))
Probit	Φ^{-1} (**P**)	Φ (η)

The complementary log-log transformation arises naturally for *in-vitro* titres since if the number of infected cells follows a Poisson distribution then the proportion $1 - P_j$ of negative wells at dilution c_j is equal to $\exp(-mc_j)$, where m is the mean number of infectious units per volume, which is equivalent to relation (**3**) with $\beta = 1$.

The parameters α and β, where α is the log mean infectious units and β the regression slope, are estimated by the method of maximum likelihood. For a given probability distribution specified by $f(y_i|\theta)$ and observations $y_1, y_2 \ldots y_n$ the log likelihood function for θ is

$$l(\theta) = \log L(\theta) = \sum \log f(y_i|\theta) \qquad (4)$$

where $L(\theta)$ is the likelihood function.

2. R code for the determination of infectious titres from SCEPA by GLM

The observed proportions of negative wells from multiple serial dilution of RML (**Table A1**) can be fitted using a GLM with binomial family complementary log-log link by the R function:

fit <-glm(cbind(positive,negative)~logdil, data = ori, family=binomial (link="cloglog"))

This code fits a 'saturated' model in which the slope parameter β is arbitrary. The 'reduced' model with a unit slope, corresponding to a Poisson model for the number of infected cells, can be fitted using the following R function:

fit <-glm(cbind(positive,negative)~1, data = ori, offset=logdil, family=binomial (link="cloglog"))

To check the fit of a GLM with binomial family and complementary log-log link we can use the analysis of deviance, a method to test whether the discrepancies between the observed and predicted values lie within an acceptable limit of experimental error.

	Saturated model	**Reduced model**
Slope	0.9608	1
Standard error	0.0969	-
Degrees of freedom	30	31
Residual deviance	26.82	26.99
AIC	106.88	105.04

The estimated value for the slope factor β is 0.9608 ± 0.0969. This allows us to test the null hypothesis that the true slope is one using the Wald test. The *p*-value corresponding to the *z*-score (0.9608-1)/ 0.0969 is 0.69, indicating no evidence of a departure from an underlying Poisson distribution for the number of infected cells. Alternatively we can test this hypothesis using the likelihood ratio test statistic (LRS),

$$LRS = -2\,[\log(L_s)/\log(L_r)] = -2\log(L_s) + 2\log(L_r) = D_s - D_r$$

where L_s and L_r are the maximised likelihoods under the saturated and reduced models, respectively, and D_s and D_r are the respective deviances. The LRS approximately follows a Chi-square distribution with degrees freedom equal to the difference in the number

of parameters fitted in the two models, here one. Here LRS = 26.99 - 26.82 = 0.17, giving a *p*-value of 0.68, approximately the same as the *p*-value from the Wald test. The reduction of AIC is a further indication of the superiority of the reduced model.

In both the saturated and reduced models, the residual deviance, which is a measure of how much the data deviates from the model, is lower than the residual degrees of freedom, indicating that the data are not overdispersed in relation to an underlying binomial distribution. The reduced model yielded an estimated titre of 8.63 ± 0.03 logTCIU/g brain for eight technical repeats of serially diluted RML I6200 brain homogenate.

3. Determination of infectious titres from bioassay using a GLM

To establish a GLM for titre determination on bioassay we performed six independent endpoint titrations by bioassay using brain homogenate RML I6200 as inoculum (**Table A2**). The proportion of positive wells and the fitted proportions from the complementary log-log and probit models are shown in **figure 3.3**. The complementary log-log and probit models resulted in estimated titres of 8.54 ± 0.54 and 8.71 ± 0.53, respectively. A corresponding titre with a slightly higher standard error (8.66 ± 0.80 log LD_{50} units/g brain) was calculated by the Spearman Karber method and a GLM was used for all subsequent titre determinations. For a direct comparison of the sensitivity levels between SCEPA *versus* bioassay we therefore repeated an endpoint titration experiment.

Table A1: *In-vitro* endpoint titration of RML I6200

Serially diluted RML I6200 was transferred onto layers of prion-susceptible PK1 cells and the number of positive and negative wells was determined by SCEPA as described in materials and methods (**section 2.2.3**). Data represent eight technical assay repeats of serially diluted homogenate.

Dilution	Wells	Repeats SCEPAs 1	2	3	4	5	6	7	8
10^{-7}	positive	12	12	12	12	12	12	12	12
	negative	0	0	0	0	0	0	0	0
$6.6x10^{-8}$	positive	12	12	12	12	12	12	12	12
	negative	0	0	0	0	0	0	0	0
$3.3x10^{-8}$	positive	11	12	12	12	11	10	12	10
	negative	1	0	0	0	1	2	0	2
10^{-8}	positive	9	6	8	9	7	8	8	6
	negative	3	6	4	3	5	4	4	6
$6.6x10^{-9}$	positive	6	4	4	4	3	7	6	4
	negative	6	8	8	8	9	5	6	8
$3.3x10^{-9}$	positive	4	6	2	4	1	4	3	3
	negative	8	6	10	8	11	8	9	9
10^{-9}	positive	0	3	0	1	0	2	2	0
	negative	12	9	12	11	12	10	10	12

Table A2: Serial mouse bioassays to determine endpoint titres of RML I6200

Five aliquots of RML brain homogenate I6200 (10 %, w/v) were each serially diluted 1:10 into uninfected CD1 brain homogenate (10 %, w/v) and kept frozen at -80 °C until further use. For mouse bioassays, groups of six Tga20 mice were inoculated intracerebrally with 30 µl brain homogenates and attack rates and scrapie incubation times were determined. Data represent five independent bioassays.

Dilution	Scrapie	Repeats SCEPAs 1	2	3	4	5
10^{-5}	sick	6	6	6	5	6
	healthy	0	0	0	0	0
10^{-6}	sick	6	6	6	3	5
	healthy	0	0	0	1	1
10^{-7}	sick	3	3	3	4	3
	healthy	3	3	3	2	2
10^{-8}	sick	0	0	1	2	1
	healthy	5	6	5	3	5
10^{-9}	sick	1	0	0	0	1
	healthy	5	5	6	6	5